8-2017

Watershed Sub-Basin Scale Forest Fire Impacts on Soil Chemistry : A Case Study in Delaware State Forest, Pennsylvania, USA

Jason Scott Darley
Montclair State University

ABSTRACT

Forest fires can affect soil chemistry and soil properties depending on the fire intensity and type of biomass burned, changing the local environment. For this study, soil and ash samples were examined post-fire from the 16-Mile fire event in the Delaware State Forest, Pennsylvania, to understand the pedosphere chemistry within the watershed sub-basin. The main goal of this project was to study the major and trace elements of ash and soil samples of the 16-Mile Fire in the burned area and compare to samples upstream and downstream of the watershed sub-basin. Inductively coupled plasma mass spectroscopy was conducted for major and trace elemental analysis of the samples to determine if a fire signature is present. Calcium, manganese, copper and barium were found at higher concentrations within the fire extent compared to up and downstream of the fire. Copper and barium concentrations show to be fire signatures that are unique to the 16-Mile fire event. Comparing the 2-month sampling to the 8-10-month sampling indicates that the concentrations of copper and barium are remaining within the soil horizons, where in some sites concentrations are moving vertically down through the soil horizons. GIS and RUSLE were used to further model conditions of the fire extent to determine if erosion and runoff would mobilize fire signatures throughout the sub-basin. Results indicate that due to the shallow slopes within the fire extent, along with factors of soil structure, rainfall, slope, and land cover management, erosion is not likely and fire signatures will reside down the soil horizon. Further research is needed to further investigate how long the fire signatures will reside in the soil horizons within this area.

MONTCLAIR STATE UNIVERSITY

Watershed Sub-Basin Scale Forest Fire Impacts on Soil Chemistry: A Case Study in Delaware State Forest, Pennsylvania, USA

by

Jason Scott Darley

A Master's Thesis Submitted to the Faculty of

Montclair State University

In Partial Fulfillment of the Requirements

For the Degree of

Master of Science, Earth and Environmental Science

August 2017

School College of Science and Mathematics

Department Earth & Environmental Studies

Thesis Committee:

[redacted]

Dr. Gregory Pope
Thesis Sponsor

[redacted]

Dr. Joshua Galster
Committee Member

[redacted]

Dr. Jennifer Callanan
Committee Member

Watershed Sub-Basin Scale Forest Fire Impacts on Soil Chemistry: A Case Study in Delaware State Forest, Pennsylvania, USA

A THESIS

Submitted in partial fulfillment of the requirements

For the degree of Master of Science in Earth and Environmental Science

By

Jason Scott Darley

Montclair State University

Montclair, NJ

2017

ACKNOWLEDGEMENTS

I would like to thank my thesis advisor, Dr. Gregory Pope, and committee member, Dr. Jennifer Callanan for allowing me to join on this research project. Greg, thank you for your enthusiasm and support throughout my thesis and for being an amazing mentor. Jenn, thank you for picking up the phone for my random calls of doubt and helping me follow the data. I would also like to thank my committee member, Dr. Joshua Galster, for spending time with me on GIS analysis and continued motivation to finish my thesis. Accessing the 16-Mile Fire would not have been possible without the support and help of the Pennsylvania Department of Conservation and Natural Resources (PA DCNR) team, in particular, Matthew Hazen, who spent the time guiding the research team to the different sampling sites and for providing data throughout the project. Tim Dugan, District Forester and Greg Czarnecki, Climate Change & Research Coordinator who both assisted in getting approval of the project to work on the site. Thanks to the William Paterson University research team, Katherine Espinal, Dennis Grune, Mariola Lach, who assisted in field sampling and soil properties analysis. I would like to thank Dr. Matthew Gorring for his help in geochemical analysis and for taking the time to meet with me on multiple occasions to answer my random chemistry questions.

After 11 years of studying in the Department of Earth and Environmental Studies I have been very fortunate to have been mentored by many of the department's professors. I would like to thank the entire EAES department for their guidance over the years. Completing my masters would not have been possible without the support of Dr. Stephanie Brachfeld and Dr. Sandra Passchier who both have assisted me over the years in keeping my education on track and not letting me give up. I would like to thank my

peers Melissa Hanson, Alexa Marques, Michael Ayers, Daniel Ciarletta, Jennifer Light, Allison Lepp, Taylor Wieczerak, and Mitch Clay for assisting me on my thesis, destressing sessions and all the great times we had during my masters.

A special thanks to my wife, Rachel, my everything, I thank you to the moon and back for your support and love through my education, my thesis and most importantly putting up with me for the past 9 years and many more. I would like to thank my entire family for their support during my graduate studies. I dedicate this thesis to my brother-in-law, Jonathan Perez, who was the most humble and helpful person I have ever known. Jonathan, you are dearly missed. Thank you for watching over us.

Table of Contents

LIST OF FIGURES

LIST OF TABLES

1. INTRODUCTION

Wildfires can produce both positive and negative impacts on forest ecosystems. Despite being similarly categorized, these ecosystems vary from location to location and their responses to wildfires will vary depending on the type of vegetation, soil, surrounding environment, and severity of the fire (Neary *et al.*, 2005). Collectively, ecosystems are part of the Earth's critical zone, which according to Brantley *et al.* (2006), is the area of the Earth's surface containing vegetation, extending down to bedrock, including groundwater, which are essential to supporting life. These complex systems (biosphere, geosphere, and hydrosphere) are all interconnected by soil. Soil controls the availability of nutrients used by forest ecosystems (as well as human agriculture), while also acting as a natural filter for water that enters the groundwater system. Soil can take upwards of thousands of years to develop, while fire has the ability to change soil properties, both physically and chemically, over a much shorter time-frame (Figure 1.1) and often with adverse effects on future soil formation (Santín & Doerr, 2016). To better understand the effects of wildfires on soil geochemistry within a watershed it is necessary to investigate elemental signatures between burned and unburned soil, using signatures to trace temporal differences within the landscape. This study builds off previous research by Pope *et al*. (2012), where ash chemistry was assessed to determine if fire signatures exist within major elements of burned soil samples.

Flannigan *et al*. (2000) mentions, that since 1989 through 1998, an average of 3,000,000 acres burned annually (acres vary year from year) from wildfires in the United States, with most occurring in the western part of the country. Effects of climate change

have caused an increase in high-intensity wildfires worldwide over the past few decades. This increase in wildfires due to changes in climate is the result of more frequent droughts brought on by warmer temperatures, resulting in longer dry seasons (Flannigan *et al.,* 2000; Westerling *et al.,* 2006). According to Santín & Doerr (2016) and Flannigan *et al.* (2000), global circulation models (GCM's) indicate an overall increase in temperatures worldwide over the next century which can lead to the recurrence of wildfires.

While the impacts of humans on the natural environment and changes in climate have increased wildfires, it is the fire ecology that determines fire damage. The severity of wildfires is based on the intensity and duration of the fire, which is dependent on the fuel being burned and other environmental factors (Certini, 2005). High-intensity wildfires can have adverse effects on soil and water quality, especially within the major and minor elemental chemistry. Severe wildfires cause contamination in soil and water within the vicinity of the fire due to the transfer of heavy metals and other contaminants from fuel and manmade materials burned (Bladon, Emelko, Silins, & Stone, 2014). Degradation of soil and water in post-wildfire settings is preserved in the environment for years to decades depending on the concentration of contaminates. Contaminated water from wildfires affects not only water used for human consumption but aquatic ecosystems as well (Bladon *et al.*, 2014).

1.1 Ash-Soil-Water Interaction

Ash resulting from wildfires is composed primarily of organic and inorganic residue including minerals and trace metals. Although most ash is derived from biomass, the upper organic material in soil layers can also be combusted during wildfires. The

major elements in wood ash are magnesium (Mg), calcium (Ca), potassium (K), phosphorous (P), sodium (Na) and sulfur (S), with minor elements of aluminum (Al), manganese (Mn), iron (Fe), silicon (Si) and zinc (Zn) (Bodí *et al*., 2014; Demeyer *et al*., 2001; Etiégni & Campbell, 1991; Marion *et al*., 1991). Etiégni and Campbell (1991) showed the concentrations of major and trace elements of wood ash at various temperatures (Figure 1.2), which indicate what elements could possibly leach out from ash into the surrounding environment. Campos *et al*., (2016) and Demeyer *et al*., (2001) mention trace elements arsenic (As), lead (Pb), nickel (Ni), chromium (Cr), cadmium (Cd), mercury (Hg), vanadium (V), and cobalt (Co) found in soil after a wildfire.

Combustion completeness of fuels is dictated by the intensity and duration of the fire. Bodí *et al*. (2014) suggests that fire temperatures below 450° C yields ash that is organic-rich while temperatures that reach 450° C and above will have almost all organic matter volatilized yielding a higher pH, increased oxidations and increased mineral content. Ashes where the combustion volatizes most organic matter are highly mobile and are rapidly transported from the vicinity of the fire, especially in windy conditions (Bodí *et al*., 2014). This allows ash to be transferred to soil and water not only in the burn zone but also unburned areas. The transfer of elements from ash to soil is a simple process considering ash is insoluble, especially in instances where fire temperatures reach > 500° C. Initially, the pH of soils can increase due to the transfer of alkaline elements and organic material from ash fall (Alauzis, Mazzarino, Raffaele, & Roselli, 2004; Badía & Martí, 2003; Blank & Zamudio, 1998; Bodí *et al*., 2014; Certini, 2005; Demeyer *et al*., 2001), then over time will decrease as the major elements are leached and mobilized from the soil (Demeyer *et al*., 2001). The concentration of elements that is retained by soil

depends on soil texture, soil water retention and repellency, cation exchange capacity (CEC) of the individual elements (Demeyer *et al.*, 2001; Marion *et al.*, 1991) and the regrowth of vegetation, which can also absorb elements.

Ash may also contribute to the change of physical properties within soil. In soils where the ash was not completely combusted (fire temperatures < 450° C), organic matter is still retained in the ash and can cause the soil color change to darker hues. Ash that is high in organic matter will also support transfer of nutrients into the soil and vegetation (Demeyer *et al.*, 2001). Ulery & Graham (1993) reported in their study that high intensity fires where ash was completely combusted, the soil had more of a reddish hue. Samples that were reddish in color had white ash at the surface, indicating temperatures > 500° C. According to Schwertmann & Fechter (1984), it is the extreme heat that oxidizes the mineral goethite to hematite and maghemite, both of which have reddish hues to them.

Soil erosion and hydrology can be altered by the accumulation of ash on the surface of soil after wildfires. In a literature review conducted by Bodí *et al*., (2014), previous studies indicate contradicting findings where an increase in soil erosion is noted in some studies while others note the reduction of soil erosion. Much of this is dependent on the thickness of the ash layers deposited on top of the soil and other post-fire conditions. Two separate studies conducted by Onda *et al*. (2008) and Woods & Balfour (2010) found that the ash layer formed a crust at the surface due to the compaction from raindrops, which resulted in water runoff in the months after the fire. This crust leads to increased water runoff with ash and soil eventually eroding into water sources in the vicinity. Erosion will be higher if the accumulation of ash and altered soil is along

hillside slopes. Based on preliminary results of the sampled sites, this is not occurring at our study area.

Ash can affect water quality by the addition of suspended sediments (containing concentrations of trace elements and metals) into streams, rivers, and other water bodies. Johansen *et al*. (2003) simulated rainfall to quantify ^{137}Cs concentrations from ash deposits and runoff after the May 2000 Cerro Grande wildfire within the Pajarito Watershed. Sampling took place in both burned and unburned areas. The results of ash indicate that the concentrations of ^{137}Cs are elevated in the ground vegetation compared to above ground vegetation. Sediment has elevated concentrations of ^{137}Cs, but due to the erosion of ash into water, it is transitory. The redistribution of suspended sediments is short-term for this study but other trace elements such as Pb and Fe can remain in water resources especially if they are not diluted. This can have long-term effects on aquatic organisms that are sensitive to minute changes. Suspended sediments from ash can also create more turbidity in water, which can lead to a decrease in water quality, particularly in urban areas that acquire water supplied from surface water.

According to Certini (2005) the extent of degradation is not only dependent on the temperature of the fire, but also soil properties, fire reoccurrence frequency, and the environmental conditions post-fire. Depending on the quality and quantity of biomass (fuel), the temperature at the surface of the soil can exceed 700° C with heat dissipating as one moves vertically down the horizon to ~30 cm (Debano, 2000a). Depending on fire duration, this determines how much heat will be dispersed down horizon. Organic carbon can be completely combusted/reduced when temperatures reach greater than 450° C in the soil, creating long and short-term transformations in the biochemical structure used

for ecological productivity (Arocena & Opio, 2003; Certini, 2005). Studies conducted by Arocena & Opio (2003), Certini (2005) and Iglesias *et al.* (1997) all show that as temperatures increase and organics are completely combusted, the pH of the soil becomes more alkaline and an increase in electrical conductivity occurs (Hernández *et al*., 1997; Naidu & Srivasuki, 1994). As previously mentioned, excessive temperatures can cause alteration (dehydroxlation and decomposition) of clay minerals such as kaolinite, illite and vermiculite within the soil horizons (Reynard-Callanan *et al*., 2010). In a study done by Iglesias *et al*. (1997) alterations were seen to kaolinite and vermiculite due to high temperatures with the formation of calcite in the soil due to the combustion of the tree species *Q. pyrenaica*. Iron oxide minerals are known to be transformed at even lower temperatures, especially minerals residing in the O/A horizon (Certini, 2005).

Few studies have been conducted to investigate changes and redistribution of trace elements in soils. Trace elements are found everywhere in nature, but become an environmental concern when found at higher concentrations(Campos *et al*., 2016). They include heavy metals that are highly toxic and can accumulate over time. Contaminated soil could grow vegetation that is then consumed by animals hunted as game or crops grown for human consumption. Risk can also come to the ecosystem itself requiring years for recovery (Smith *et al*., 2011). Low amounts of heavy metals can naturally accumulate over time, whereas wildfires can cause a greater risk of toxic trace elements and heavy metals accumulating in a short time frame (Campos *et al.,* 2016; Costa, *et al.,* 2014; Pinedo-Gonzalez *et al.,* 2016).

Campos *et al.* (2016) examined major and trace elements from a wildfire which occurred in July 2010, near the parish of Ermida, Portugal. The study took a series of soil

(eucalypt and pine forests) and ash samples at six sites along hill slopes. Samples were collected directly after the fire, and respectively four, eight and fifteen months later. Major and minor trace elements of the samples were analyzed using Inductively coupled plasma mass spectrometry (ICP-MS). Of special interest were the trace elements V, Mn, Co, Ni, Cu, Cd and Pb. The analyzed ash samples show high concentrations of Mn and Pb, while the lowest concentrations were Co and Cd. Burnt soil samples from the initial sampling showed concentrations of V, Mn, Ni, Cd, and Pb, compared to unburned soil, with Mn having the highest concentration. The other samples show a decrease in most concentration of these trace elements due to rainfall and erosion, except for Cu and Pb which remain at relatively the same levels even in the 15-month sampling.

Costa *et al*. (2014) investigated a wildfire originating from an airplane crash in June 2006, in the Marao River watershed, Portugal. Landsat TM remote sensing images were used in the study to calculate how much biomass was burned during the fire and to document the recovery of vegetation over time. Three samples of ash and soil were collected within the burn area to conduct chemical analysis five and eleven months after the fire. Water samples for chemical analysis, as well as pH and electrical conductivity, were collected upstream from the burn area, within the burn area and downstream. Results from the chemical analysis of soil in ashes showed high concentrations of Mn, Mg, Fe, Cu, and Zn. Zn and Mn were only seen in high concentrations in the five-month samples and decreased after the 11-month sample results. This indicates that Mn and Zn leached from the soil samples and were most likely carried away by water runoff from rain water transported to the river system (Costa *et al*., 2014). Fe and Cu remain relatively the same between both sampling times in this study, but Cu concentrations vary

in other studies. Water chemistry results had concentrations of Mg, Mn, Na, and Ca in the samples collected 5 months after the fire and Mn was still high even after the 11-month water sampling. Excessive heat can cause the soil to become water repellent, lessening infiltration rates. According to Debano (2000), heat going vertically down through the soil dehydrates organic particles, which release waxes that attach to clay sized particles forming an impermeable layer. This can increase runoff and erosion leading to ash-flow into nearby water sources. Flooding can occur due to this increase of deposition of soil into river and streambeds that displace water.

Pinedo-Gonzalez *et al*. (2016) investigated size partitioning of metals transported due to storm runoff from wildfires in the September 2012 San Gabriel Mountains in greater Los Angeles County. Storm water runoff was collected in three different catchment sites of both unburned and burned areas. One catchment was inside a burn area, one was a reference site that was not burned and the last site was an urban area. ICP-MS was used to analyze all the samples measuring the concentrations of Cd, Co, Mo, Ni, Fe, Cu, Zn, Pb, and V. Both unburned and urban area yield results where runoff concentrations of Cd, Co, Mo, Ni, Fe, Cu, Zn, Pb, and V are the same compared to previous studies and were within range of what is found in nature and where human activity exists (Davis *et al*., 2001; Joshi & Balasubramanian, 2010; Yoon *et al*., 2006). Higher concentrations of Fe, Cu, Zn, Pb and V were found in the burn area which were higher than natural background and comparable to those concentration levels found in urban areas. Size partitioning was seen in Pb and Fe where wildfires can modify the colloidal and soluble phases of these two elements (Pinedo-Gonzalez *et al*., 2016).

1.2 Effects of Wildfires on Water Quality and Chemistry

Wildfires can have negative impacts on both the physical and chemical aspects of water. According to Tecle & Neary (2015), transported debris including ash, soil, charred trees and vegetation can enter water sources and cause an increase in turbidity. If the fire is close to the water source, the temperature of the water can also increase and kill off aquatic life sensitive to temperature changes. Erosion and stormflow has also been known to increase peak river and stream flows that affect discharge areas outside the vicinity of the fire (Tecle & Neary, 2015). Water chemistry can change from the fire and can affect water quality for long durations. According to Smith *et al*. (2011), trace elements of Fe and Mn can change both the color of water as well as taste. Elevated concentrations of Pb, Al, and Hg are toxic to both humans and wildlife and can have long-term effects. Smith *et al.* (2011) mentions that there is a lack of data for post-fire trace element concentrations in streams and other water bodies.

Burton *et al*. (2016) looked at the trace elements in stormflow and streams following the September 2009 Station Fire at the Angeles National Forest in Los Angeles, CA. The primary purpose of the study was to identify toxic trace elements in ash and soil and compare them to stormflows in streams. For this study 32 samples of ash, 18 samples of burned soil, 4 samples of unburned soil and 13 sites for stream water sampling were collected. Results from the burned and unburned soil showed that trace elements of As, Ni, Pb, Zn and Fe were relatively the same to each other. Comparing the burned soil to ash, trace elements in the ash had higher concentrations of Cu, Pb, and Zn where Fe was higher in the burned soil samples. Burton *et al*. (2016) establish that Fe mainly derives from minerals in the soil where Cu, Pb, and Zn are primarily found in

vegetation. Sources of As, Mn and Ni come from burned vegetation and soil. Buildings were also destroyed during this fire and elements of As, Cu, Pb, Ni and Zn can also derive from these sources. High concentrations of Pb, Ni, and Zn were found in the samples from streams close to the vicinity of the fire. These concentrations were found to be higher than what is recommended for certain types of aquatic life.

In summary, wildfires can cause physical and chemical changes to soils and water resources. These changes are short and long-term and can have adverse effects on the environment. It has been discussed in this chapter that burned biomass (ash) and high temperatures from the fire can alter soil properties while also adding/changing major and minor elements. Concentrations of trace elements and metals can reside in soils for extended periods and can be transferred to water sources by erosion due to repellency layers created during the fire. The concentration of trace elements in water sources poses a threat to aquatic species, drinking water for human consumption and ecosystems.

Historically, fire regimes within this region have consisted of low intensity fires used to clear land by Native Americans and during the Industrial Revolution more intense burning for use as a raw material and fuel (Brose *et al*., 2001). In more recent times, forest management have set low intensity, prescribed fire regimes to destroy diseased trees, invasive plants and insects. The 16-Mile Fire burned much hotter and at a longer duration compared to past wildfires in this area. The nature of this fire is consistent with fire regimes that are seen in Western United States.

1.3 Project Aim

This project investigates the impacts of wildfire on major and trace elements in soil from the April 2016, 16-Mile Wildfire at the Delaware State Forest, Pennsylvania

(Warner, 2016). The goal of this project was to determine if there is an identifiable trace element signature in the forest soil following the fire. Concentrations of heavy metals and trace elements can accumulate from the burning of biomass and other material (such as building materials), during wildfires, possibly leading to an increase of trace elements in soil and surrounding watershed. Soil sampling was conducted within burned study areas as well as unburned areas that are immediately adjacent to the fire. The unburned soil outside the burn zone will be used as control for the study. Inductive coupled plasma mass spectroscopy (ICP-MS) is utilized to identify the major and minor composition of ash and soil of each site. Bedrock samples were also analyzed by ICP-MS to determine the elemental composition of the parent material of the soil pre-fire. Samples are point specific, so elemental signatures can then be used within a geographic information system (GIS) to identify where concentrations of trace elements and heavy metals might possibly reside within areal fire extent and surrounding sub basin. Specifically, this information can be used to determine the amount of change to the soil from the wildfire. In addition, forest and wildlife management professionals can use this information to manage natural resources and sensitive ecosystems from the potential change in soil and water chemistry.

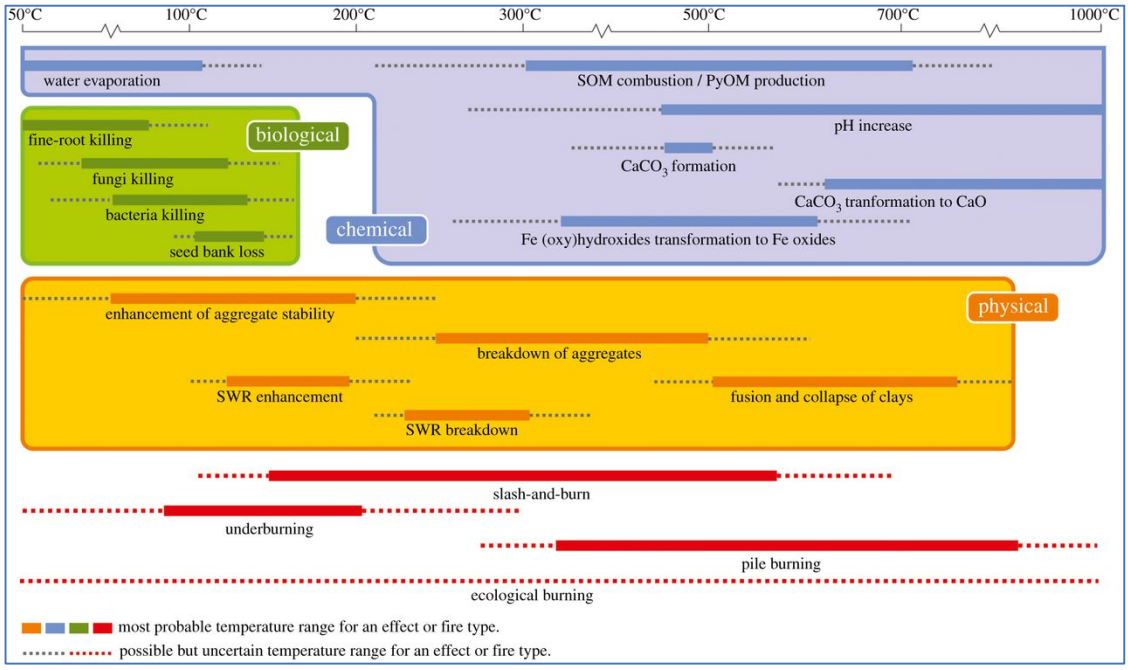

Figure 1.1 Effects of fires on soils chemical, biological, and chemical properties (Santín & Doerr, 2016).

Table 1.1 Elemental concentrations of wood ash at various temperatures (°C) in ppm (Etiégni & Campbell, 1991).

Element	*Temperature (°C)*					
	538	*649*	*760*	*871*	*982*	*1 093*
Aluminum	10 415	12 825	13 115	10 115	13 415	11 015
Antimony	264	142	65	91	94	208
Arsenic	< 20	< 20	< 20	54	74	59
Barium	1 301	1 490	1 640	1 463	1 601	1 530
Beryllium	< 5	< 5	< 5	< 5	< 5	< 5
Bismuth	< 30	< 30	< 30	< 30	< 30	< 30
Cadmium	< 2	< 2	< 2	< 2	< 2	< 2
Calcium	187 480	217 480	241 180	216 080	238 980	264 580
Cerium	< 40	< 40	< 40	< 40	< 40	< 40
Chromium	52	37	49	20	39	622
Cobalt	< 3	< 3	< 3	< 3	< 3	< 3
Copper	345	620	588	380	437	422
Iron	8 796	11 951	9 981	8 219	22 411	16 781
Lanthanum	< 10	< 10	< 10	< 10	< 10	< 10
Lead	51	75	200	39	43	685
Lithium	35	55	70	10	30	10
Magnesium	59 730	68 060	76 970	69 170	80 470	89 100
Manganese	10 549	11 789	13 489	11 859	16 609	21 680
Molybdenum	18	21	26	39	56	192
Nickel	59	64	151	63	497	8 979
Phosphorus	16 950	19 060	21 720	19 370	21 030	25 460
Potassium	110 500	86 590	47 720	79 860	51 970	4 026
Selenium	< 50	< 50	< 50	< 50	< 50	< 50
Silicon	33 867	39 777	42 647	31 997	46 477	35 267
Sodium	2 961	4 947	4 365	1 643	1 479	< 100
Titanium	780	1 060	1 012	777	957	796
Vanadium	13	18	23	17	26	234
Ytterbium	3	3	3	2	5	3
Zinc	2 678	2 139	1 001	177	26	55
Zirconium	14	14	16	15	19	23
Carbonates (%)	62·8	60·0	58·4	54·9	53·3	51·4

2. METHODS

It is useful to investigate the elemental signatures between burned and unburned soils in order to understand the effect wildfires have on soil geochemistry within a watershed. These signatures are then used to trace temporal differences within the landscape. The effects of wildfires on soil geochemistry within a watershed is necessary to investigate elemental signatures between burned and unburned soil, using signatures to trace temporal differences within the landscape. Sampling is needed for the study area to determine if fire signatures can be used to delineate the mobility of trace elements within the fire extent and adjacent area soil.

2.1 Study Area

The study area, designated as the 16-Mile fire, is located within the Delaware State Forest in northeastern Pennsylvania. The Delaware State Forest covers approximately 335 km^2, spanning across four counties, with the fire occurring in Pike and Monroe counties (Figure 2.1). The fire occurred in April of 2016 due to arson, burned 32.5 km^2 (Figure 2.2 & 2.3) over a five day period and destroyed more than 11 structures within the state forest (PA Department of Conservation and Natural Resources, 2016). This wildfire was severe due to the ecological conditions of fuel (tree species) burned, which was caused by climatic circumstances and trees that were diseased by gypsy moths, present during the time of the fire (Callanan *et al*., 2017b). According to Callanan *et al.* (2017), the main climatic conditions that contributed include a drier spring with less than normal precipitation and more temperate winter (Philadelphia/Mount Holly Weather Forecast Office, 2017). Much of the ground vegegation within the fire extent has grown back since, but much of the trees burned are still present (Figure 2.4).

Tree species found within the fire extent and surrounding area consist mainly of *Quercus montana* (chestnut oak) found in association with both *Quercus velutina* (black oak) and *Quercus alba* (white oak) (Callanan *et a*l., 2017b). The wildfire burned near the center of the state forest with a stream, Big Bushkill Creek, bisecting the burn zone. Big Bushkill Creek is a tributary approximately 48 km long that drains into the Delaware River with headwaters from Pecks Pond and Porter Lake (U.S. Geological Survey, 1979). The Big Bushkill Creek and Delaware State Forest are part of the Middle Delaware-Mongaup Brodhead Watershed (Figure 2.5) (United States Department of Agriculture, Natural Resources Conservation Service, 2009). The burned portion of the Delaware State Forest is used for recreational fishing, hunting, hiking and lumber resources.

The bedrock lithology of the of the 16-mile and surrounding area, consists of upper Devonian Long Run and Walcksville members of the Catskill Formation (Figure 2.6) (Harper, 1999). The Catskill Formation is part of the greater Catskill deltaic wedge that was created from the Acadian orogeny (Brezinski *et al*., 2009; Ettensohn, 1985; Harper, 1999). According to Harper (1999), the Catskill wedge is classified in five broad facies with the Catskill formation consisting of deposited sediments of sandstone and mudstone. The parent material for the soil of the 16-Mile Fire is sandstone with much of the soil texture ranging from coarse loamy to loamy skeletal, based on the soil survey (Figure 2.7). Within the 16-mile Fire extent, 28 soil series are present (Figure 2.8), with Morris, Lackawanna, and Arnot series being most dominant (USDA-NRCS, n.d.). Soil development and partial parent material can also be coming from glacial till from the Wisconsin Ice Age which extended south past the Delaware State Forest (PA Department

of Conservation and Natural Resources, 2000). The presence of small boulders of differing lithology from that of the local bedrock in the region is evidence of glacial till.

2.2 Field Methods

Site Nomenclature

To properly site and reference project samples, an identification system was constructed using codes for the following information: event id (16MF), time frame (Tx), sample site (Sx), and horizon/material (xxx) (example: 16MF-T1-S2-O). In this case, the 'time frame' classification indicated each sample's time of collection post-fire. Any sample obtained one month after the 16-Mile Fire was denoted as T1, while those from the eight and ten-month collection were denoted as T2. A total of 11 sites were sampled with six sample sites in the burn area (16MF-T1-A1, 16MF-T1/2-S3, 16MF-T1/2-S4, 16MF-T1/2-S7a/b, and 16MF-T1/2-S10) and 5 sample sites outside the burn area (16MF-T1-S2, 16MF-T1/2-S5, 16MF-T1/2-S9, 16MF-T1-S12, and 16MF-T2-S12) (Table 2.1).

Soil Survey

Soil samples were obtained by excavating short pits, where soil was dug to the B/C horizon, to expose three sides to determine horizon boundaries. Soil sampling was separated based on soil horizons. Sampling also included gathering samples of ash and charred tree in areas, where present post-fire, along with an unburned branch to use as a control for ash samples. A soil pit was also dug to determine the typical soil profile of this region (Figure 2.9). To determine the parent material, a bedrock sample was collected, analyzed and compared to soil samples. GPS coordinates were collected for all sites for use in mapping the area (Figure 2.10) of interest and GIS analysis.

2.3 Laboratory Methods

Bulk soil samples were first placed in 50ml beakers with approximately 40ml of sample and oven dried at 75°C for 48 hours to remove water content within the samples. The dried samples were then crushed with an agate mortar and pestle to fine powder for flux-fusion preparation to be later analyzed by ICP-MS. A modified version of Murray *et al. (2000)* flux-fusion preparation is used at Montclair State University's geochemical laboratory (Hansen & Passchier, 2016). Murray . (2000) uses a tolerance of +/- 0.0005g of lithium metaborate ($LiBO_2$) and an initial concentration of 10% HNO_3, whereas a tolerance of +/- 0.0020 g $LiBO_2$ and an initial concentration of 7% HNO_3 are used in our flux-fusion preparation. Each sample was weighed using an analytical balance on weighing paper with sample masses between 0.0995 – 0.1005 g (tolerance of 0.5%). $LiBO_2$ was then added to the sample with the masses between 0.398 – 0.402 g (tolerance of 0.5%). The sample and $LiBO_2$ were mixed and positioned into a graphite crucible and placed in a muffle furnace for pyrolysis at 1050°C for approximately 35 minutes. After the allocated time, the homogenous molten bead was carefully transferred from the crucible to a Teflon beaker (with magnetic stir rod) filled with 50ml of 7% HNO_3 where the sample would shatter. To further dissolve the bead in HNO_3 the Teflon beakers are placed on magnetic stir plates to completely dissolve the fused sample. The solution was filtered into 60ml Nalgene bottles. The 50ml of 7% HNO_3 dilutes the sample to a factor of 500x. To run the 500x solution on ICP-MS, 0.50ml of the 500x solution was pipetted into 15ml tubes along with 9.5 ml of 2% HNO_3 creating a 10,000x dilution. The 15ml tubes of 10,000x sample solutions along with standards and blank samples were all placed on an auto-sampler rack and were measured on a Thermo Scientific iCAP Q ICP-

MS. To account for variation, all samples were replicated 3 times for major and minor elemental analysis.

Along with the soil samples, ten standards were created from United States Geological Survey (USGS) and National Institute of Standards and Technology (NIST) geochemical standards (Table 2.2), which have known compositions. These standards are used to calibrate the analyzed results testing the calibration of major and minor elements. Three blank samples were made for the entire set of samples to measure for any contamination of the entire flux-fusion preparation through analyzing the samples on the ICP-MS. The blanks contain no sample except $LiBO_2$ measuring between 0.398 – 0.402g. Drift solution was also used during ICP-MS analysis, to account for any fluctuation of the instrument while measuring the samples. Drift solution was measured every fifth sample and used post ICP-MS analysis using an Excel™ post processing spreadsheet. All post processing of ICP-MS data was done using Microsoft Excel 2017™ on a spreadsheet template where the raw data was input in counts per second (CPS). Data was then corrected for drift, measured for accuracy by standards calibration (USGS & NIST), and corrected against blanks. Final data for major elements (SiO_2, TiO_2, AlO_3, Fe_2O_3, MnO, MgO, CaO, Na_2O, K_2O and P_2O_5) were in weight percent whereas minor elements (Sc, V, Cr, Co, Ni, Cu, Zn, Ga, Rb, Sr, Y, Zr, Nb, Cs, Ba, La, Ce, Pr, Nd, Sm, Eu, Gd, Dy, Ho, Er, Tm, Yb, Lu, Hf, Ta, Pb, Th, and U) were finalized in parts per million (ppm). This analysis is similar to those carried out by Burton *et al*. (2016) & Campos *et al*. (2016), who also utilized ICP-MS for trace chemical analysis of ash, soil and water samples from forest fires. Statistical analysis was carried out using IBM's SPSS™.

Analysis of variance (ANOVA) was used to test each individual element for differences in element concentrations in burned versus unburned soils.

2.4 Geographic Information System Analysis

GIS mapping and analysis was accomplished using ESRI ArcMap 10.5 Desktop Advanced, which is the industry standard when conducting geospatial research. All shapefiles and data were downloaded from the Pennsylvania Spatial Data Access website (http://www.pasda.psu.edu/) and imported and organized in ArcMap. To delineate the sub-basin of the Middle Delaware-Mongaup-Brodhead watershed, a 1-meter digital elevation model (DEM) for Pike and Monroe counties were processed in ArcMap using the surficial hydrology modeling toolset. The fill tool was first used to remove any depressions artifacts inherent within the DEM. Flow direction and flow accumulation was then used to determine the direction of surface runoff and to then establish which cells have the most concentration of flow based on flow direction. Accumulation points were then designated within the flow accumulation model to derive the sub basin.

The Revised Universal Soil Loss Equation (RUSLE) is used to model soil loss potential of the 16-Mile extent and surrounding area in ArcMap, soil loss based on the following parameters using methods from Fu *et al*., (2006) and Panagos *et al*., (2015):

$$A = R\ x\ K\ x\ LS\ x\ C\ x\ P$$

Where "R" is the climate factor (rainfall erosivity), "K" is the soil factor (soil erodibility), "LS" is the topography factor (slope length and steepness in degrees), "C" is the land-use factor (cover-management), "P" is support practice (if the land was maintained for crop rotation), and "A" is soil loss by unit measure (tons/ha/yr) (Fu *et al*., 2006). The rainfall erosivity, "R" factor, for this model was based on the average isoerodent values, the

study area has an isoerodent value of 137 ton/hr/yr (Renard *et al*., 1997). The value was added to the sub-basin polygon shapefile and converted to a raster. The soil erodibility, which is based on soil properties (texture and structure), is included in the soil survey. The soil survey maps for Monroe and Pike Counties were converted to raster using the k factor. Slope length and degree factor, "LS" were derived using the flow accumulation map for the sub basin and slope raster (in degrees). To calculate the LS- factor the following formulas were used, where m = 0.4 and n = 1.4 (Fu *et al.*, 2006; Haan *et al.*, 1994):

$$S = \left(\frac{\sin\left(0.01745\ x\ \theta deg\right)}{0.09}\right)^{n}$$

$$L = (m+1)\left(\frac{\lambda_{\mathrm{A}}}{22.1}\right)^{m}$$

The cover-management, "C" factor for this project was derived using a land cover shapefile for the 16-Mile fire and surrounding area, utilizing C factor values by (Fu *et al*., 2006; Haan *et al*., 1994). Typically, C factor values are generated using land cover and NDVI satellite imagery for the area of interest that are site specific. The RUSLE model of this study is experimental due to the unknown land cover from post-fire conditions, hence the use of predetermined C values. The support practice factor "P" is based on the different practices for contouring cropland and rangeland. Since the study area is within a state forest with no disturbance to the soil, we used a value of 1. Once all rasters were created, all the factors were entered in the raster calculator using the RUSLE to calculate soil loss within the sub basin watershed. Validation of the RUSLE model is needed to determine the accuracy of the model results. The slope raster map was employed to validate the RUSLE model by overlaying both rasters and comparing the RULSE model

results to the slope of the 16-Mile Fire extent. Areas of increased slope steepness aligned with the RUSLE model results.

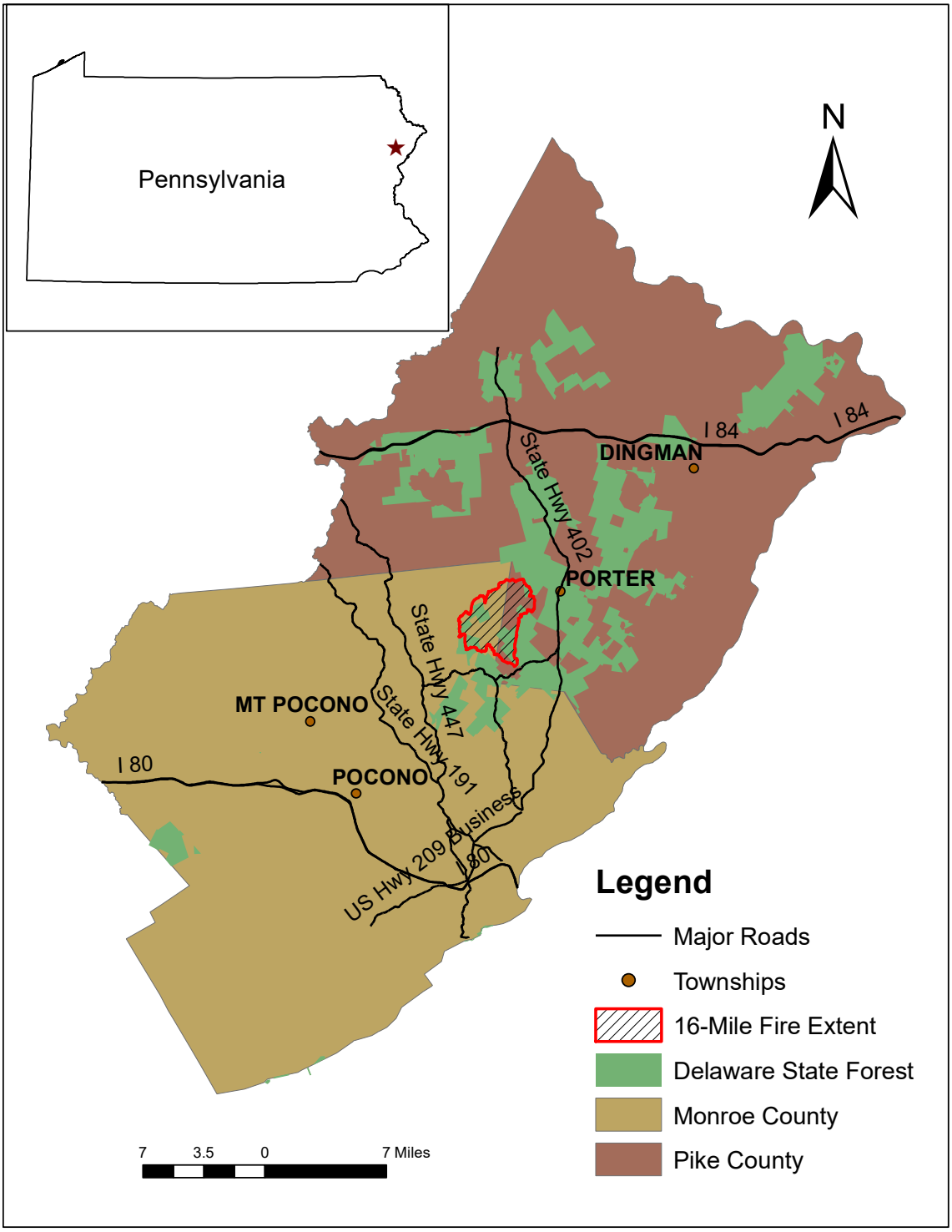

Figure 2.1 Location of 16-mile fire in Monroe and Pike Counties, PA.

Figure 2.2 Aerial view of the 16-Mile Fire (Hazen, 2016).

Figure 2.3 Forestry workers and firefighters trying to control the fire from spreading (Hazen, 2016).

Figure 2.4 Vegetation growing back 10 months after the 16-Mile Fire event (Callanan, 2017).

Figure 2.5 Extent of the Middle Delaware-Mongaup Brodhead Watershed (United States Department of Agriculture Natural Resources Conservation Service, 2009).

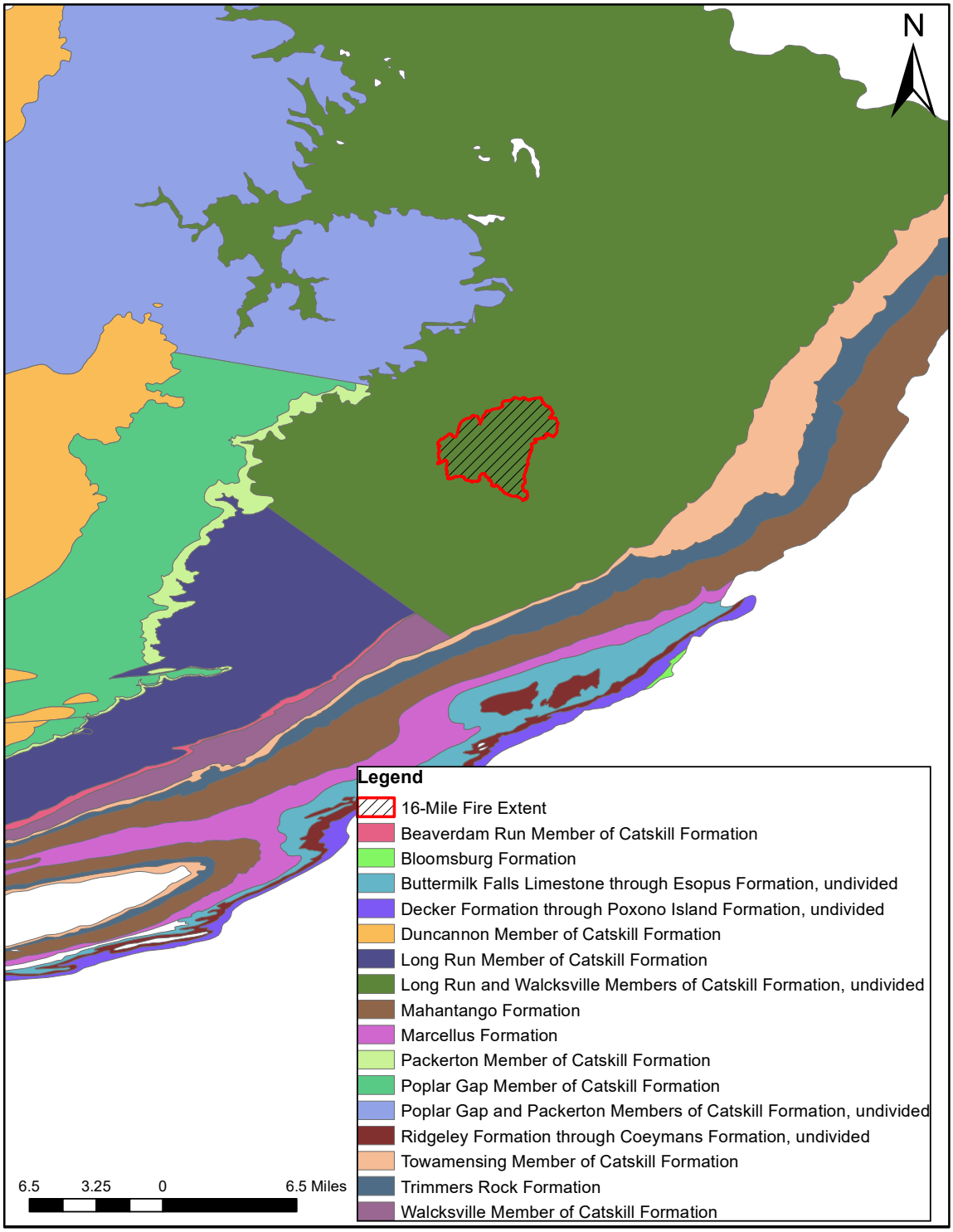

Figure 2.6 Bedrock geology of 16-Mile fire and surrounding region.

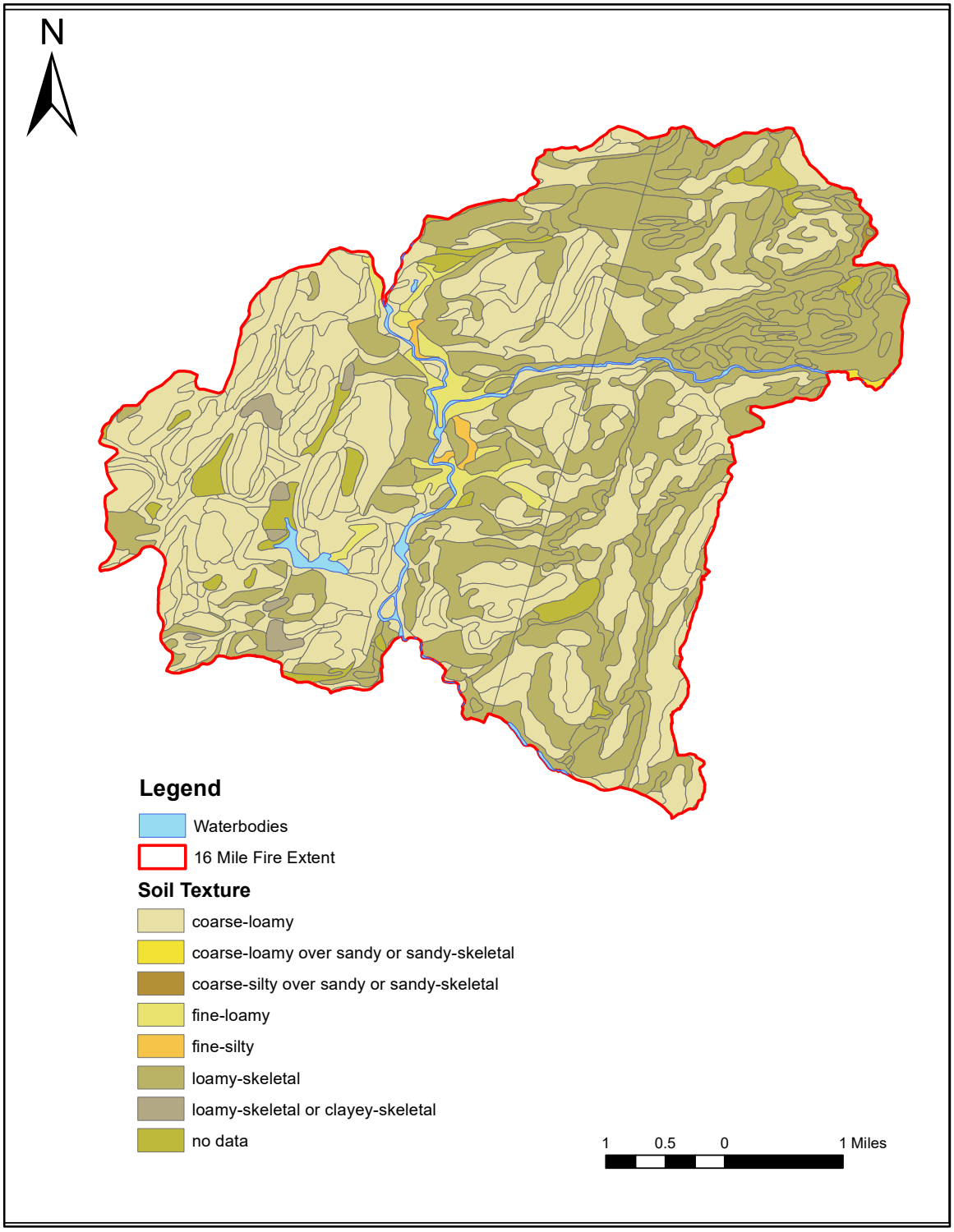

Figure 2.7 Soil texture map of the 16-Mile fire.

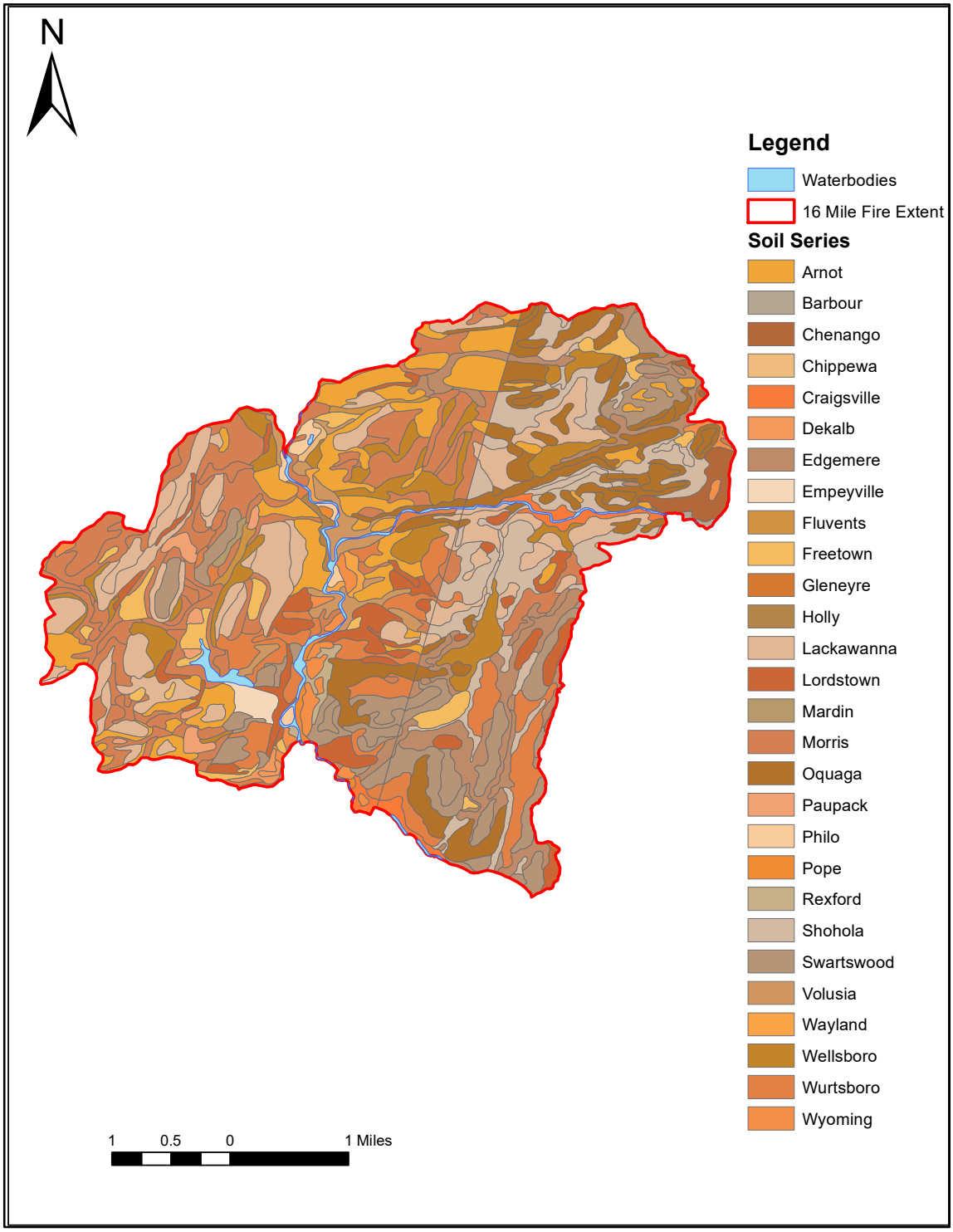

Figure 2.8 Soil series of the 16-Mile fire extent.

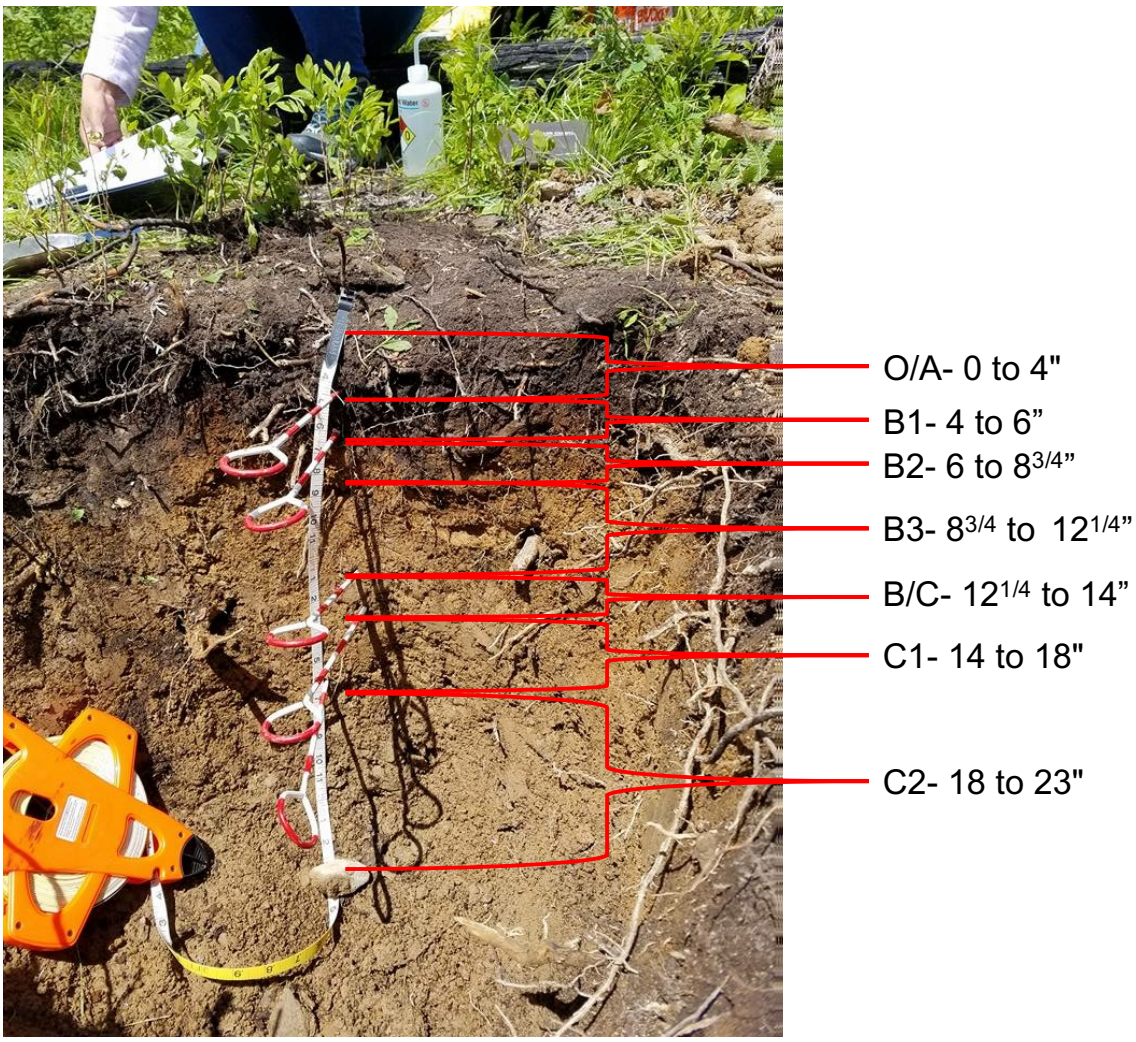

Figure 2.9 Soil profile at Site 10, showing depths of each horizon (Callanan, 2017).

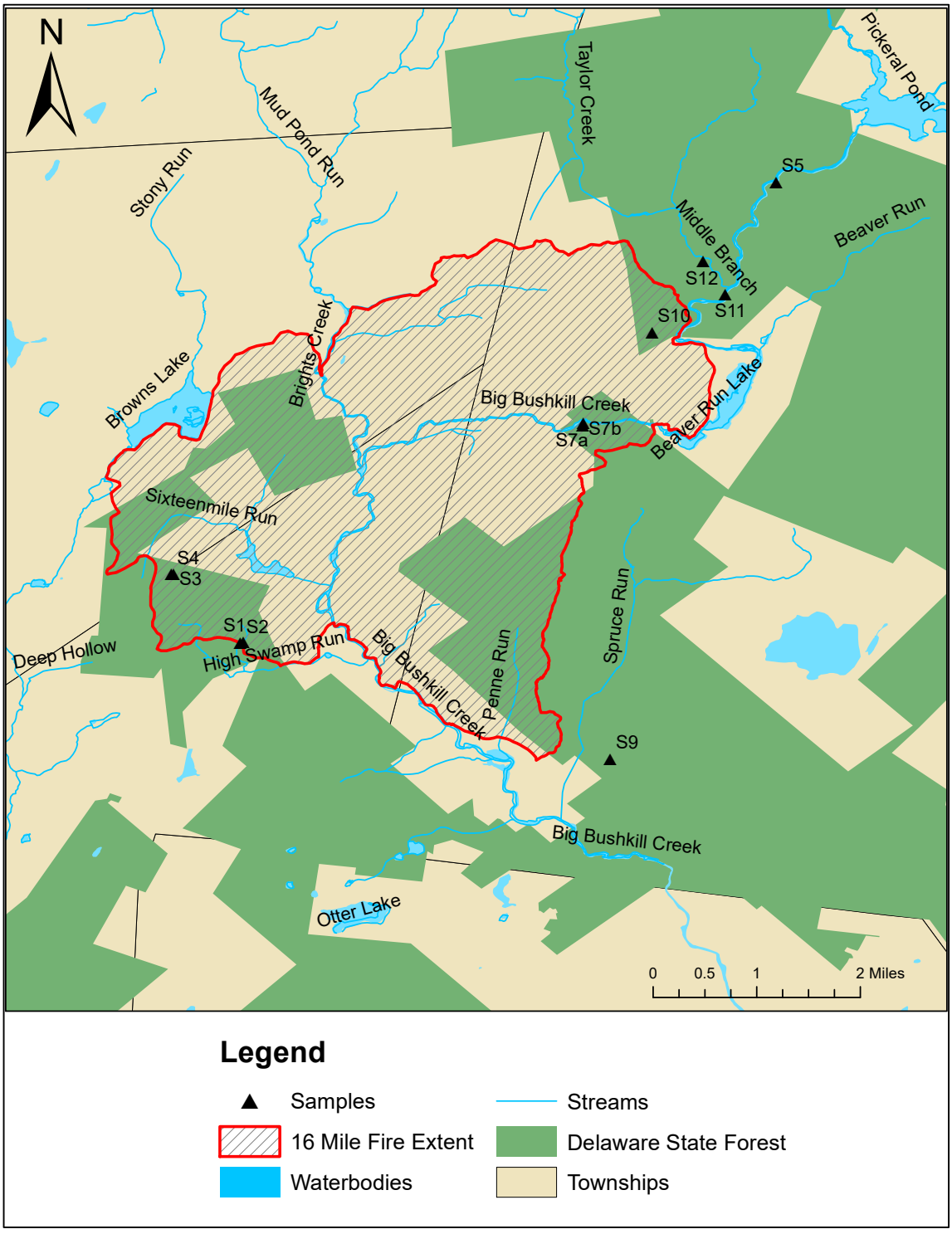

Figure 2.10 Map of 16-Mile fire extent and surrounding area, Delaware State Forest, PA.

Table 2.1 Sampled sites and their properties.

Site #	Sample ID	Date Surveyed	Latitude	Longitude	Elevation (ft)	Horizon	Fire Impact	Soil Series	Notes
1	16MF-T1-A1-ASH	05/18/16	41°10'46.19"N	75°10'20.65"W	1051	ASH	burned	N/A	black ash
2	16MF-T1-S2-OA	05/18/16	41°10'45.42"N	75°10'22.13"W	1060	O/A	unburned	Chippewa-Norwich	
2	16MF-T1-S2-OAB	05/18/16	41°10'45.42"N	75°10'22.13"W	1060	O/A/B	unburned	Chippewa-Norwich	
2	16MF-T1-S3-BBC	05/18/16	41°10'45.42"N	75°10'22.13"W	1060	B/BC	unburned	Chippewa-Norwich	
3	16MF-T1-S3-ASH	05/18/16	41°11'20.48"N	75°10'55.69"W	1198	ASH	burned	N/A	white ash
3	16MF-T1-A3-DUFF	05/18/16	41°11'20.48"N	75°10'55.69"W	1198	Duff	burned	Wellsboro	
3	16MF-T1-S3-O	05/18/16	41°11'20.48"N	75°10'55.69"W	1198	O	burned	Wellsboro	
3	16MF-T1-S3-A	05/18/16	41°11'20.48"N	75°10'55.69"W	1198	A	burned	Wellsboro	
3	16MF-T1-S3-B1	05/18/16	41°11'20.48"N	75°10'55.69"W	1198	B1	burned	Wellsboro	
3	16MF-T1-S3-B2	05/18/16	41°11'20.48"N	75°10'55.69"W	1198	B2	burned	Wellsboro	
3	16MF-T1-A3-TREE	05/18/16	41°11'20.48"N	75°10'55.69"W	1198	Tree	burned	N/A	
3	16MF-T2-S3-O	12/14/16	41°11'20.48"N	75°10'55.69"W	1198	O	burned	Wellsboro	
3	16MF-T2-S3-OA	12/14/16	41°11'20.48"N	75°10'55.69"W	1198	O/A	burned	Wellsboro	
3	16MF-T2-S3-B1	12/14/16	41°11'20.48"N	75°10'55.69"W	1198	B1	burned	Wellsboro	
4	16MF-T1-A4-ASH	05/18/16	41°11'20.20"N	75°10'56.83"W	1217	ASH	burned	N/A	log white ash
4	16MF-T1-S4-OA	05/18/16	41°11'20.20"N	75°10'56.83"W	1217	O/A	burned	Morris	burnt
4	16MF-T2-S4-O	12/14/16	41°11'20.20"N	75°10'56.83"W	1217	O	burned	Morris	burnt O hzn
4	16MF-T2-S4-A	12/14/16	41°11'20.20"N	75°10'56.83"W	1217	A	burned	Morris	burnt A hzn
4	16MF-T2-S4-BE	12/14/16	41°11'20.20"N	75°10'56.83"W	1217	B/E	burned	Morris	
4	16MF-T2-S4-B2	12/14/16	41°11'20.20"N	75°10'56.83"W	1217	B2	burned	Morris	
4	16MF-T2-S4-Tree	12/14/16	41°11'20.20"N	75°10'56.83"W	1217	Tree	burned	N/A	burnt wood
5	16MF-T1-S5-TS	05/18/16	41°14'37.16"N	75°05'52.99"W	1164	TS	unburned	Chenango	
5	16MF-T1-S5-Core15	05/18/16	41°14'37.16"N	75°05'52.99"W	1164	Core	unburned	Chenango	core to 15cm
5	16MF-T2-S5-O	12/14/16	41°14'37.16"N	75°05'52.99"W	1164	O	unburned	Chenango	
5	16MF-T2-S5-A	12/14/16	41°14'37.16"N	75°05'52.99"W	1164	A	unburned	Chenango	
5	16MF-T2-S5-B	12/14/16	41°14'37.16"N	75°05'52.99"W	1164	B	unburned	Chenango	
7A	16MF-T1-S7A-O	06/02/16	41°12'36.23"N	75°07'29.91"W	1086	O	burned	Craigsville-Wyoming	burnt O hzn
7A	16MF-T1-S7A-A	06/02/16	41°12'36.23"N	75°07'29.91"W	1086	A	burned	Craigsville-Wyoming	
7A	16MF-T1-S7A-B1	06/02/16	41°12'36.23"N	75°07'29.91"W	1086	B1	burned	Craigsville-Wyoming	
7A	16MF-T2-S7A-O	01/27/17	41°12'36.23"N	75°07'29.91"W	1086	O	burned	Craigsville-Wyoming	
7A	16MF-T2-S7A-OA	01/27/17	41°12'36.23"N	75°07'29.91"W	1086	O/A	burned	Craigsville-Wyoming	
7A	16MF-T2-S7A-A	01/27/17	41°12'36.23"N	75°07'29.91"W	1086	A	burned	Craigsville-Wyoming	
7A	16MF-T2-S7A-Tree	01/17/17	41°12'34.76"N	75°07'30.10"W	1088	Tree	burned	N/A	burnt wood
7B	16MF-T2-S7B-OA	01/27/17	41°12'34.76"N	75°07'30.10"W	1088	O/A	burned	Craigsville-Wyoming	
7B	16MF-T2-S7B-B	01/27/17	41°12'34.76"N	75°07'30.10"W	1088	B	burned	Craigsville-Wyoming	

Site #	Sample ID	Date Surveyed	Latitude	Longitude	Elevation (ft)	Horizon	Fire Impact	Soil Series	Notes
9	16MF-T1-S9-O	06/02/16	41°09'47.00"N	75°07'16.27"W	1153	O	unburned	Oquaqa	
9	16MF-T1-S9-AC	06/02/16	41°09'47.00"N	75°07'16.27"W	1153	A/C	unburned	Oquaqa	
9	16MF-T2-S9-O	12/14/16	41°09'47.00"N	75°07'16.27"W	1153	O	unburned	Oquaqa	
9	16MF-T2-S9-A	12/14/16	41°09'47.00"N	75°07'16.27"W	1153	A	unburned	Oquaqa	
10	16MF-T1-S10-ASH	06/22/16	41°13'21.62"N	75°06'55.20"W	1204	ASH	burned	N/A	
10	16MF-T1-S10-O1	06/22/16	41°13'21.62"N	75°06'55.20"W	1204	O1	burned	Lordstown-Swartswood	
10	16MF-T1-S10-O2	06/22/16	41°13'21.62"N	75°06'55.20"W	1204	O2	burned	Lordstown-Swartswood	
10	16MF-T1-S10-ASH/Tree	06/22/16	41°13'21.62"N	75°06'55.20"W	1204	ASH/Tree	burned	N/A	
10	16MF-T2-S10-O	01/27/17	41°13'21.62"N	75°06'55.20"W	1204	O	burned	Lordstown-Swartswood	
10	16MF-T2-S10-A	01/27/17	41°13'21.62"N	75°06'55.20"W	1204	A	burned	Lordstown-Swartswood	
10	16MF-T2-S10-B	01/27/17	41°13'21.62"N	75°06'55.20"W	1204	B	burned	Lordstown-Swartswood	
11	16MF-T1-S11-O	06/22/16	41°13'40.98"N	75°06'18.53"W	1134	O	unburned	Edgemore-Shohola	
11	16MF-T1-S11-OA	06/22/16	41°13'40.98"N	75°06'18.53"W	1134	O/A	unburned	Edgemore-Shohola	
11	16MF-T1-S11-B	06/22/16	41°13'40.98"N	75°06'18.53"W	1134	B	unburned	Edgemore-Shohola	
12	16MF-T2-S12-O	01/27/17	41°13'58.65"N	75°06'29.31"W	1163	O	unburned	Wyoming	
12	16MF-T2-S12-A	01/27/17	41°13'58.65"N	75°06'29.31"W	1163	A	unburned	Wyoming	
12	16MF-T2-S12-B	01/27/17	41°13'58.65"N	75°06'29.31"W	1163	B	unburned	Wyoming	
Control	16MF-T2-C-ROCK	12/14/16				ROCK			bedrock (sandstone)
Control	16MF-T2-C-Ash	12/14/16				ASH			control ash

Table 2.2 U.S. Geological Survey and National Institute of Standards and Technology geochemical standards.

USGS/NIST Standards	Location	Type
RGM-1	Califorina	Rhyolite
AGV-2	Oregon	Andesite
MAG-1	Massachusetts	Marine Sediment
G-2	Rhode Island	Granite
BHVO-2	Hawaii	Basalt
SCo-1	Wyoming	Shale
QLO-1	Oregon	Quartz Latite
DNC-1	North Caroline	Dolerite
GSP-2	Colorado	Granodiorite
Montana Soil-2	Montana	Agricultural Soil

3. RESULTS

Field sampling of burned sites within the fire extent showed indication of intense temperatures from the fire. Sites 3, 4, 7A, and 10 all had an ash layer on the surface of the ground. Site 7B was the site of a cabin that was burned during the fire event, which during the second interval of sampling was removed and soil samples were collected to determine differences where structures were present and not present. Ground vegetation was not thick in a number of these areas, except for the presence of various species of oak trees. During the second interval for sampling ash was removed at all of these sites.

3.1 Geochemistry of Major Elements

Major elemental data for all of the sites and control samples are reported in normalized weight percent (Table 3.1) and trace elemental data are reported in ppm (Table 3.2). The following samples (16MF-T1-S3-Ash, 16MF-T1-A3-Duff, 16MF-T1-A1-Ash, 16MF-T1-S10-Ash/Tree, 16MF-T2-S3-Tree, 16MF-T2-S12-Ash, and 16MF-T2-S7A-Tree) had various individual elemental values that were recorded as negative values due to overall low counts per second (cps) from ICP-MS analysis due to blank and drift correction in post processing. To correct for this, negative values were replaced with a zero value. For all major and trace element line graphs (Figures 3.1 through 3.22), solid lines denote horizons in time series 1 and dashed lines denote horizons in time series 2. Complete data tables shown in tables 3.1 and 3.2.

Each site had noticeable concentration in aluminum ranging from 11.81 weight percent at Site 12 to 23.06 weight percent at Site 9. O horizons have the highest amount of aluminum compared to other horizons. Unburned sites also show a slight concentration with calcium that averages out to be 1.87 weight percent and manganese that averages

out to be 1.86 weight percent. The unburned soils show a similar trend in major elements compared to the control rock (Figure 3.11) (sandstone parent material).

The burned sites (Figures 3.2, 3.3, 3.5, 3.6, 3.8) have aluminum concentrations ranging from 11.50 to 46.99 weight percent's, which is similar to the same trend seen in the unburned samples, although some burn samples have higher weight percents. Calcium peaks range from 1.23 to 20.53 weight percent and are seen in all the burned sites. The ash sample from site 3 shows the highest calcium peak (69.29 weight percent) out of all samples analyzed, including the control ash (58.08 weight percent). Site 4 is the only site to show an increase in aluminum and calcium from time series 1 to time series 2. Site 7A & B both show manganese peaks throughout all of the horizon samples in both time series. All other major elements have relatively the same weight percent throughout all of the burned and unburned samples. Unburned calcium samples have an average normalized weight percent of 1.87 with the greatest weight percent 2.87 in sample 16MF-T1-S5-TS. Burned samples have a normalized weight percent of 6.62 with the highest in the soil samples having a weight percent 10.25 in sample 16MF-T2-S4-O (Figure 3.25). Unburned manganese samples have an average weight percent of 0.23 with the greatest weight percent of 1.05 in sample 16MF-T1-S9-AC. Burned soil samples have a normalized weight percent of 1.10, with the highest normalized percent weight in the B horizon of sample 16MF-T1-S7A-B1 (Figure 3.26).

Differences of major elemental concentrations can be seen in horizons from each other at all the sites (Figures 3.1through 3.10). The O, OA horizons have the highest concentrations whereas the A and B horizons have less concentrations. Within the unburned samples where A horizons are present, Site 2 (Figure 3.1), Site 9 (Figure 3.7),

Site 12 (Figure 3.10), the A horizon has slightly higher concentrations of manganese to O horizons of the sites. Within burn sites, aluminum, magnesium, sodium and potassium have consistent concentrations within all of the horizons.

Changes between sites over time is visible on all of the sites (Figures 3.1 through 3.10), but do not have any consistency between sites. Sites 3 (Figure 3.2), Site 5 (Figure 3.4), Site 10 (Figure 3.8) show overlapping concentrations of major elements between time interval one and two.

3.2 Geochemistry of Trace Elements

Most trace elements are negligible with concentrations < 20 ppm. Some elements such as vanadium, nickel, copper, rubidium, strontium, zirconium, barium, lanthanum, cerium and neodymium, have noticeably higher concentrations. Trace amounts of vanadium, rubidium, strontium, yttrium, and lead are found in all the burned and unburned samples. Zirconium is shown as a prominent concentration in all samples, with the burned samples +/- 278 ppm and the unburned slightly higher with an average of 374 ppm. Site 9 (unburned) and site 10 (burned) show a similar trend with zirconium, having a higher concentration in time series 2 compared to time series 1. Copper has higher concentrations in the burned samples averaging 28 ppm, whereas 18 ppm in the unburned samples with site 7B having the highest concentrations. Barium has the highest concentration out of any of the elements present with the higher concentrations found in the burned samples. Site 7A has the highest concentration with 2082 ppm in the B horizon, and 1295 ppm in the O horizon in time series 1. Site 4 shows a trend of increased barium from the OA horizon time series 1 (300 ppm) compared to the O horizon (498 ppm) and A horizon (618 ppm) in time series 2. Ash at site 3 also has a

high concentration of barium compared to all other ash samples except the control ash which has a concentration of 2697 ppm.

Results of copper over time between burned and unburned through the different horizons (Figure 3.27) show higher concentrations of copper in burned sites to unburned sites. Copper concentrations are staying relatively the same between the two sampling time intervals in both burned and unburned samples (Figure 3.28). Concentrations within the horizons are also consistent with burned samples with the exception of site 7B which has higher concentrations in time interval two but cannot be compared since 7B was not sampled during time interval one. Comparing barium concentrations of burned and unburned between the time intervals through the different horizons (Figure 3.29) have higher concentrations within the burned sites to unburned sites. Like copper, barium concentrations remain the same between the two sampling intervals and stay within the horizons (Figure 3.30).

Using rare earth elements (REE's) lanthanum (La), cerium (Ce), praseodymium (Pr), neodymium (Nd), samarium (Sm), europium (Eu), gadolinium (Gd), terbium (Tb), dysprosium (Dy), holmium (Hm), erbium (Er), thulium (Tm), ytterbium (Yb) and lutetium (Lu) results of O horizons site 3, site 9 for the two time intervals were plotted along with the control rock sample. These concentrations were then normalized against upper continental crust values (Taylor & McLennan, 1995) to investigate any differences between the parent material to burned and unburned samples. REE's (Figure 3.24) show similar trends between the control rock and site 9 T1, whereas site 9 T2 has slightly lower values in La, Ce, Pr, Nd, Er, Tm, Yb, and Lu. The burned samples compared to unburned and control rock show an overall lower concentration in all REE's with both burned

having a depletion in Ce. Burned sample site 3 T1 compared to site 3 T2 shows a further depletion of all REE's indicating the fire event has a continuing effect.

3.3 Statistical Analysis

The analysis of variance (ANOVA) tested for statistically significant differences in the element concentrations, comparing two groups, burned soils and unburned soils. A total of 51 samples were included in the analysis. Manganese, calcium, copper, barium, sodium, strontium and tantalum were shown to be statistically significant in differentiating burned versus unburned soils ($p < 0.05$). Copper showed the most clear-cut differentiation. No other elements were statistically significant. The results of the ANOVA test for the significant elements is shown in (Table 3.3).

Table 3.1 Major element concentrations in normalized wt % for all samples.

Site #	Sample Id	Fire Impact	SiO_2	TiO_2	Al_2O_3	Fe_2O_3	MnO	MgO	CaO	Na_2O	K_2O	P_2O_5
1	16MF-T1-A1-ASH	burned	20.83	0.59	38.11	10.31	1.93	5.91	19.61	0.09	0.08	2.53
2	16MF-T1-S2-OA	unburned	68.58	1.11	18.83	4.59	0.05	2.10	2.32	1.09	1.05	0.29
2	16MF-T1-S2-OAB	unburned	64.81	1.15	18.73	8.05	0.06	2.46	1.93	0.69	1.79	0.34
2	16MF-T1-S2-BBC	unburned	76.36	0.88	13.77	4.23	0.03	1.49	1.36	0.84	0.94	0.11
3	16MF-T1-S3-ASH	burned	0.00	0.59	15.94	3.61	5.94	3.02	69.29	0.30	0.00	1.30
3	16MF-T1-A3-DUFF	burned	14.44	0.47	46.99	9.48	2.77	6.42	16.95	0.06	0.00	2.42
3	16MF-T1-S3-O	burned	35.04	1.62	38.68	10.11	0.37	5.20	6.61	1.03	0.09	1.25
3	16MF-T1-S3-A	burned	66.25	1.12	19.23	5.94	0.10	2.35	2.93	0.84	0.72	0.51
3	16MF-T1-S3-B1	burned	76.49	0.83	13.56	4.30	0.08	1.48	1.66	0.68	0.81	0.11
3	16MF-T1-S3-B2	burned	78.68	0.85	12.01	4.27	0.07	1.41	1.23	0.47	0.81	0.18
3	16MF-T1-A3-TREE	burned	24.28	0.84	36.09	8.53	1.64	4.79	20.53	0.18	0.97	2.15
3	16MF-T2-S3-O	burned	52.89	0.86	28.59	6.99	0.60	3.52	5.83	0.16	0.01	0.55
3	16MF-T2-S3-OA	burned	75.96	0.88	14.38	4.12	0.05	1.58	1.81	0.35	0.70	0.17
3	16MF-T2-S3-B1	burned	78.77	0.73	12.39	3.93	0.05	1.36	1.42	0.49	0.74	0.14
4	16MF-T1-A4-ASH	burned	76.50	0.68	11.50	3.46	0.22	1.44	4.78	0.30	0.71	0.42
4	16MF-T1-S4-OA	burned	76.77	0.80	12.31	3.59	0.20	1.52	3.58	0.45	0.43	0.35
4	16MF-T2-S4-O	burned	52.28	1.13	23.50	6.58	1.04	3.17	10.25	0.39	0.57	1.08
4	16MF-T2-S4-A	burned	68.03	0.80	14.34	4.29	0.72	1.90	8.20	0.38	0.61	0.72
4	16MF-T2-S4-BE	burned	78.72	0.78	12.92	3.30	0.05	1.46	1.86	0.34	0.48	0.10
4	16MF-T2-S4-B2	burned	78.21	0.78	12.38	4.40	0.07	1.43	1.37	0.45	0.69	0.22
4	16MF-T2-S4-TREE	burned	13.13	0.45	56.41	10.92	0.45	6.95	11.63	0.06	0.00	0.00
5	16MF-T1-S5-TS	unburned	65.72	0.97	18.21	6.66	0.38	2.29	2.87	1.11	1.36	0.41
5	16MF-T1-S5-CORE15	unburned	74.31	0.78	12.78	6.35	0.47	1.37	1.32	0.89	1.61	0.12
5	16MF-T2-S5-O	unburned	63.46	0.87	19.46	8.24	0.43	2.35	2.63	0.67	1.43	0.47
5	16MF-T2-S5-A	unburned	74.46	0.81	14.84	4.57	0.06	1.61	1.60	0.81	1.09	0.14
5	16MF-T2-S5-B	unburned	77.46	0.81	12.05	5.10	0.08	1.35	1.16	0.93	1.03	0.05
7a	16MF-T1-S7A-O	burned	64.56	0.74	14.51	7.02	2.10	1.69	7.08	0.61	1.06	0.62
7a	16MF-T1-S7A-A	burned	71.24	0.77	13.75	7.03	1.86	1.67	1.60	0.86	0.88	0.34
7a	16MF-T1-S7A-B1	burned	68.02	0.83	14.34	7.92	3.58	1.68	1.48	0.80	1.03	0.33
7a	16MF-T2-S7A-O	burned	70.14	0.81	13.40	7.06	2.21	1.57	2.83	0.72	0.84	0.43
7a	16MF-T2-S7A-OA	burned	68.69	0.84	14.39	8.18	2.76	1.65	1.51	0.76	0.89	0.33
7a	16MF-T2-S7A-A	burned	71.56	0.81	13.76	7.26	1.60	1.66	1.41	0.80	0.86	0.28
7a	16MF-T2-S7A-TREE	burned	13.02	0.46	55.89	10.94	0.30	6.82	12.10	0.10	0.34	0.02
7b	16MF-T2-S7B-OA	burned	66.95	0.92	16.02	8.21	2.07	1.91	1.70	0.81	0.99	0.41
7b	16MF-T2-S7B-B	burned	68.63	0.88	15.26	8.44	1.28	1.87	1.35	0.77	1.22	0.29

Site #	Sample Id	Fire Impact	SiO_2	TiO_2	Al_2O_3	Fe_2O_3	MnO	MgO	CaO	Na_2O	K_2O	P_2O_5
9	16MF-T1-S9-O	unburned	60.73	1.07	23.06	6.67	0.58	2.86	2.72	0.73	0.70	0.89
9	16MF-T1-S9-AC	unburned	69.59	0.78	16.29	5.88	1.05	1.95	1.74	0.65	1.45	0.62
9	16MF-T2-S9-O	unburned	75.03	0.79	14.11	4.67	0.23	1.74	1.66	0.54	1.02	0.21
9	16MF-T2-S9-A	unburned	75.05	0.83	13.58	4.88	0.35	1.76	1.72	0.67	0.92	0.23
10	16MF-T1-S10-ASH	burned	67.79	0.96	17.30	6.01	0.40	2.15	3.29	0.50	1.00	0.61
10	16MF-T1-S10-O1	burned	62.10	1.00	21.13	6.11	0.34	2.66	4.74	0.52	0.89	0.52
10	16MF-T1-S10-O2	burned	70.93	1.05	16.51	5.75	0.05	1.86	1.87	0.51	1.25	0.22
10	16MF-T1-S10-ASH/TREE	burned	12.93	0.46	55.14	10.59	0.92	7.19	11.94	0.04	0.00	0.79
10	16MF-T2-S10-O	burned	69.22	0.96	16.15	4.73	0.48	2.03	4.17	0.76	1.05	0.44
10	16MF-T2-S10-A	burned	77.58	0.85	12.07	5.06	0.04	1.38	1.50	0.53	0.81	0.18
10	16MF-T2-S10-B	burned	74.89	0.83	13.43	5.69	0.06	1.53	1.37	0.55	1.47	0.18
11	16MF-T1-S11-O	unburned	65.25	1.12	20.56	6.31	0.17	2.38	2.69	0.56	0.54	0.41
11	15MF-T1-S11-OA	unburned	71.82	0.97	16.82	5.12	0.05	1.82	1.99	0.53	0.69	0.19
11	16MF-T1-S11-B	unburned	73.72	0.91	14.26	5.80	0.05	1.64	1.46	0.62	1.41	0.13
12	16MF-T2-S12-O	unburned	77.78	0.94	12.81	3.84	0.04	1.51	1.71	0.51	0.67	0.19
12	16MF-T2-S12-A	unburned	78.94	0.91	11.81	4.18	0.06	1.30	1.42	0.40	0.80	0.17
12	16MF-T2-S12-B	unburned	76.08	0.73	13.29	5.20	0.05	1.41	1.42	0.44	0.99	0.39
control	16MF-T2-C-ROCK		73.50	0.87	13.37	5.78	0.14	1.99	1.31	0.85	2.08	0.10
control	16MF-T2-C-ASH		6.95	0.34	22.87	4.45	2.66	3.93	58.08	0.04	0.00	0.68

Table 3.2 Trace element concentrations in ppm.

Site #	Sample Id	Fire Impact	Sc	V	Cr	Co	Ni	Cu	Ga	Rb	Sr	Y	Zr	Nb	Cs	Ba	Hf	Pb	Th	U
1	16MF-T1-A1-ASH	burned	1.709	21.079	14.422	7.997	17.742	28.832	9.002	16.589	155.197	7.964	8.058	1.298	1.141	598.592	0.306	18.202	0.447	0.328
2	16MF-T1-S2-OA	unburned	5.299	60.115	29.826	2.610	13.244	14.533	12.213	46.974	54.508	22.240	241.799	5.863	3.334	208.779	5.713	16.941	6.314	1.915
2	16MF-T1-S2-OAB	unburned	9.527	98.061	57.219	7.583	23.903	29.101	16.787	101.077	65.593	28.808	227.662	16.442	6.294	321.100	6.176	31.222	10.982	2.949
2	16MF-T1-S2-BBC	unburned	8.154	72.145	35.896	3.121	9.626	11.686	15.081	72.233	54.586	25.993	409.078	15.131	4.616	233.487	10.070	36.729	8.155	2.188
3	16MF-T1-S3-ASH	burned	0.614	26.020	9.237	3.054	22.849	52.046	7.048	9.129	1100.500	5.552	24.304	0.245	0.400	1567.898	0.632	21.617	0.661	0.206
3	16MF-T1-A3-DUFF	burned	0.983	15.152	6.523	2.883	11.387	25.704	8.258	9.033	70.751	7.589	1.734	0.253	0.324	527.337	0.069	15.704	0.000	0.112
3	16MF-T1-S3-O	burned	2.325	32.971	19.484	2.903	15.854	19.388	8.305	18.974	39.222	13.440	126.024	1.552	1.109	145.361	2.994	16.749	2.455	0.859
3	16MF-T1-S3-A	burned	5.204	57.582	34.559	3.935	22.984	43.107	11.632	41.655	50.577	24.151	270.607	6.740	2.415	174.847	6.697	20.413	5.473	2.036
3	16MF-T1-S3-B1	burned	6.359	56.152	26.812	4.089	10.621	15.390	14.026	59.808	23.147	26.667	428.789	13.858	3.150	175.948	10.132	52.629	6.972	2.320
3	16MF-T1-S3-B2	burned	6.081	48.625	31.534	5.768	11.176	9.902	10.731	58.327	35.864	26.373	399.355	11.238	3.457	170.134	9.425	21.790	7.951	2.301
3	16MF-T1-A3-TREE	burned	2.127	29.585	17.834	2.650	14.796	34.924	9.203	24.154	158.351	9.012	53.555	3.156	1.226	596.967	1.394	15.445	1.136	0.567
3	16MF-T2-S3-O	burned	2.365	25.325	13.768	3.060	11.659	16.078	9.604	19.926	33.747	12.271	119.705	7.849	1.096	311.083	3.108	23.580	1.726	0.732
3	16MF-T2-S3-OA	burned	6.092	56.569	28.530	3.372	12.204	16.536	14.755	51.346	24.333	24.982	357.778	12.506	2.441	169.246	8.925	56.955	7.778	2.205
3	16MF-T2-S3-B1	burned	6.409	51.949	28.912	5.814	14.485	15.121	12.955	58.023	24.232	29.408	479.947	14.022	3.075	188.571	11.714	27.512	7.917	2.416
4	16MF-T1-A4-ASH	burned	5.889	47.113	27.287	5.090	18.147	34.443	12.879	69.206	161.695	23.298	419.395	13.712	3.489	374.213	10.365	48.875	7.076	2.211
4	16MF-T1-S4-OA	burned	4.811	49.159	27.190	2.604	16.150	32.363	11.086	35.326	101.429	21.930	504.424	13.579	2.158	300.632	12.087	40.007	6.016	2.054
4	16MF-T2-S4-O	burned	3.122	30.375	25.911	3.183	21.205	42.298	8.912	32.522	141.446	14.777	152.766	6.179	2.145	498.045	3.981	16.460	3.367	1.177
4	16MF-T2-S4-A	burned	4.842	46.788	34.830	3.781	26.281	58.226	11.809	46.590	212.173	20.992	269.883	10.865	2.908	618.438	7.058	24.175	5.712	1.887
4	16MF-T2-S4-BE	burned	5.575	51.569	27.305	2.748	11.049	16.414	13.839	45.485	34.153	23.022	324.636	12.411	2.749	174.165	8.126	63.671	6.240	2.130
4	16MF-T2-S4-B2	burned	5.707	52.560	30.375	5.591	17.165	20.045	12.376	56.681	41.772	27.636	359.739	11.658	3.528	178.281	8.574	22.045	8.199	2.182
4	16MF-T2-S4-TREE	burned	0.788	12.606	4.630	1.631	7.450	7.918	8.514	3.665	18.640	5.336	0.000	0.000	0.020	42.096	0.000	16.331	0.000	0.035
5	16MF-T1-S5-TS	unburned	6.075	58.870	30.808	8.992	19.676	24.812	12.103	61.693	67.396	21.327	230.900	7.894	4.221	368.756	5.720	21.404	6.304	2.065
5	16MF-T1-S5-CORE15	unburned	10.116	83.233	44.836	24.006	12.925	14.972	16.856	104.831	49.703	30.152	459.515	17.140	6.902	446.997	11.990	49.311	11.522	3.398
5	16MF-T2-S5-O	unburned	5.876	58.142	28.669	12.713	16.659	16.120	12.877	53.793	36.710	22.355	187.126	7.481	3.761	348.908	4.742	65.255	5.240	1.962
5	16MF-T2-S5-A	unburned	8.839	71.870	39.097	5.318	13.740	13.142	16.377	55.417	41.543	29.787	448.597	14.262	4.882	314.813	11.412	81.867	9.265	3.233
5	16MF-T2-S5-B	unburned	8.188	65.910	38.277	5.521	9.534	5.547	14.417	64.364	55.956	26.936	336.808	15.678	5.428	284.678	8.503	29.704	9.814	2.630
7a	16MF-T1-S7A-O	burned	7.321	66.219	34.731	16.599	29.800	38.323	14.418	95.924	252.538	23.725	332.719	13.642	4.680	1295.313	8.966	81.234	8.778	2.786
7a	16MF-T1-S7A-A	burned	9.367	76.121	45.571	17.236	24.726	25.031	15.203	68.984	59.699	31.252	431.681	14.785	4.568	796.512	11.135	38.626	10.362	3.573
7a	16MF-T1-S7A-B1	burned	10.217	77.845	45.588	28.493	35.668	26.305	16.481	86.745	57.443	38.646	380.267	17.354	6.141	2082.880	9.730	28.189	12.772	4.594
7a	16MF-T2-S7A-O	burned	7.585	65.808	36.531	17.804	22.593	25.061	13.818	82.686	100.234	25.672	325.554	14.594	5.051	906.419	8.475	25.714	9.906	3.365
7a	16MF-T2-S7A-OA	burned	10.991	78.247	45.490	24.818	31.133	32.394	17.155	84.551	56.674	38.844	429.488	16.279	6.286	1112.318	10.586	41.216	13.961	4.462
7a	16MF-T2-S7A-A	burned	8.944	67.851	40.589	14.649	24.326	28.313	14.908	77.130	50.401	30.469	396.771	15.055	5.612	723.492	10.074	28.294	10.729	3.897
7a	16MF-T2-S7A-TREE	burned	0.765	19.291	4.524	1.612	11.140	13.248	7.889	13.825	20.219	5.117	0.000	0.000	0.190	27.602	0.000	15.297	0.000	0.041
7b	16MF-T2-S7B-OA	burned	9.842	77.920	48.543	21.901	29.936	55.203	16.474	77.344	55.207	39.520	311.035	15.360	6.669	763.528	7.923	56.021	12.155	4.354
7b	16MF-T2-S7B-B	burned	14.366	91.909	59.036	24.513	31.519	39.557	18.747	92.708	59.097	48.474	445.237	16.457	8.186	636.417	11.646	33.996	14.740	6.421

Site #	Sample Id	Fire Impact	Sc	V	Cr	Co	Ni	Cu	Ga	Rb	Sr	Y	Zr	Nb	Cs	Ba	Hf	Pb	Th	U
9	16MF-T1-S9-O	unburned	4.329	38.283	21.299	6.020	18.506	24.498	9.443	34.081	33.104	27.058	209.073	7.304	1.952	193.720	5.556	17.263	4.710	1.777
9	16MF-T1-S9-AC	unburned	9.143	67.373	38.903	13.033	29.150	36.153	15.565	76.355	31.724	40.380	319.059	12.369	4.649	370.290	8.334	70.749	10.779	3.739
9	16MF-T2-S9-O	unburned	6.746	55.539	33.077	7.274	21.360	17.880	13.864	63.248	26.772	31.366	388.345	12.771	3.340	345.072	9.937	53.066	8.931	2.687
9	16MF-T2-S9-A	unburned	6.292	56.024	37.387	7.548	30.294	37.430	12.796	57.085	48.147	33.710	469.386	12.978	3.449	302.854	11.275	35.449	8.758	2.817
10	16MF-T1-S10-ASH	burned	5.167	52.021	31.683	3.366	16.578	28.154	11.872	59.502	66.184	17.200	227.321	11.427	3.712	305.429	5.900	18.111	5.744	1.690
10	16MF-T1-S10-O1	burned	4.250	45.402	25.689	3.447	14.520	22.322	12.106	35.533	56.989	15.975	214.396	6.366	2.170	271.241	5.304	26.454	4.669	1.476
10	16MF-T1-S10-O2	burned	5.743	63.099	33.154	2.490	14.480	30.829	13.524	52.323	44.383	22.658	285.680	14.079	3.125	307.166	7.638	26.362	8.075	2.201
10	16MF-T1-S10-ASH/TREE	burned	0.748	12.730	5.034	1.698	7.871	12.140	7.936	6.071	31.531	5.146	0.000	0.000	0.148	111.185	0.000	15.347	0.000	0.056
10	16MF-T2-S10-O	burned	4.753	47.649	27.923	2.921	11.910	28.426	11.973	47.495	84.806	20.038	364.132	9.538	3.039	302.936	9.224	26.660	6.437	1.888
10	16MF-T2-S10-A	burned	6.647	62.757	33.140	2.509	13.575	21.307	14.264	69.174	49.138	26.633	509.662	15.813	3.879	173.882	12.643	33.434	8.512	2.618
10	16MF-T2-S10-B	burned	9.320	79.070	46.071	9.194	20.117	19.465	16.011	87.735	39.767	27.839	501.502	16.360	5.228	321.202	12.627	35.177	11.521	3.167
11	16MF-T1-S11-O	unburned	4.630	49.186	29.269	2.496	11.228	12.000	12.006	31.553	44.440	17.808	175.903	11.178	2.550	191.594	4.859	20.445	5.689	1.674
11	15MF-T1-S11-OA	unburned	7.149	73.823	36.269	3.524	13.630	15.191	16.170	39.906	32.590	25.885	392.524	13.705	2.790	199.454	9.888	37.912	8.324	2.654
11	16MF-T1-S11-B	unburned	9.766	84.780	52.549	8.365	22.521	15.079	16.976	74.859	42.176	31.370	465.682	18.610	5.315	354.786	12.167	27.423	12.976	3.540
12	16MF-T2-S12-O	unburned	5.296	50.000	30.041	2.446	13.586	20.062	12.035	51.253	43.582	22.180	447.110	14.410	3.055	160.695	10.800	37.538	7.392	2.342
12	16MF-T2-S12-A	unburned	7.211	55.857	28.992	3.165	8.744	9.185	13.571	64.975	24.974	26.768	776.425	17.625	3.269	182.464	22.219	33.844	9.478	3.267
12	16MF-T2-S12-B	unburned	7.384	61.755	34.041	5.904	15.572	13.008	14.559	65.011	26.774	23.337	548.037	14.776	3.942	238.597	13.973	27.668	9.103	2.687
control	16MF-T2-C-ROCK		10.728	76.342	47.306	12.690	26.032	128.707	16.414	114.170	62.820	32.908	383.500	17.196	5.266	320.954	9.602	22.092	12.109	2.436
control	16MF-T2-C-ASH		0.815	12.262	6.073	3.736	35.224	27.506	8.395	9.850	714.120	12.904	0.000	0.152	0.131	2697.344	0.000	24.287	0.000	0.065

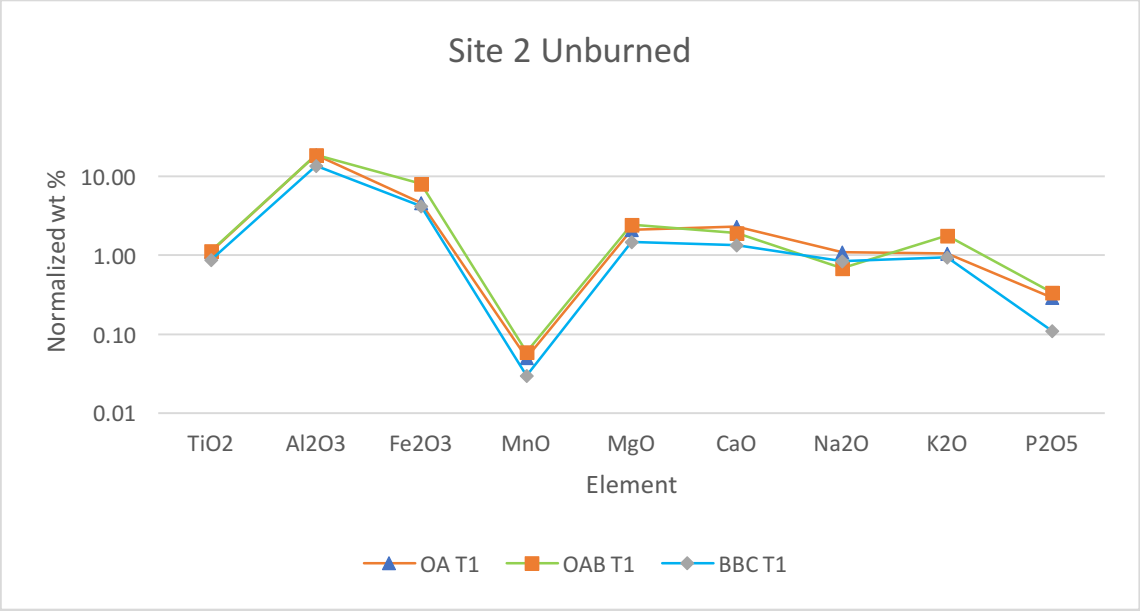

Figure 3.1 Elemental concentrations of Ti, Al, Fe, Mn, Mg, Ca, Na, K, and P at Site 2.

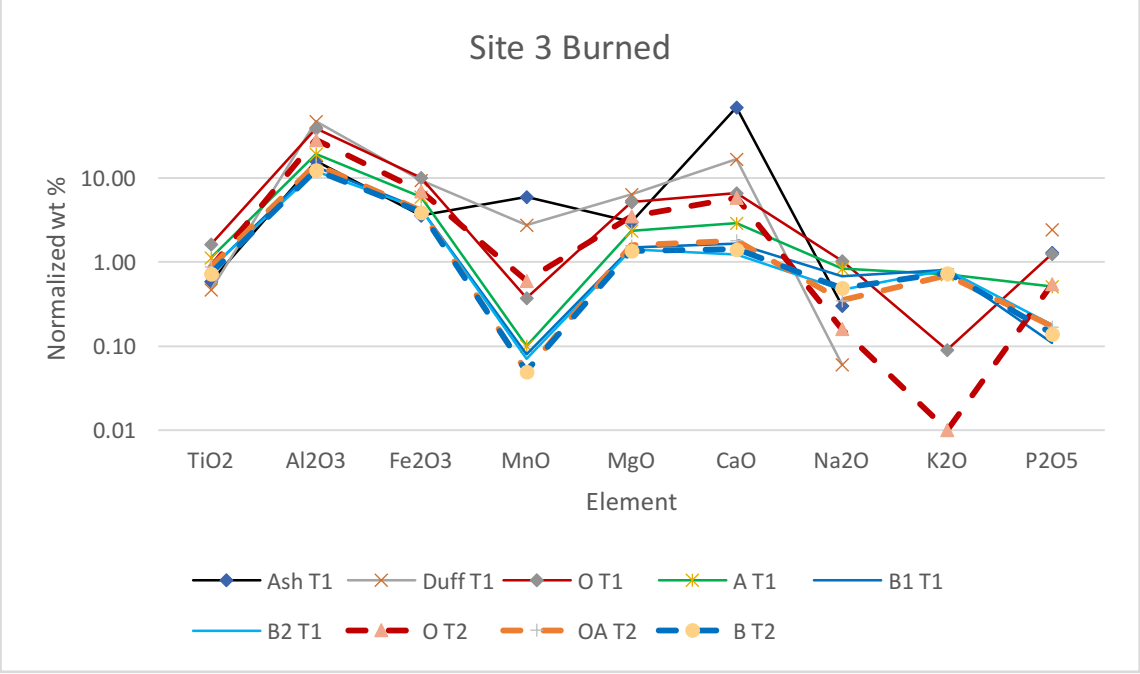

Figure 3.2 Elemental concentrations of Ti, Al, Fe, Mn, Mg, Ca, Na, K, and P at Site 3.

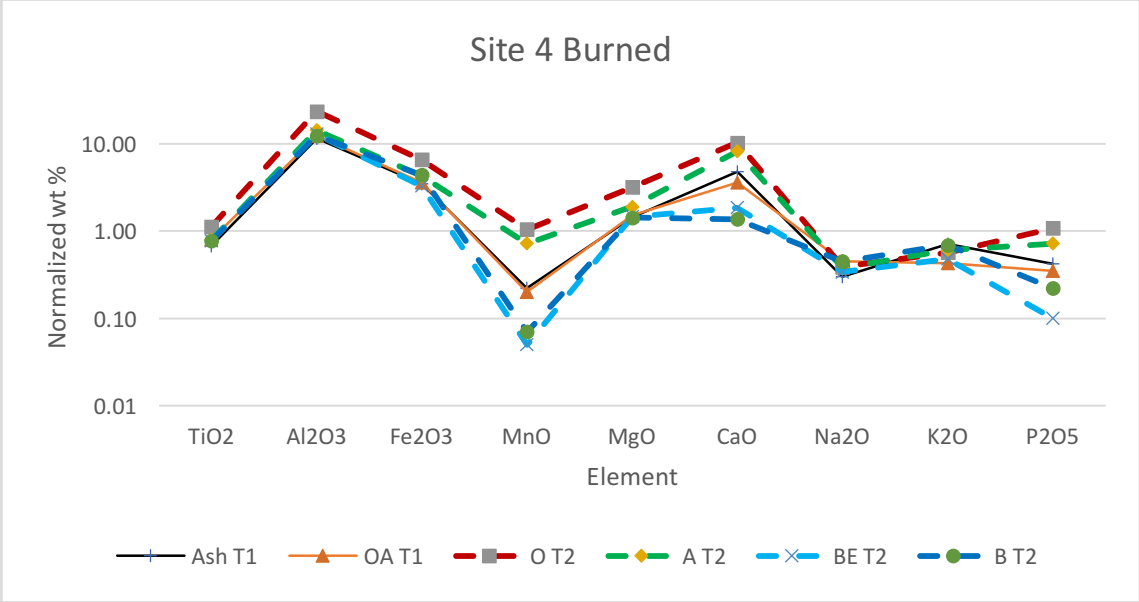

Figure 3.3 Elemental concentrations of Ti, Al, Fe, Mn, Mg, Ca, Na, K, and P at Site 4.

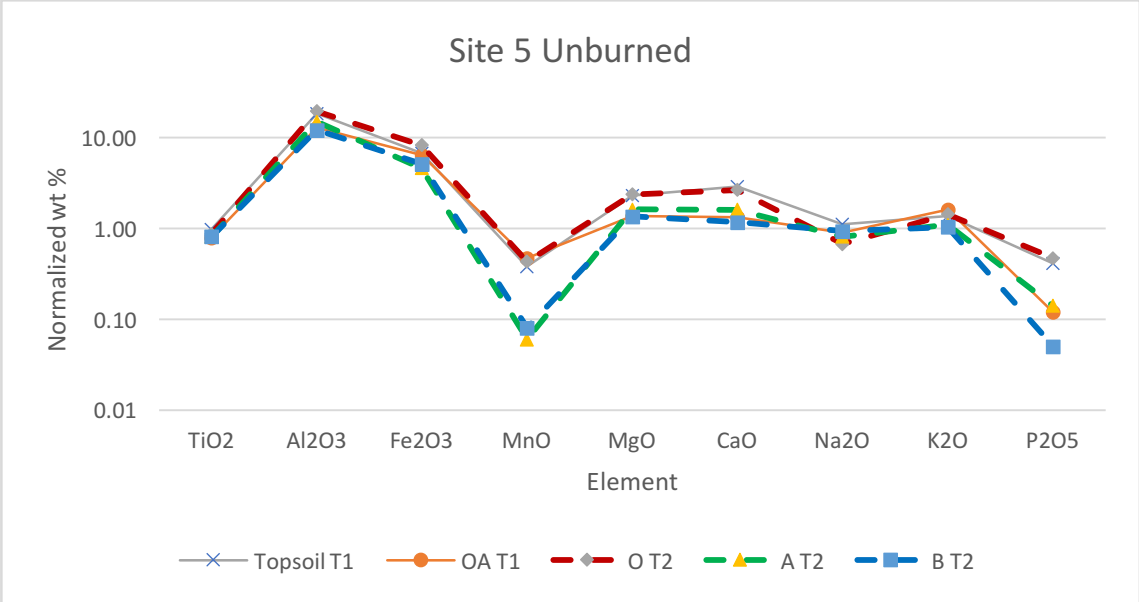

Figure 3.4 Elemental concentrations of Ti, Al, Fe, Mn, Mg, Ca, Na, K, and P at Site 5.

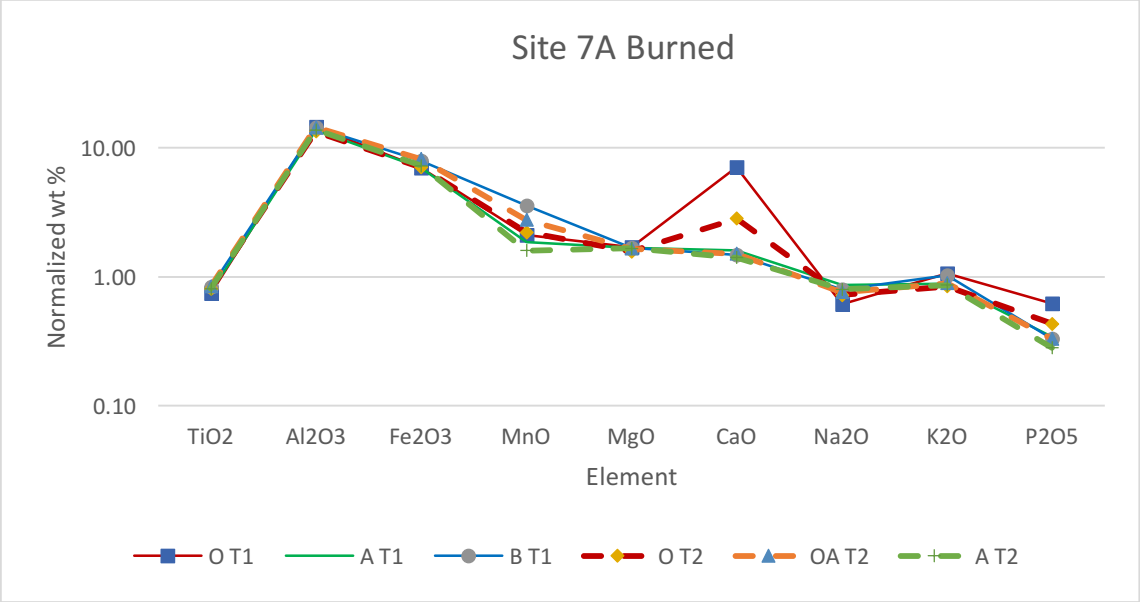

Figure 3.5 Elemental concentrations of Ti, Al, Fe, Mn, Mg, Ca, Na, K, and P at Site 7A.

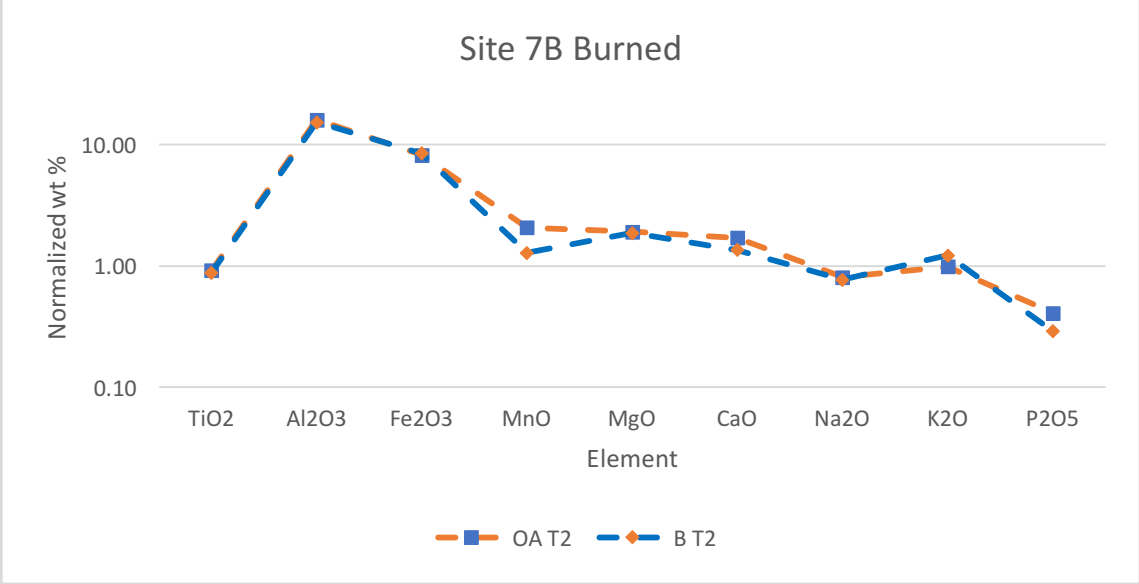

Figure 3.6 Elemental concentrations of Ti, Al, Fe, Mn, Mg, Ca, Na, K, and P at Site 7B.

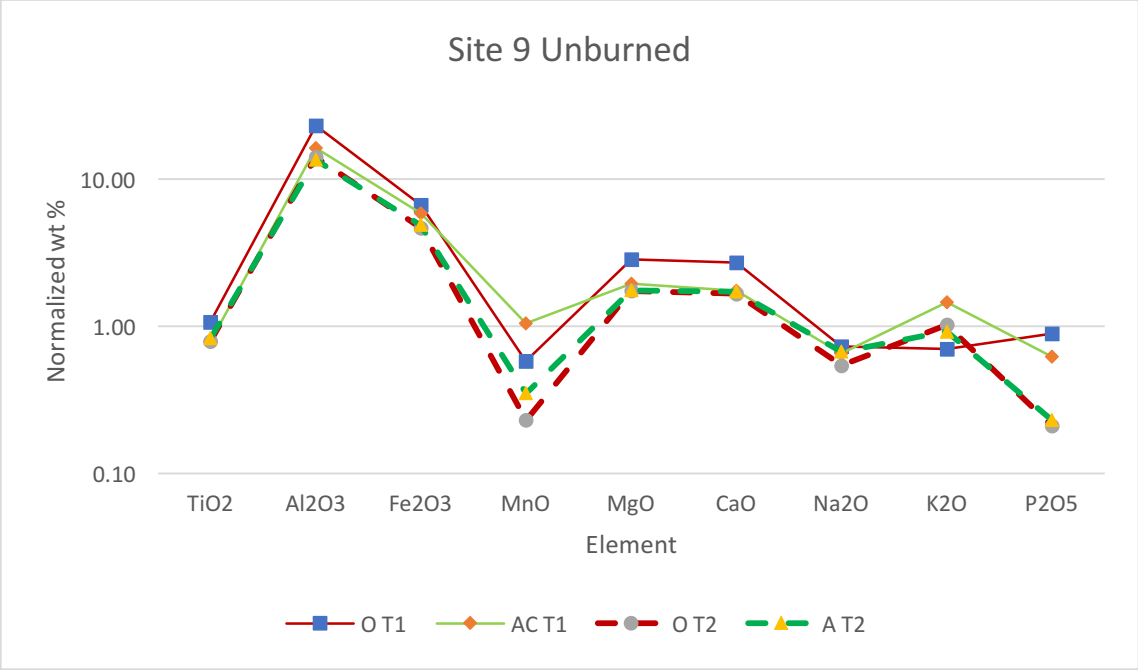

Figure 3.7 Elemental concentrations of Ti, Al, Fe, Mn, Mg, Ca, Na, K, and P at Site 9.

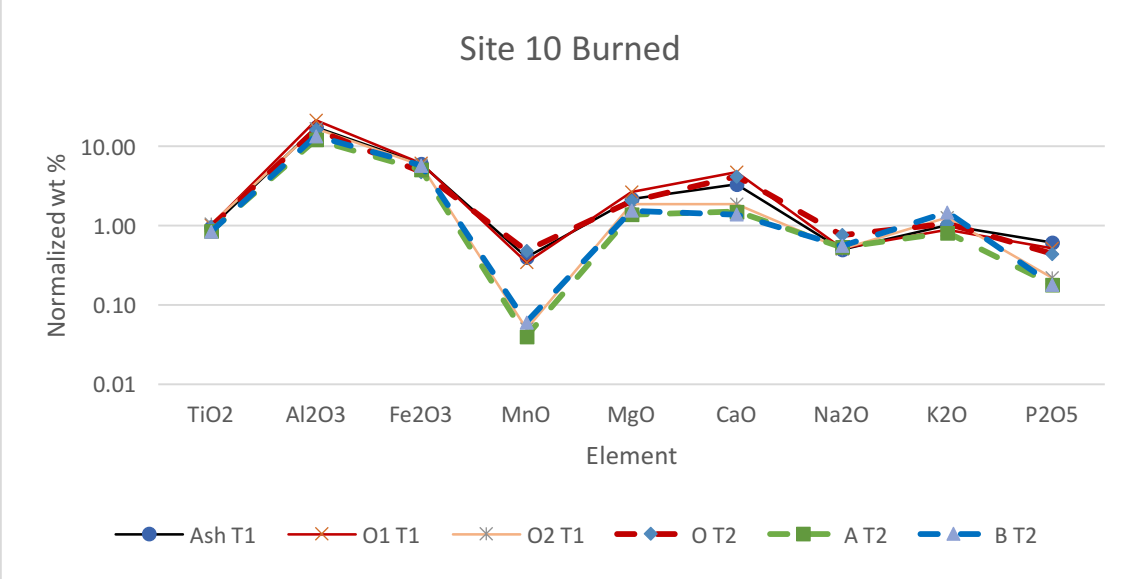

Figure 3.8 Elemental concentrations of Ti, Al, Fe, Mn, Mg, Ca, Na, K, and P at Site 10.

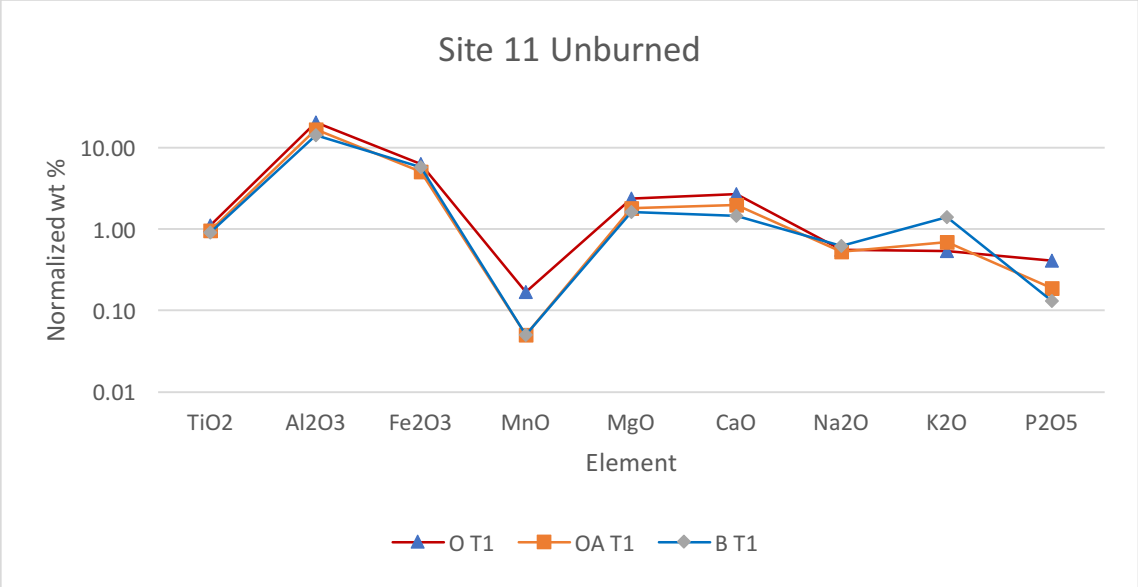

Figure 3.9 Elemental concentrations of Ti, Al, Fe, Mn, Mg, Ca, Na, K, and P at Site 11.

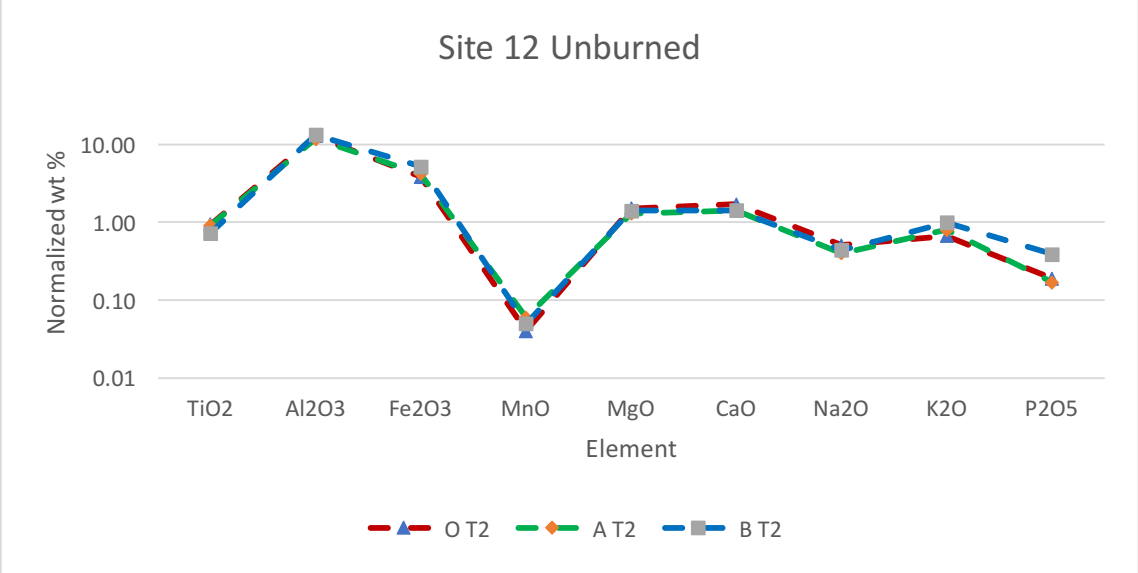

Figure 3.10 Elemental concentrations of Ti, Al, Fe, Mn, Mg, Ca, Na, K, and P at Site 12.

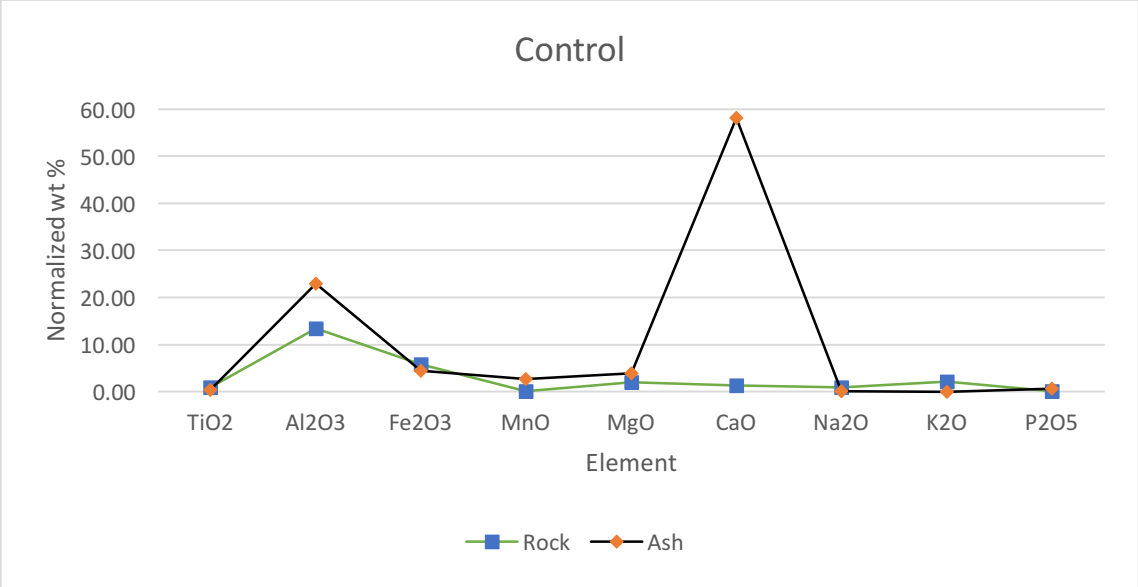

Figure 3.11 Elemental concentrations of Ti, Al, Fe, Mn, Mg, Ca, Na, K, and P for control ash and rock.

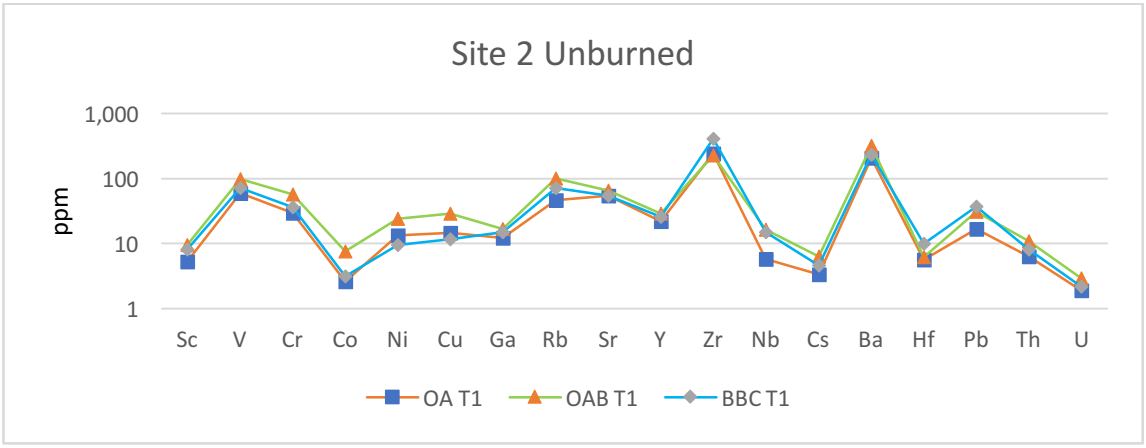

Figure 3.12 Elemental concentrations of Sc, V, Cr, Co, Ni, Cu, Ga, Rb, Sr, Y, Zr, Nb, Cs, Ba, Hf, Pb, Th and U for Site 2

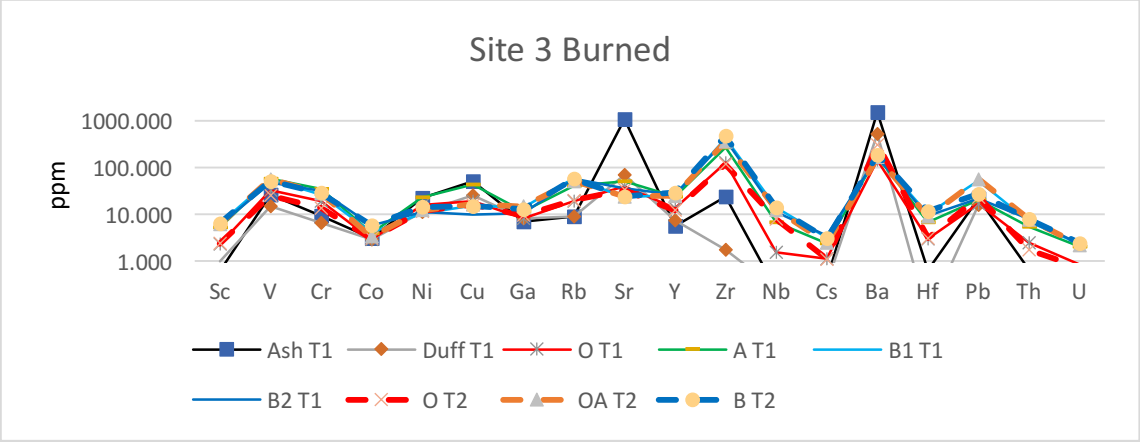

Figure 3.13 Elemental concentrations of Sc, V, Cr, Co, Ni, Cu, Ga, Rb, Sr, Y, Zr, Nb, Cs, Ba, Hf, Pb, Th and U for Site 3.

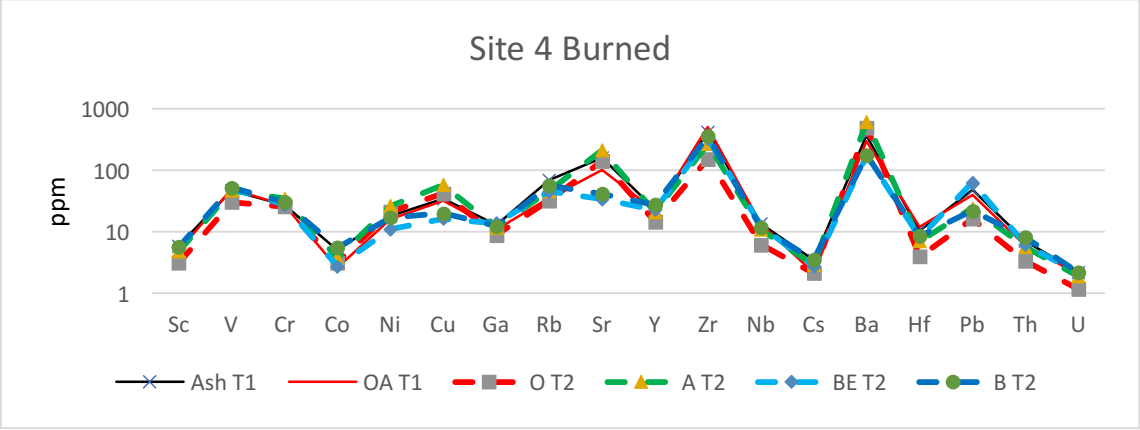

Figure 3.14 Elemental concentrations of Sc, V, Cr, Co, Ni, Cu, Ga, Rb, Sr, Y, Zr, Nb, Cs, Ba, Hf, Pb, Th and U for Site 4.

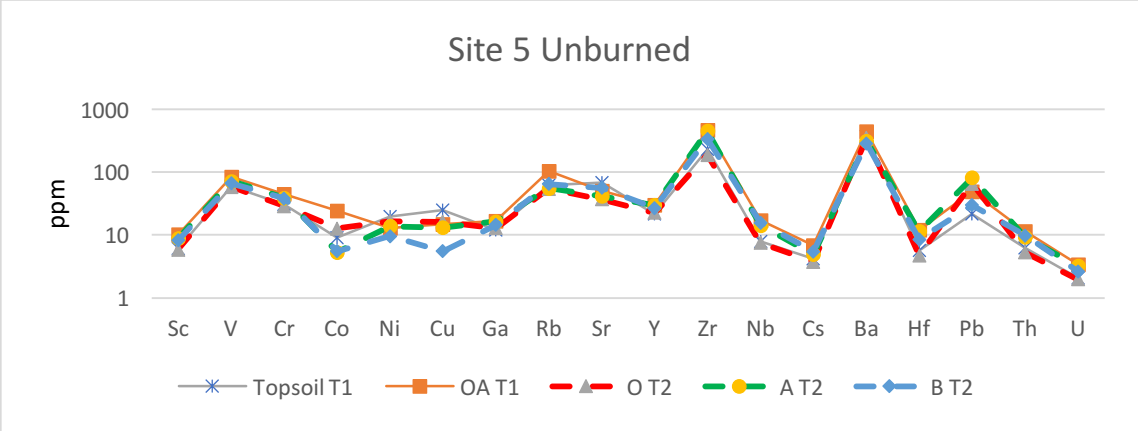

Figure 3.15 Elemental concentrations of Sc, V, Cr, Co, Ni, Cu, Ga, Rb, Sr, Y, Zr, Nb, Cs, Ba, Hf, Pb, Th and U for Site 5.

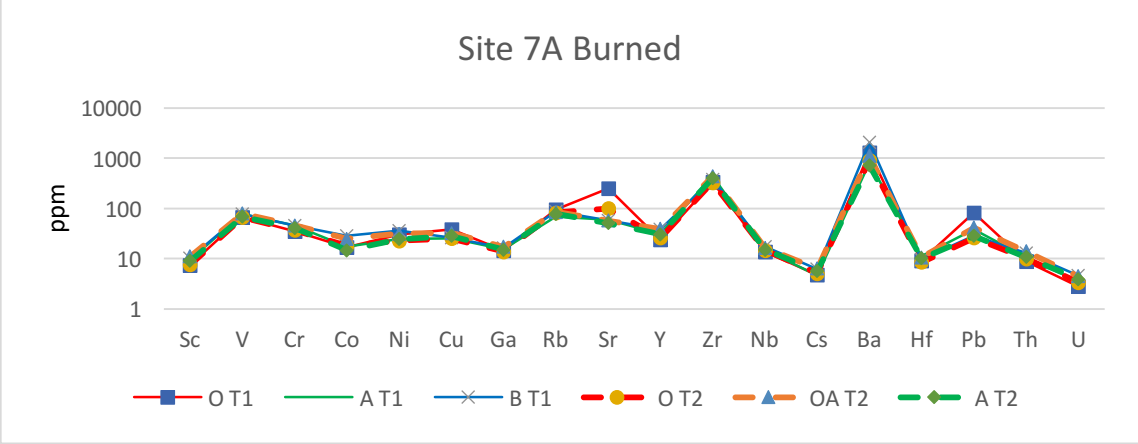

Figure 3.16 Elemental concentrations of Sc, V, Cr, Co, Ni, Cu, Ga, Rb, Sr, Y, Zr, Nb, Cs, Ba, Hf, Pb, Th and U for Site 7A.

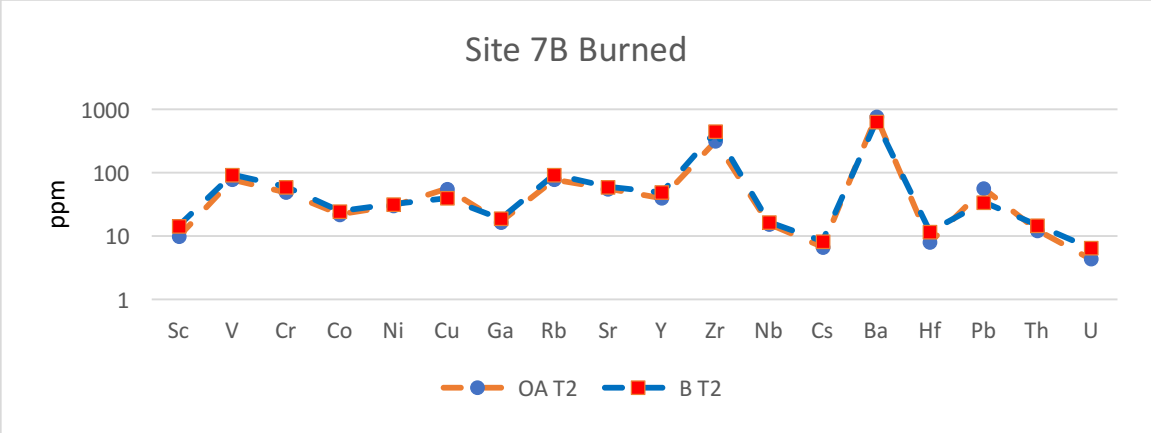

Figure 3.17 Elemental concentrations of Sc, V, Cr, Co, Ni, Cu, Ga, Rb, Sr, Y, Zr, Nb, Cs, Ba, Hf, Pb, Th and U for Site 7B.

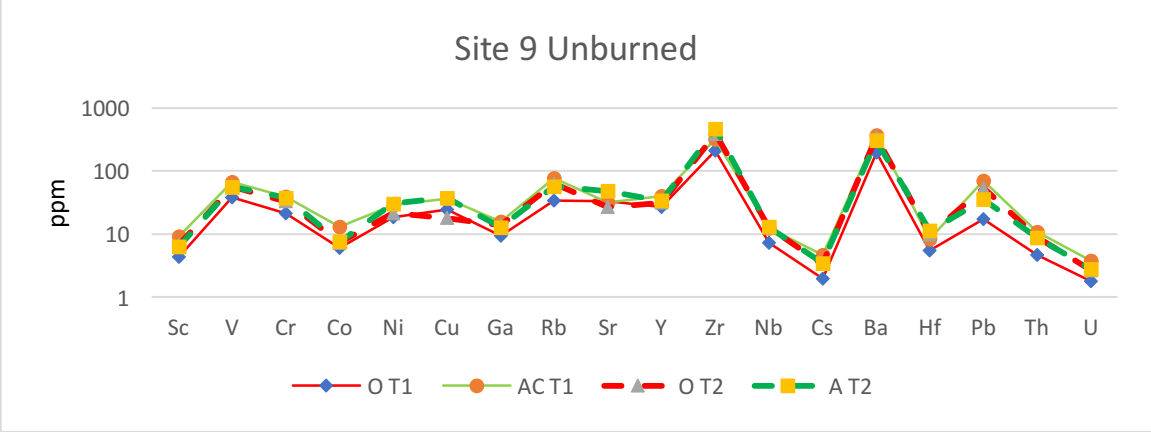

Figure 3.18 Elemental concentrations of Sc, V, Cr, Co, Ni, Cu, Ga, Rb, Sr, Y, Zr, Nb, Cs, Ba, Hf, Pb, Th and U for Site 9.

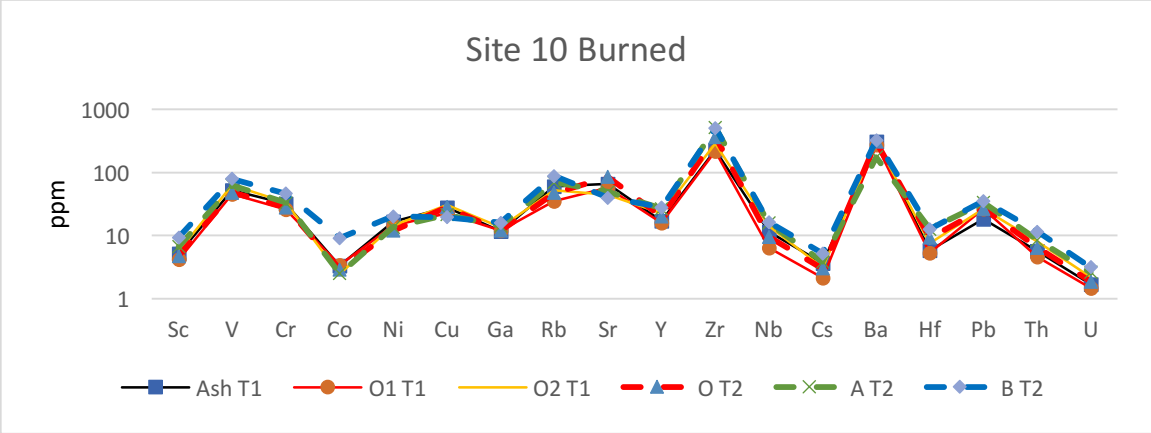

Figure 3.19 Elemental concentrations of Sc, V, Cr, Co, Ni, Cu, Ga, Rb, Sr, Y, Zr, Nb, Cs, Ba, Hf, Pb, Th and U for Site 10.

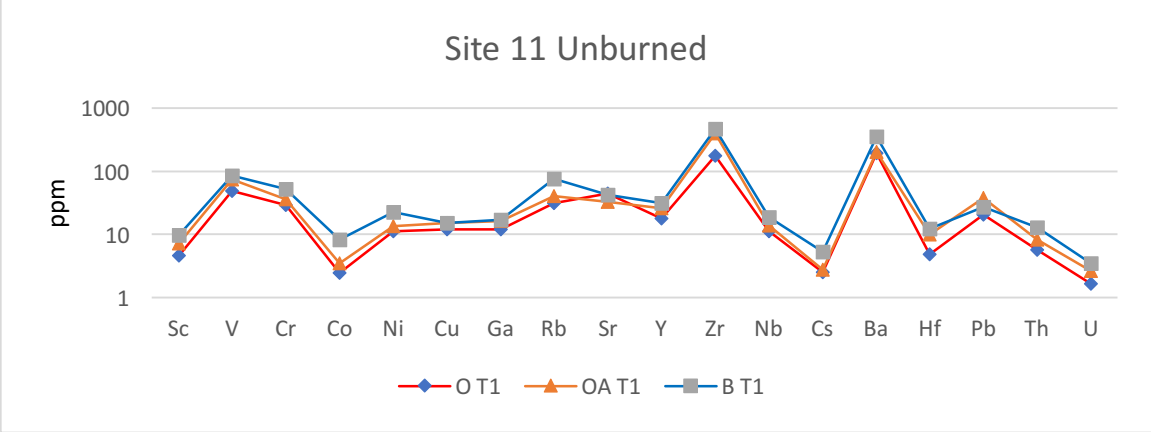

Figure 3.20 Elemental concentrations of Sc, V, Cr, Co, Ni, Cu, Ga, Rb, Sr, Y, Zr, Nb, Cs, Ba, Hf, Pb, Th and U for Site 11.

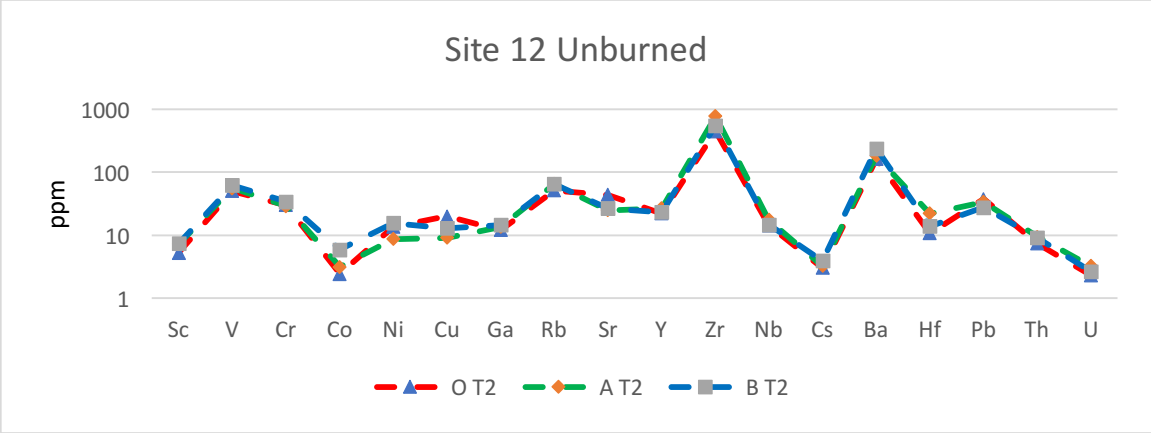

Figure 3.21 Elemental concentrations of Sc, V, Cr, Co, Ni, Cu, Ga, Rb, Sr, Y, Zr, Nb, Cs, Ba, Hf, Pb, Th and U for Site 12.

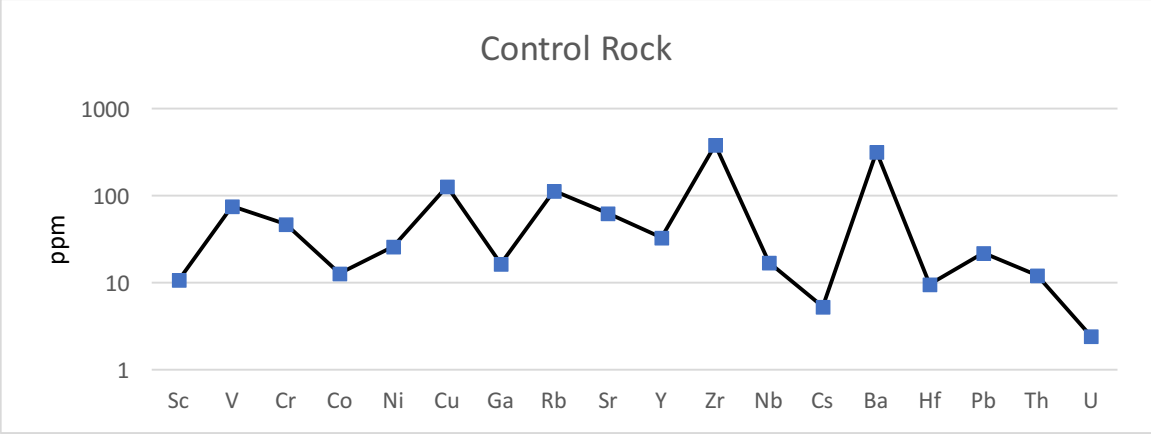

Figure 3.22 Elemental concentrations of Sc, V, Cr, Co, Ni, Cu, Ga, Rb, Sr, Y, Zr, Nb, Cs, Ba, Hf, Pb, Th and U for control rock.

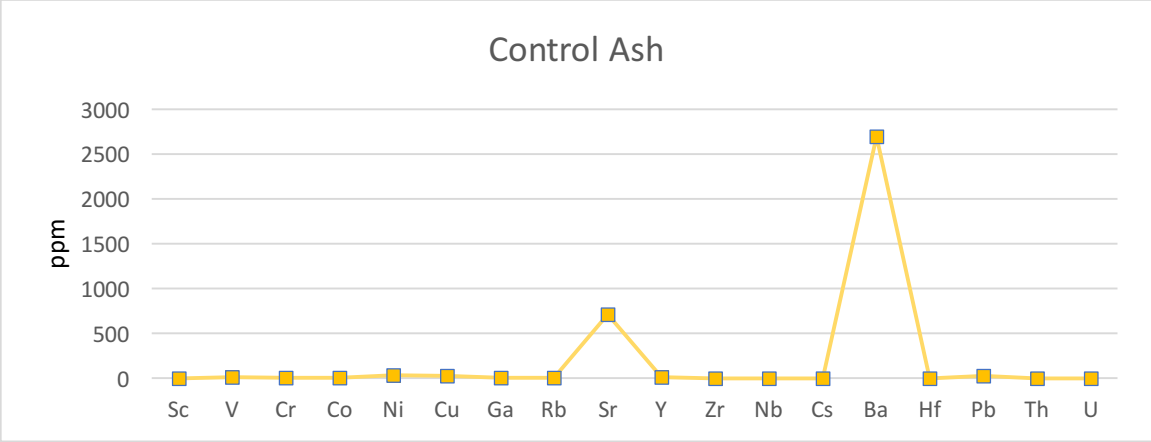

Figure 3.23 Elemental concentrations of Sc, V, Cr, Co, Ni, Cu, Ga, Rb, Sr, Y, Zr, Nb, Cs, Ba, Hf, Pb, Th and U for control ash.

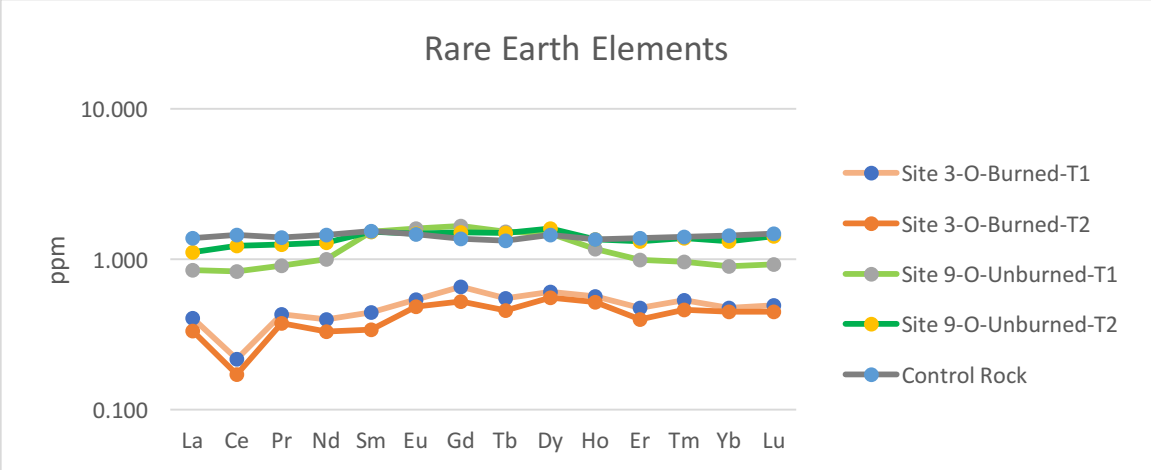

Figure 3.24 Site 3 (burned), Site 9 (unburned), and control rock plotted against upper continental crust values (Taylor & McLennan, 1995).

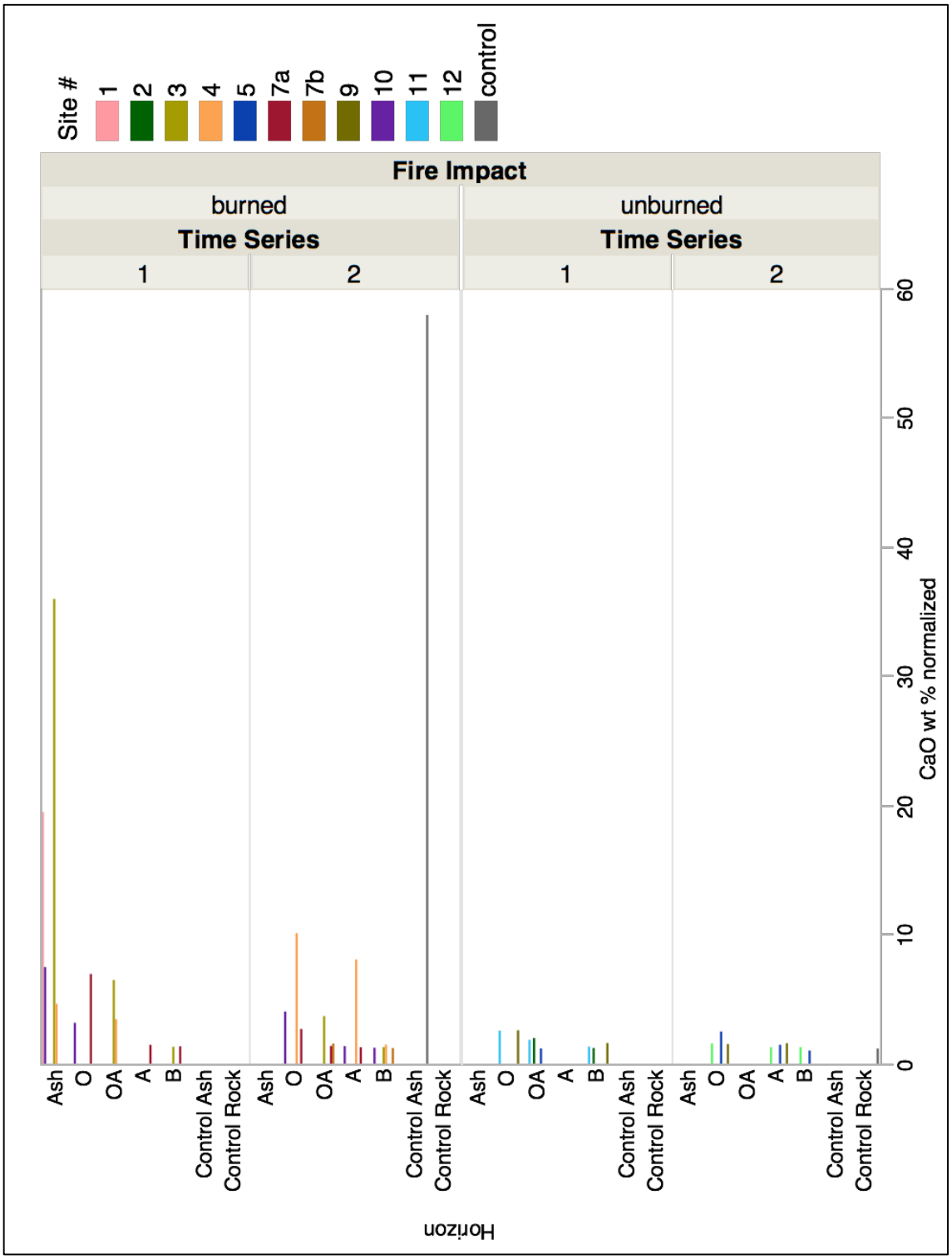

Figure 3.25 Bar graph of samples sites comparing CaO wt % normalized by horizon based on fire impact and time series.

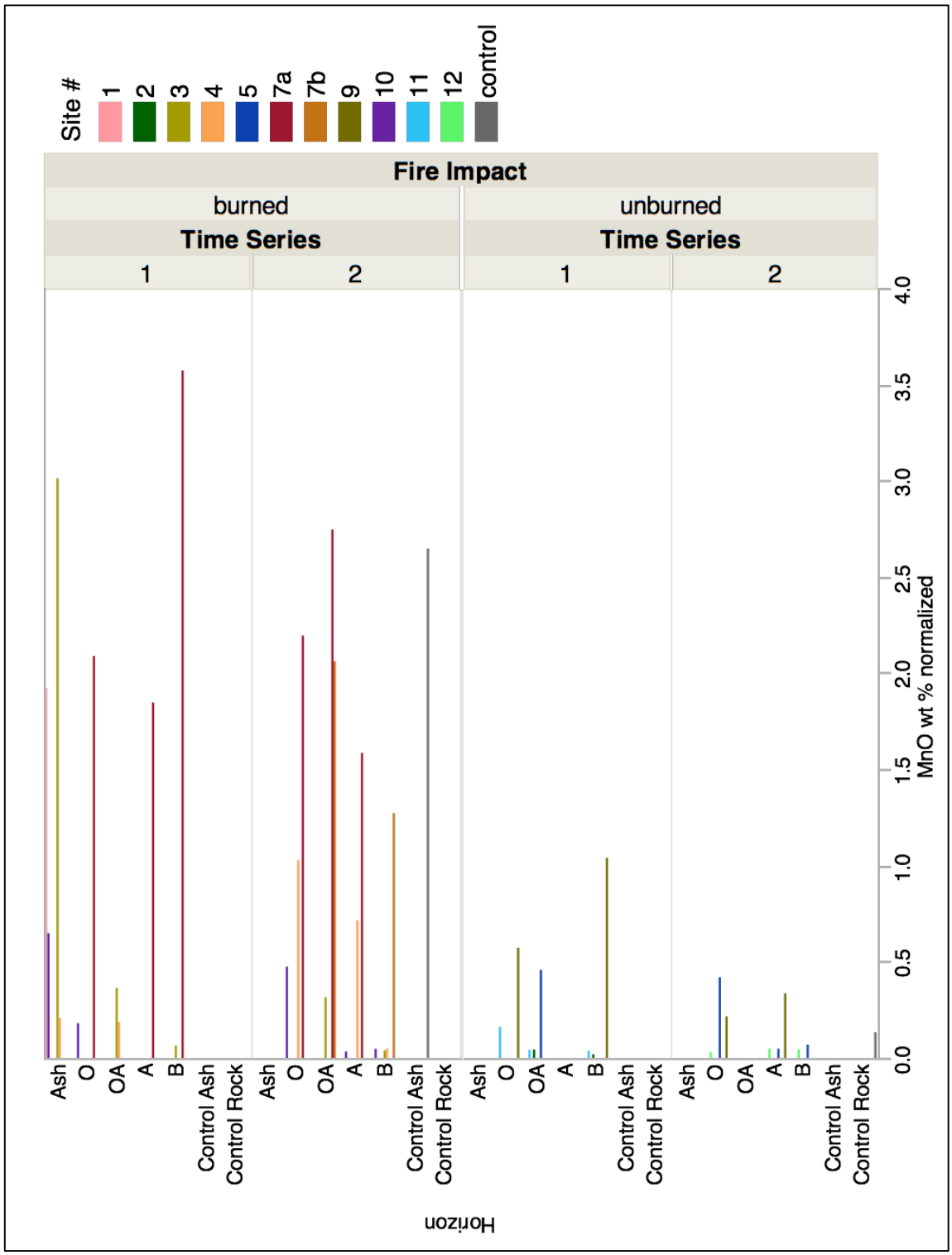

Figure 3.26 Bar graph of sample sites comparing Mn wt % normalized by horizon based on fire impact and time series.

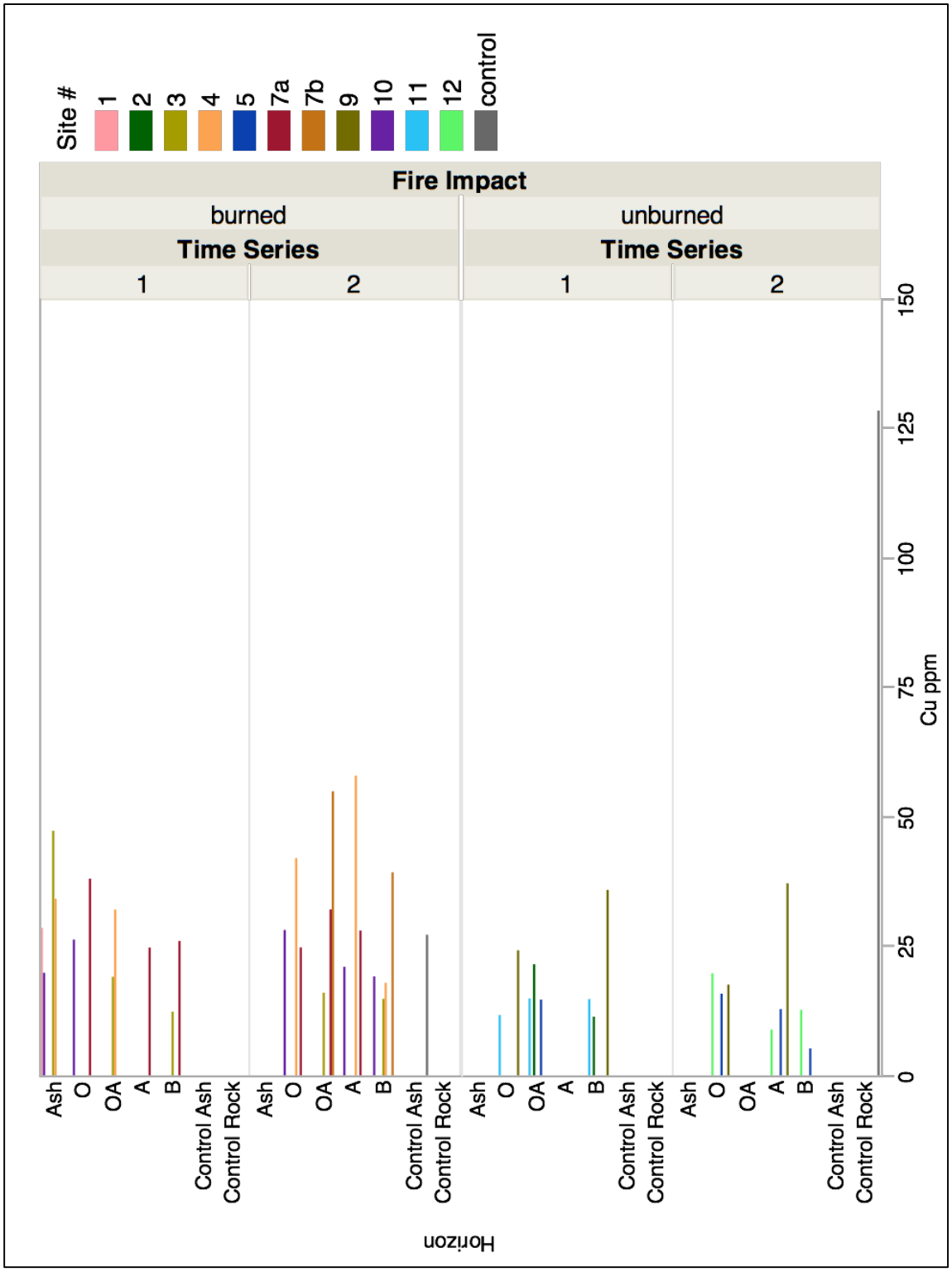

Figure 3.27 Bar graph of sites comparing Cu ppm by horizon based on fire impact and time series.

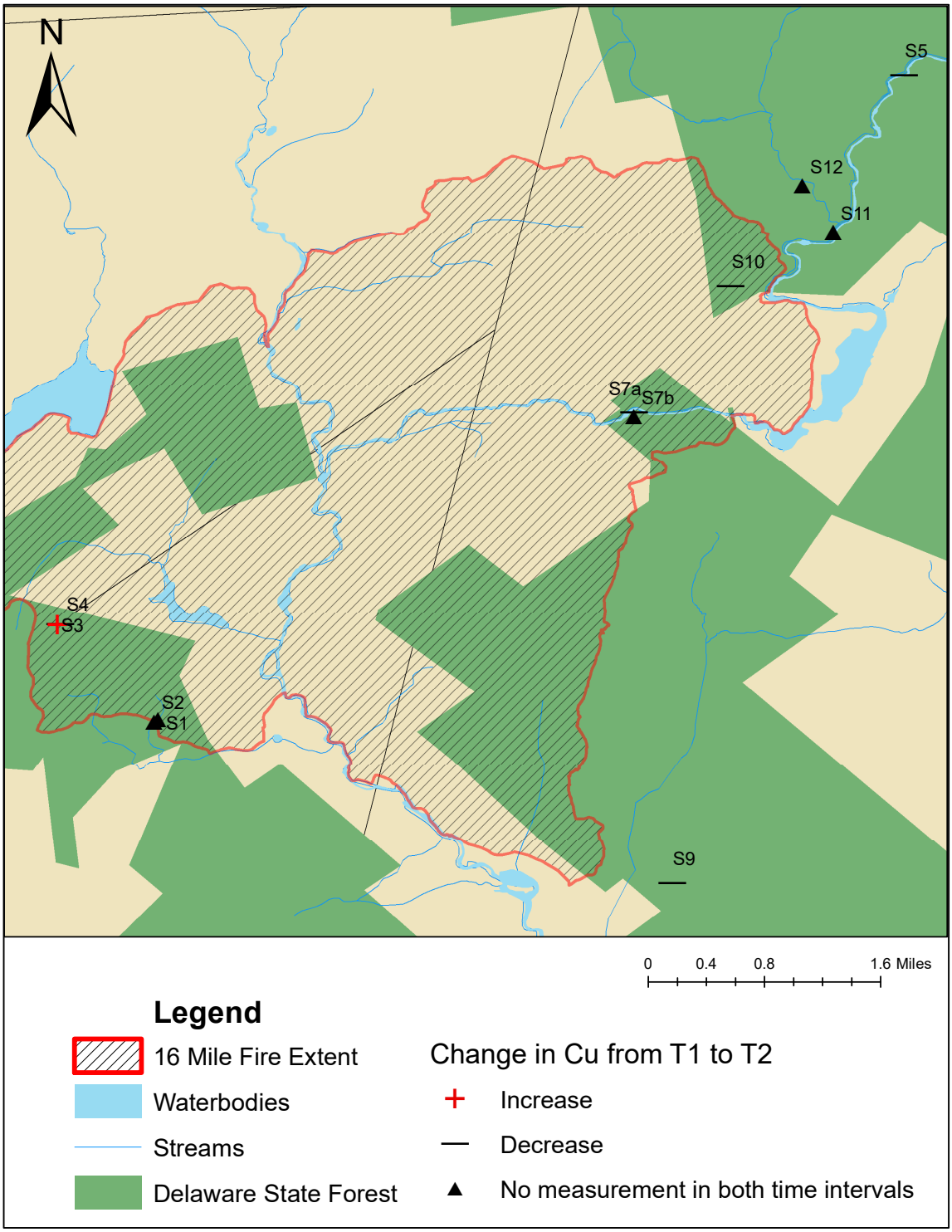

Figure 3.28 Map of sites comparing Cu ppm from burned and unburned soils between the two-time intervals.

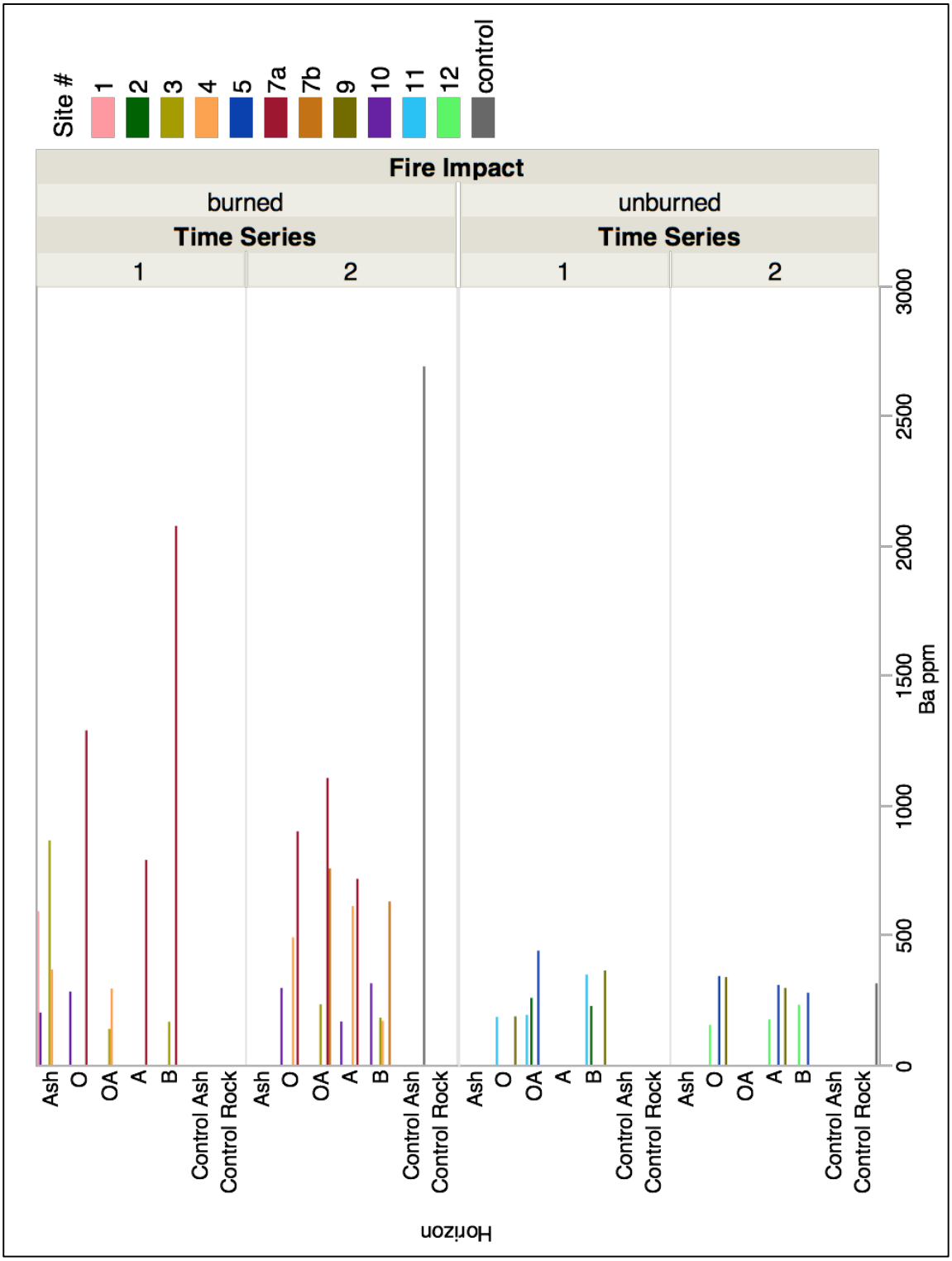

Figure 3.29 Bar graph of sites comparing Ba ppm by horizon based on fire impact and time series.

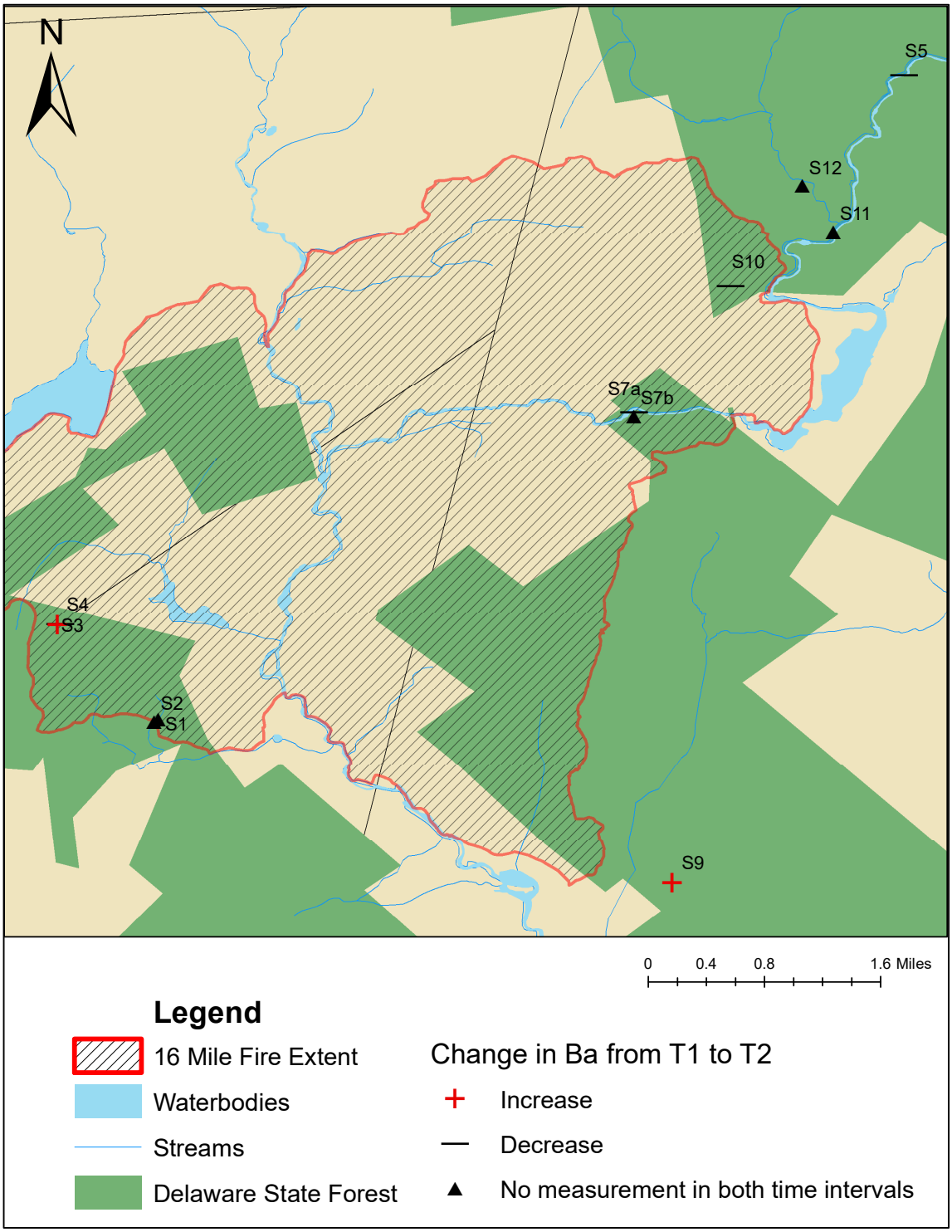

Figure 3.30 Map of sites comparing Ba ppm from burned and unburned soils between the two-time intervals.

Table 3.3 Results of analysis of variance for element concentrations comparing burned versus unburned soils, all statistically significant (p= <0.05) elements.

		Sum of Squares	df	Mean Square	F	Sig.
MnO	Between Groups	11.12	2	5.56	3.872	.027
	Within Groups	73.25	51	1.44		
	Total	84.37	53			
CaO	Between Groups	1466.29	2	733.14	5.708	.006
	Within Groups	6550.31	51	128.44		
	Total	8016.59	53			
Cu	Between Groups	6629.61	2	3314.80	14.508	.000
	Within Groups	11652.26	51	228.48		
	Total	18281.87	53			
Ba	Between Groups	2823518.38	2	1411759.19	7.303	.002
	Within Groups	9858530.83	51	193304.53		
	Total	12682049.20	53			
Na2O	Between Groups	2.08	2	1.04	4.946	.011
	Within Groups	10.75	51	0.21		
	Total	12.83	53			
V	Between Groups	2736.10	2	1368.05	3.372	.042
	Within Groups	20693.24	51	405.75		
	Total	23429.33	53			
Sr	Between Groups	222264.22	2	111132.11	4.215	.020
	Within Groups	1344513.12	51	26363.00		
	Total	1566777.33	53			
Ta	Between Groups	1.03	2	0.52	3.692	.032
	Within Groups	7.12	51	0.14		
	Total	8.15	53			

4. DISCUSSION

The main goal of this project was to study the major and trace elements of ash and soil samples of the 16-Mile Fire in the burned area and compare to samples upstream and downstream of the watershed sub-basin. Results from ICP-MS show variations between burned and unburned samples in the major elements calcium and manganese and within the trace elements copper and barium. Of these elements, copper and barium have higher concentrations and are considered to be fire signatures. Within the soil horizons the O and A have higher concentrations. Copper has higher concentrations in the second time interval compared to first time interval. Barium has relatively the same concentration between the two time intervals, with the highest concentration in the B horizon at site 7A. Copper and barium concentrations are higher in the burned area compared to the unburned areas.

4.1 Geochemistry Trends and Correlations

Burned vs Unburned Soil

ICP-MS of major elements reveals calcium and manganese are more abundant in the ash and soil samples of burned sites to unburned areas. This is directly related to the temperature of individual elements that volatize at excessive temperatures (Bodí *et al*., 2014). Ultimately, ICP-MS results yield two conclusive fire signatures of trace elements, copper and barium that are characteristic of wood ash as studied by Etiégni & Campbell (1991). It is also worth noting that calcium is much more abundant in the ash samples compared to soil, which is typical of ash to due to high concentrations in biomass and litter (Costa *et al.*, 2014). According to Bodí *et al.* (2014) and Certini (2005), an increase in calcium is common when high temperatures > 500 °C allow for various compounds

such as carbonates, oxalates, and oxides of calcium to disassociate, resulting in increased concentration in soil horizons. It is during this disassociation that alterations in calcium compounds occur both physically and chemically thus changing the mineralogy (Bodí *et al.*, 2014). Manganese displays the same trend as calcium with higher concentrations in burned soils to unburned (Figure 3.26).

Differences in the trace element copper is seen between the burned and unburned sites with burned samples containing higher concentrations (Figure 3.29). Spatially, the highest concentrations are at site 3, 7A, 7B, and 9 (Figure 3.28). Site 9 is southeast of the fire extent and might have higher concentrations of copper due to the northwest wind during the fire event (Philadelphia/Mount Holly Weather Forecast Office, 2017). The fire progression map (Figure 4.1) also indicates southeast movement of the high winds towards site 9, while also progressing further northeast as well. Ash fall may have been more predominant within that vicinity thus yielding higher concentrations of copper. The source of higher concentrations of copper in the burned samples to unburned samples can be due to the addition of ash. Burton *et al.* (2016) mentions in their study that copper can be derived from the ash remains of biomass, since the highest concentrations of copper was in ash samples compared to burned soil. Copper is also present within the parent material in our study and it is common in sandstone. Comparing our results to Campos *et al.* (2016), they found no differences between copper in burned and unburned soils. Based on the various studies reviewed and cross analyzed for copper it is of general understanding that copper as a fire signature is dependent on the type of biomass (oak trees) combusted during the fire event and the concentration present in the soil already from parent material.

ICP-MS results of barium between burned and unburned sites by horizon (Figure 3.29) show that burned samples in some cases are two times the concentration of unburned samples. All of the unburned samples and control rock are below 500 ppm, whereas the majority of burned samples are above 500 ppm. The control ash yielded the highest barium concentration, 2697 ppm. A literature review of barium and its presence in soil due to forest fire yielded no results, only being documented from the Cerro Grande Fire (Gallaher *et al.*, 2002). According to Gallaher *et al.* (2002) barium was present in high concentrations in post-fire runoff. Comparing barium present within the parent material (control rock), 320.954 ppm, to the control sites (unburned) and burned sites, we can conclude that the higher concentrations in burned sites are from the combusted biomass. Spatially barium has higher concentrations within the burn extent compared to the surrounding unburned area, with slightly lower concentrations over time at sites within the fire extent (Figure 3.30).

Geochemistry within Horizons

Most of the manganese concentrations reside in the O, OA, and A horizons except for the highest amount of manganese in the B horizon at site 7A in time series 1. This is consistent with other findings by Burton *et al.* (2016) and Campos *et al.* (2016), which also reported on having higher concentrations of manganese in soil samples post-wildfire conditions.

Overall, the concentration of copper varies between horizons in the burned samples most residing in the OA and A horizons. It can be weathered into the B horizon from the parent material or derived from organic matter that is leeching from the O horizon, which can easily adhere to clay minerals (Hough, 2010). Initial particle size

data plotted on soil texture diagrams (Figure 4.2) shows that much of the soil horizons are silt loams. One OA horizon plotted as silty clay. It is most likely that copper is adhering to the clay portion of the clay particles in the soil. While the initial sampling plan was to only sample the upper soil horizons (O and A) analytical results showed that higher concentrations where being seen in the B horizons.

The high amount of barium concentrations in this study is consistent with results by Etiégni & Campbell (1991) with having high concentrations of barium in wood ash except for Site 7b, which has the highest concentration. Based on the concentration of barium in the control ash and results by Etiégni & Campbell (1991) it can be concluded that barium is a fire signature from the combusted biomass that is being absorbed into the OA and A horizons. While the initial sampling plan was to only sample the upper soil horizons (O and A) analytical results showed that higher concentrations where being seen in the B horizons. This was unexpected in such a short period of time. One possibility is the translocation of elements from increased weathering post-fire. Callanan *et al*. (2013) found during a study that post-fire chlorite was weathered past the typical 10 cm beneath the surface. Site 7b, horizon B1 is at a depth of 15 cm. It is possible that the high intensity nature of this fire event caused for increased weathering of certain elements, which were then translocated to the B horizon in a shorter period of time.

Future work needs to be conducted on the type of barium that resides within the study area and whether or not it is easily soluble. The solubility of Ba, Cu, Mn, and Ca can have a large influence on why concentrations of these elements are being seen within the various horizons. Solubility rates should be looked at in future research of this area to have a better understanding if this is having an effect on the concentrations down horizon

and possibly residence time. Especially for REEs, which we observe as being depleted within all the soil samples. This appears to be the case that they are easily soluble within the soil. It would be interesting to see during a prescribed fire if these signatures remain between post-fire and the first rainfall event.

As previously discussed, cabins were also destroyed within the 16-Mile Fire and sampling took place where a cabin once stood at Site 7b. When comparing trace element concentrations between Site 7b and 7a, there is no increase in concentrations or distinct difference from the burned man-made materials to vegetation and soil. Therefore, the cabin did not contribute any additional trace elements to the soil or surrounding area. This could be due to the type of materials used for constructing the cabin. It is also possible that post-fire cleanup of the former cabin site included removing any material in the O horizon. Site 7b was only sampled during the 8-month field sampling after multiple weather events.

Geochemistry Over Time

The overall trend of calcium decreases from time series 1 to time series 2, except for site 4, which has an increase from a soil sampled in the OA horizon in time series 1 to an increase in O and A horizons in time series 2. While the results from this study show manganese to be about the same concentrations between the two time series, Costa *et al.* (2014) reported in their study that manganese decreases over time due to manganese's solubility, allowing it to be transported away during erosion/runoff. This difference from our study to Costa *et al.* (2014), could be due to a number of factors, but is most likely due to the difference in biomass, soil types by region and the cation exchange of manganese adhering to soil particles and duration of the study. It would be interesting to

see what changes occur after three years of sampling the area. It is possible that we would see the same results as in Costa's *et al*. (2014). Another differentiating factor of Costa's *et al*. (2014) study area is that the soil parent material consisted of metamorphic and igneous rocks (schist and granite) and vegetation that is more abundant in shrubs, that contributed to a different elemental concentration to soil formation. The 16 Mile Fire and surrounding area consists of sandstone parent material and woods containing various species of oak trees. Other major elements analyzed did not reveal any indication of fire signature or have a distinct difference between soil horizons or time interval.

While results on the major and trace elements show the presence of fire signatures, our results vary from the studies of Burton *et al.*, (2016) and Campos *et al.* (2016), where other trace elements of vanadium, cobalt, nickel, cadmium, and lead were present. It is most likely due to the variation in vegetation, soil chemistry and fire ecology that is yielding varying findings.

4.2 Sub-Basin RUSLE Model

Geographic information system analysis was done to determine the sub-basins of the Middle Delaware-Mongaup Brodhead Watershed that were affected by the fire. Surface hydrological analysis indicates that two sub-basins were disturbed by the 16-Mile fire event (Figure 4.3). The largest sub-water basin is 191.5 km^2 (labeled as watershed 1) and the smaller sub-water basin is 19.6 km^2 (labeled as watershed 2), totaling 211.1 km^2. As discussed earlier, the Big Bushkill Creek has a confluence in the center of the fire extent. With the 16-Mile Fire extent in a hydrologically active region, further investigation was conducted to determine if increased runoff would have the fire signatures of barium and copper mobilized. This is due to evidence of high intensity burning, such as white ash

and burned O horizon in various sampling sites. Another study conducted by Callanan *et al*. (2017a) coincides with this project in that it looks at the water chemistry to determine if ash and soil that was mobilized from the fire event affected water quality within the Bushkill Creek. According to Debano (2000b), during wildfires, high temperatures can penetrate down the soil horizon which cause clay layers collapse and develop a hydrophobic layer increasing water repellency thus leading to increased soil erosion from runoff.

A slope raster of the study area (Figure 4.4) shows that the 16-Mile fire extent has shallow slopes with 84 % having <9 degree slopes and 15 % with >9 degree slopes. All of the sites sampled lie in areas with slopes < 3 degrees. This indicates a low probability for runoff in our sampled sites, though that probability may be higher with steeper slopes. However, the landscape topography seems to play a role in barium as a fire signature. Comparing burned sites (1, 7A and 7B) that are lower in elevation and close to the creek (group 1) with burned sites (3, 4, and 10) at higher elevation (group 2), there is a statistically significant difference in the amount of barium, with lesser amounts of barium at the higher elevations, based on ANOVA analysis ($p<0.0005$) (Figure 4.5). This difference is similar to that comparing burned to unburned samples at the same topographic expression, lower elevation and close to the creek (sites 1, 7a, and 7b burned, group 1, and sites 5, 11, and 12, unburned, group 3), also statistically significant ($p<0.0003$), with less barium at the unburned sites (Figure 4.6). This difference in barium concentration in burned sites near Bushkill Creek could be due to different vegetation that develops in proximity to the stream, which may have higher concentrations compared to vegetation that burned elsewhere. To confirm this, vegetation outside of the

burn zone near the creek should be investigated for elemental analysis for barium concentrations. Other elements were evaluated to see if topography played a similar role with increased concentrations near lower elevation. No other elements show similar trend like Barium.

The RUSLE evaluates other factors that play a role in soil erosion. The RUSLE model (Figure 4.7) shows that the majority of the study area is in a 0 to 0.009 tons/ha/yr. range of soil loss. Only regions that are adjacent to streams or on steeper slopes have a higher potential for increased soil erosion. This indicates that the elemental fire signatures are less likely to be mobilized throughout the sub-basin from soil erosion and runoff. Additionally, it coincides with the chemical analysis results of fire signatures increasing over time and moving down the soil horizon. Areas that have steeper slopes (but not sampled during this study) could see soil loss ranging from 0.02 to 2.3 tons/ha/yr. These areas have the potential to disperse fire signatures and other concentrations of trace elements to other areas that might have lower concentrations. Another factor that can influence the amount of erosion in this area is the precipitation and infiltration capacity of soil or soil moisture. If soil near the Bushkill Creek is consistently moist there, a higher chance for soil erosion is possible. Since it will take time for vegetation to provide stability to the soil, areas with rills created by surface runoff will increase erosion. This is based on what Miller *et al*. (2011) found, where erosion rates increase due to the amount of precipitation causing wetter soil and increasing the amount of erosion instead of surface conditions playing a major role in erosion. Furthermore, soil sampling within these areas is needed to determine if this is in fact valid for the 16-Mile Fire study area. While this gives an estimate of potential soil

loss within the fire extent, further analysis is needed along with updated coverage factor values for the study area to account for vegetation that is no longer present.

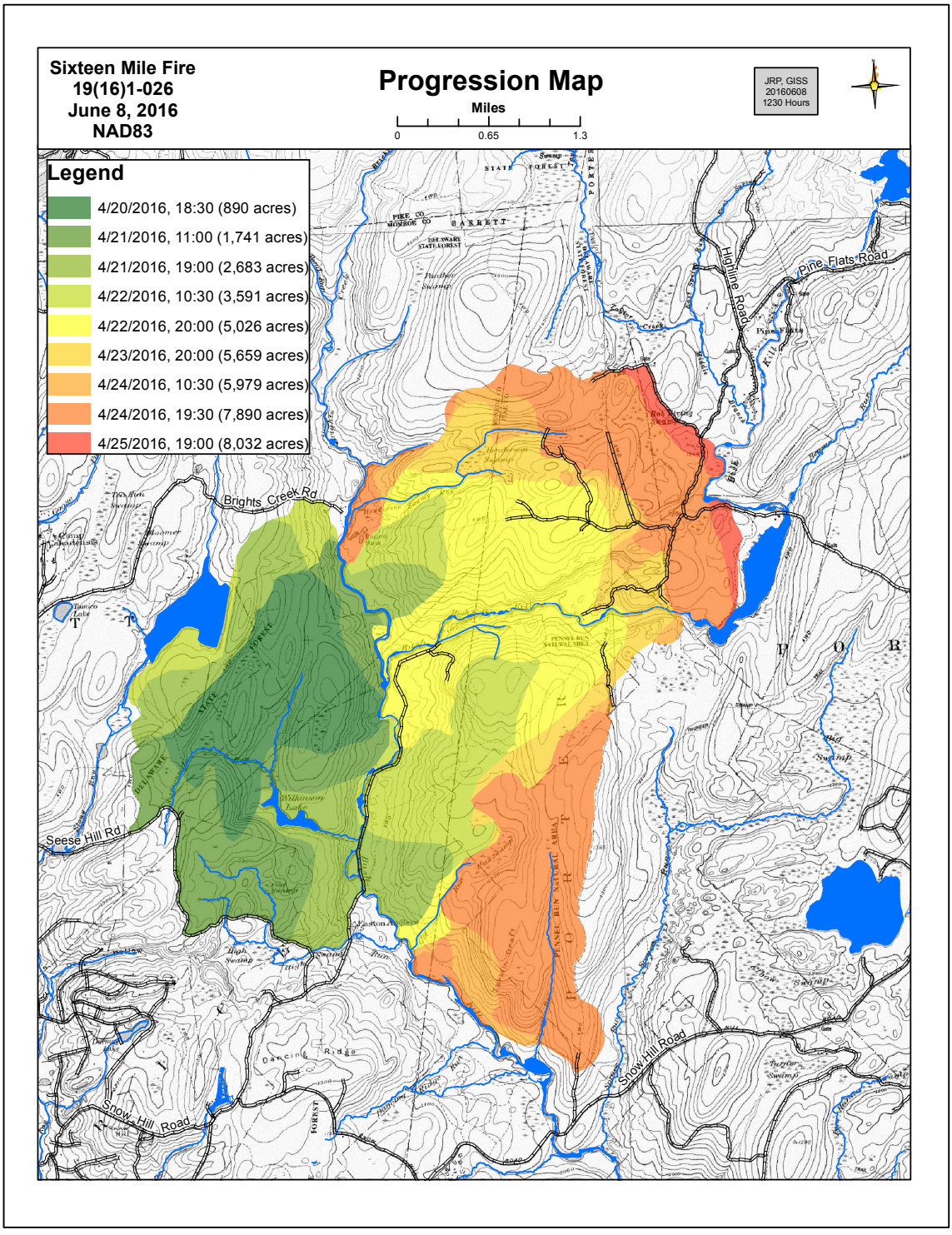

Figure 0.1 Fire progression map of the 16-Mile Fire (Hazen, 2016).

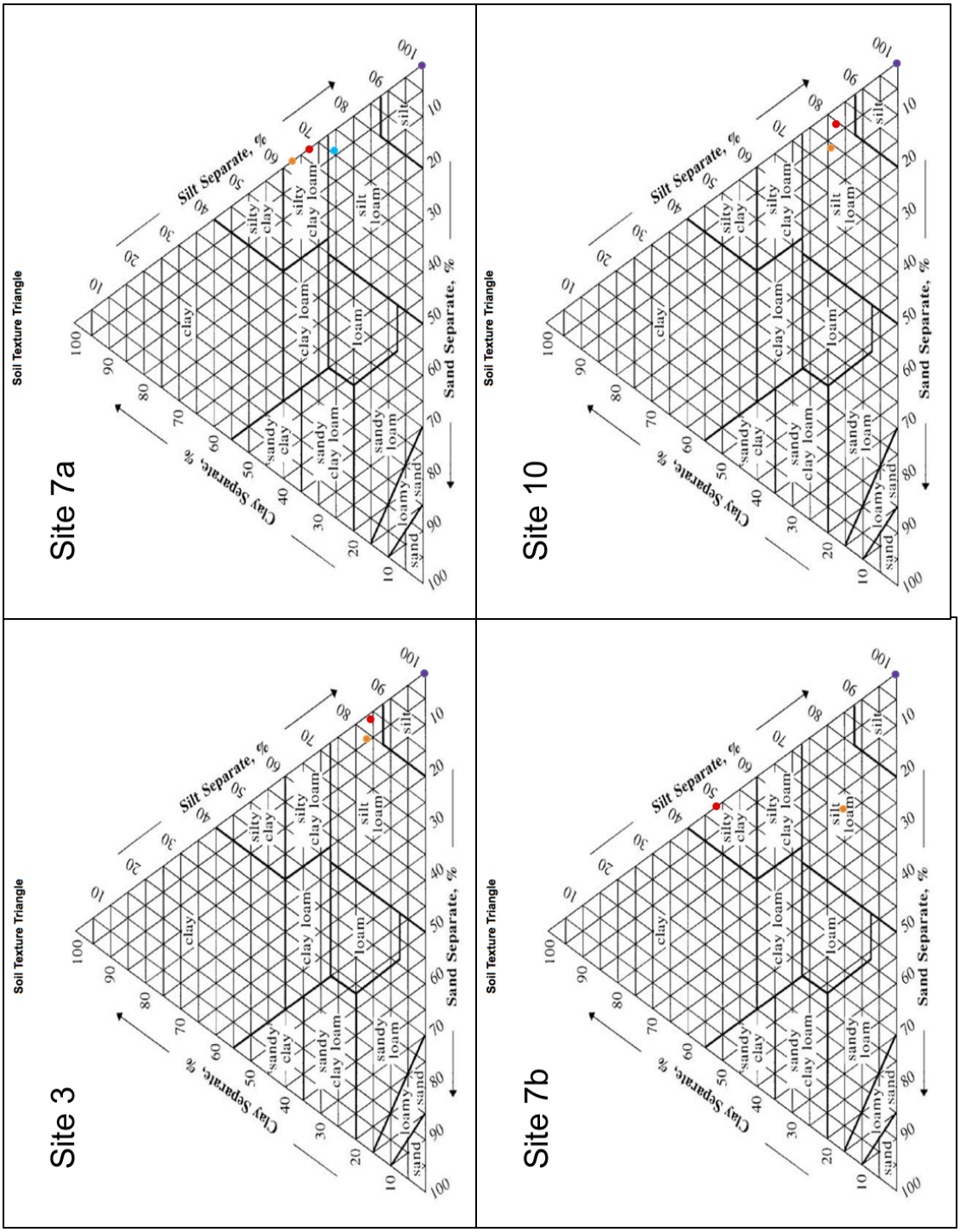

Figure 0.2 Soil texture triangles of Sites 3, 7a, 7b, and 10. Most all horizons plot as silt loam, except for the O and A horizon at Site 7a, silty clay loam and the OA horizon at Site 7b, silty clay.

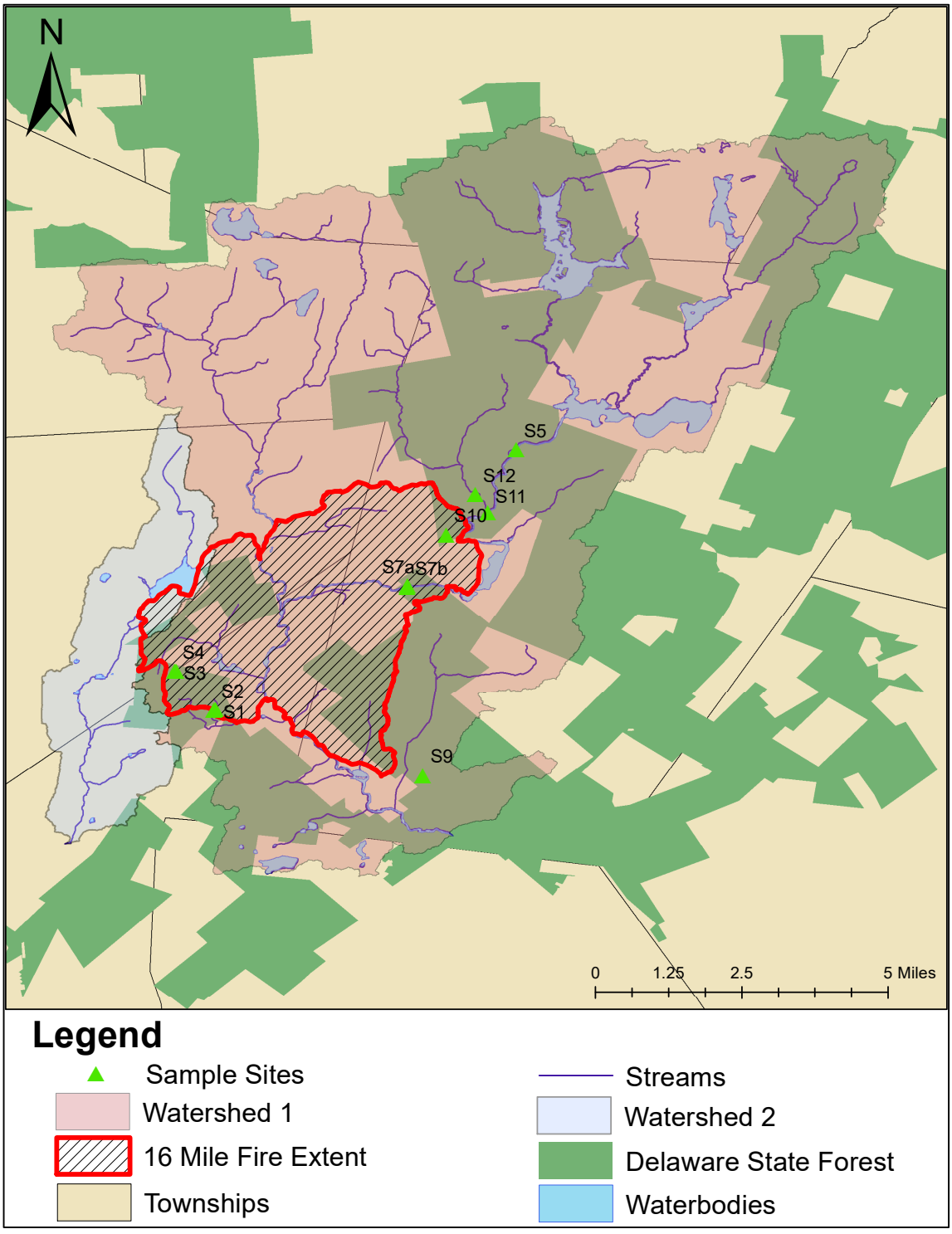

Figure 0.3 Map showing the extents of the sub watersheds that are affected by the 16-Mile fire.

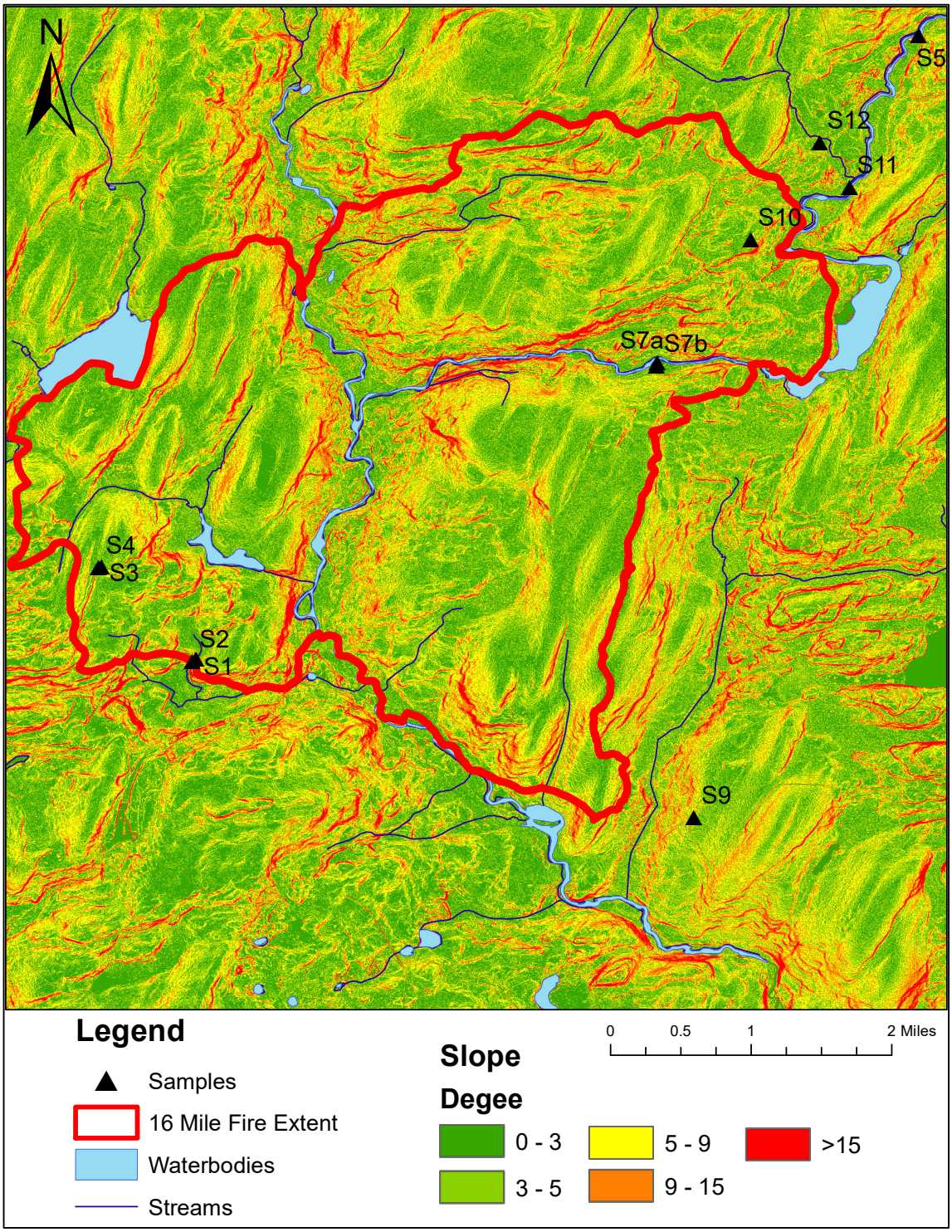

Figure 0.4 Map showing the various slopes within the fire extent.

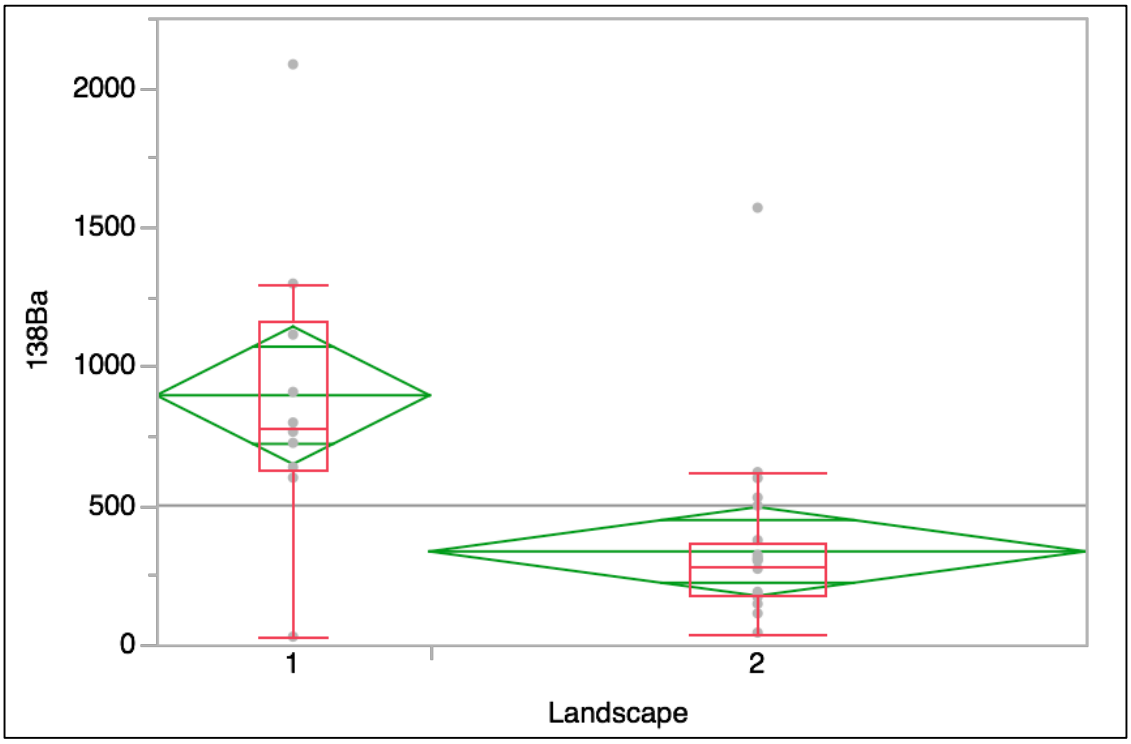

Figure 0.5 Box chart graph of ANOVA analysis showing the difference of burned sites at low elevation near the creek (1) to burned sites at high elevation (2) $p<0.0005$.

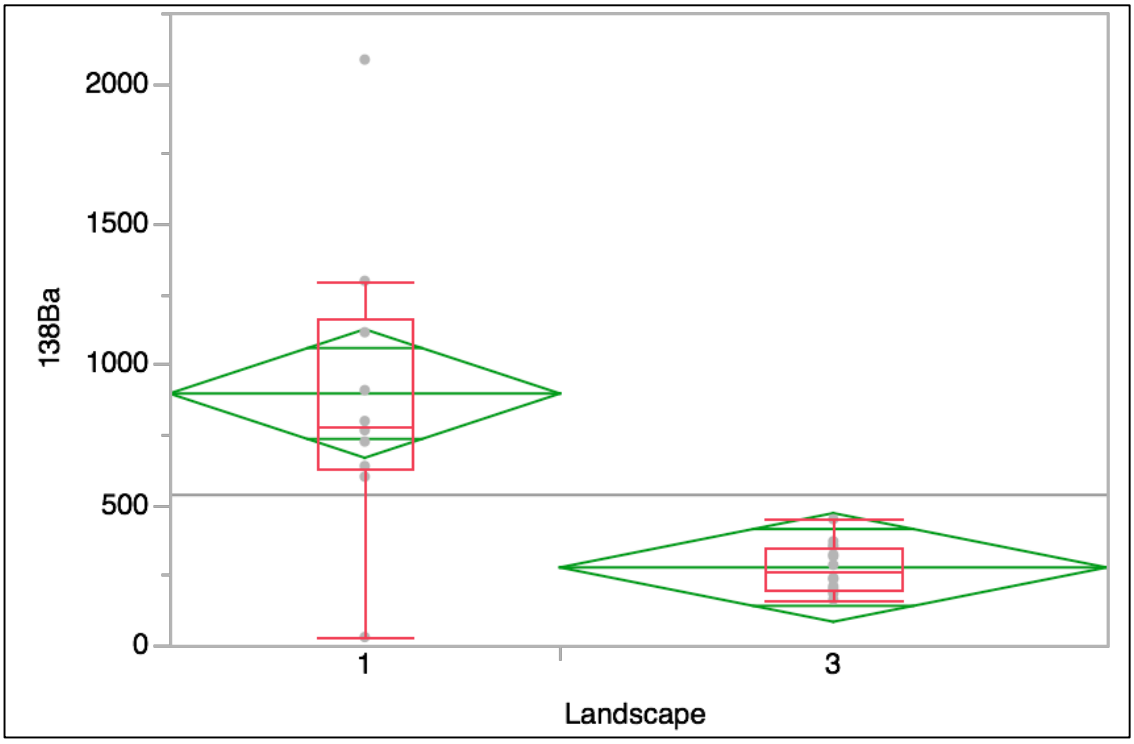

Figure 0.6 Box chart graph of ANOVA analysis showing the difference of burned sites at low elevation near the creek (1) to unburned sites at low elevation near the creek (2) $p<0.0003$.

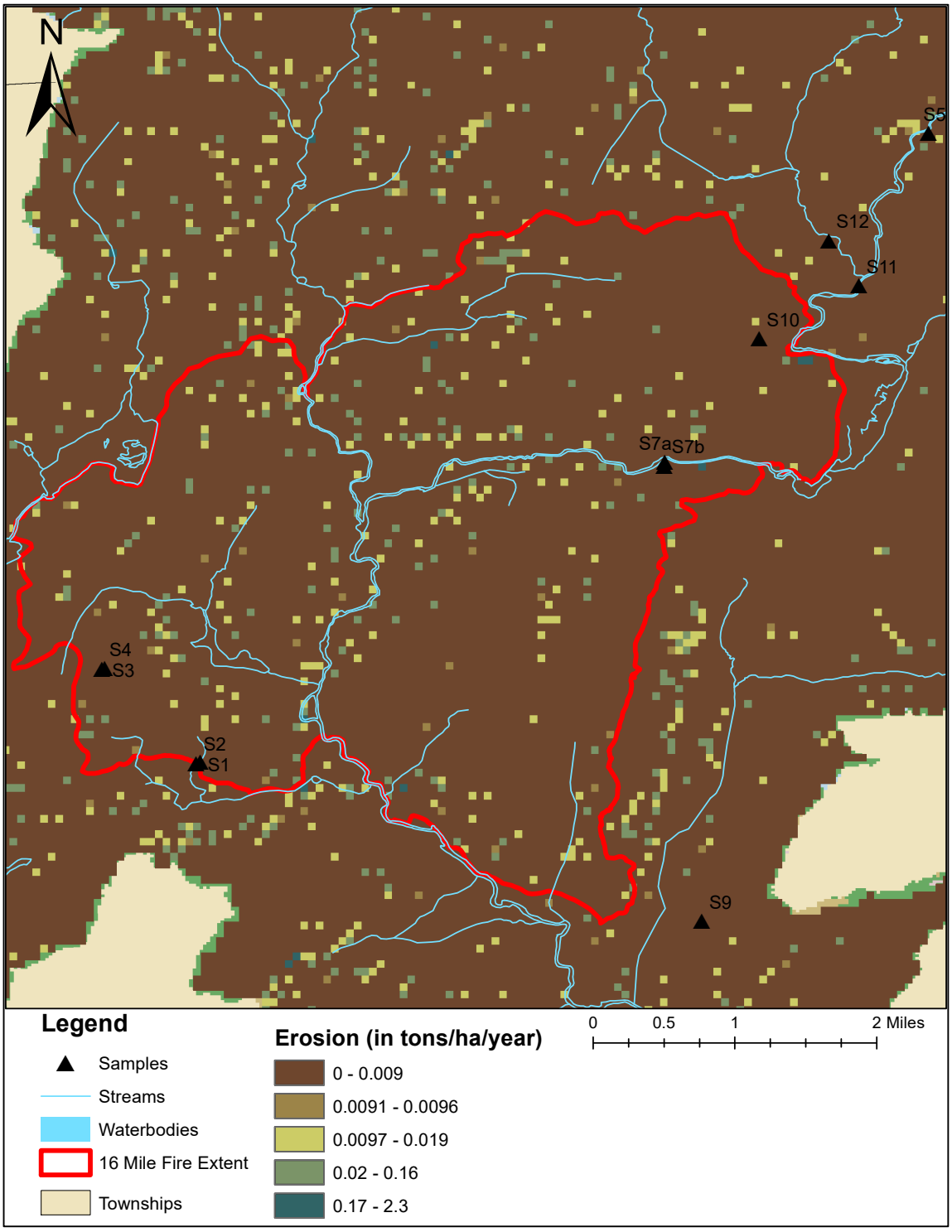

Figure 0.7 Map showing the results (in tons/ha/year) of the RUSLE model indicating the amount of erosion within the fire extent.

4 CONCLUSION

Soil and ash samples were collected within the 16-Mile fire extent of the Delaware State Forest, PA and surrounding area to investigate the presence of fire signatures of major and trace elements within the samples and how these signatures are distributed spatially. Burned soil and ash samples show distinct fire signatures in trace elements copper and barium and higher concentrations of calcium and manganese of burned to unburned samples. Comparing the 2-month sampling to the 8-10-month sampling indicates that the concentrations of copper and barium are remaining within the soil horizon, where in some sites concentrations are moving vertically down through the soil horizons.

Using geographic information system analysis of surface hydrology, a DEM was able to determine the sub-basins that are directly affected by the 16-Mile fire. A slope raster along with revised universal soil loss equation model of the sub-basin indicates that the majority of the 16-Mile fire extent has a shallow slope with low soil erodibility. This conclusion can be made on the summations of the land cover, soil structure, topography, and climatic variability, indicating that soil erosion will be low over time and the mobility of the found fire signatures will reside in the vertical horizon.

Further research needs to be done to investigate how long the fire signatures will reside in the soil horizons. As ecological succession returns to this area sampling needs to be monitored to see if vegetation will sequester copper and barium. Sampling should be continued at the same sites making sure the same soil horizons are collected each time interval to better monitor changes in geochemistry. Sampling of the B horizon at sites already sampled should continue to identify if further translocation or illuviation of other

elements occurs over time. While some B horizons at site already showed higher concentrations of Ba or Mn, other elements might take a longer time and are not easily mobilized.

Additional sampling should be done in the southeast region just adjacent to the fire extent to see if soil in that area has increased fire signatures due to atmospheric conditions during the fire allowing ash to accumulate. Decomposed surface vegetation should be collected to see if this can add higher concentrations of trace elements to the O and A horizons. It is possible that as vegetation decomposes, the organic matter will be the first to be absorbed by soil and plants, leaving behind trace elements. This would not contribute the amount of trace elements from wildfires, but this area did have a high abundance of diseased vegetation leading to possible higher amounts of surface mulch.

To better understand how this fire affects water resources, sediment samples at the bottom of the Big Bushkill Creek should be sampled. The data reported here is preliminary and is the first results following the 16-Mile fire, as more samples are collected and analyzed they could portray a better idea of where fire signatures reside and its impact on the local environment. This fire regime that occurred within the Delaware State Forest is not typical of wildfires that occur in Eastern United States. As climate changes within this region, the reoccurrence of similar conditions (drought, diseased vegetation, mild winter) will continue to grow with the possibility of more intense wildfires. Increases in high-intensity wildfires will have adverse effects on natural resources for sustaining the natural environment and the future generations that rely on them.

6. REFERENCES

Alauzis, M. V., Mazzarino, M. J., Raffaele, E., & Roselli, L. (2004). Wildfires in NW Patagonia: Long-term effects on a Nothofagus forest soil. *Forest Ecology and Management*, *192*(2–3), 131–142. https://doi.org/10.1016/j.foreco.2003.11.014

Arocena, J. M., & Opio, C. (2003). Prescribed fire-induced changes in properties of sub-boreal forest soils. *Geoderma*, *113*(1–2), 1–16. https://doi.org/10.1016/S0016-7061(02)00312-9

Badía, D., & Martí, C. (2003). Plant Ash and Heat Intensity Effects on Chemicaland Physical Properties of Two Contrasting Soils. *Arid Land Research and Management*, *17*(1), 23–41. https://doi.org/10.1080/15324980301595

Bladon, K. D., Emelko, M. B., Silins, U., & Stone, M. (2014). Wildfire and the future of water supply. *Environ.Sci.Technol.*, *48*(1520–5851 (Electronic)), 8936–8943. https://doi.org/10.1021/es500130g

Blank, R. R., & Zamudio, D. C. (1998). The Influence of Wildfire on Aqueous-Extractable Soil Solutes in Forested and Wet Meadow Ecosystems Along the Eastern Front of the Sierra-Nevada Range, California. *International Journal of Wildland Fire*, *8*(2), 79–85. Retrieved from http://dx.doi.org/10.1071/WF9980079

Bodí, M. B., Martin, D. A., Balfour, V. N., Santín, C., Doerr, S. H., Pereira, P., … Mataix-Solera, J. (2014). Wildland fire ash: Production, composition and eco-hydro-geomorphic effects. *Earth-Science Reviews*, *130*, 103–127. https://doi.org/10.1016/j.earscirev.2013.12.007

Brantley, S. L., White, T. S., White, A. F., Sparks, D., Richter, D., Pregitzer, K., … Amundson, R. (2006). *Frontiers in Exploration of the Critical Zone: Report of a workshop sponsored by the National Science Foundation (NSF)*. Newark, DE.

Brezinski, D. K., Cecil, C. B., Skema, V. W., & Kertis, C. A. (2009). Evidence for long-term climate change in Upper Devonian strata of the central Appalachians. *Palaeogeography, Palaeoclimatology, Palaeoecology*, *284*(3–4), 315–325. https://doi.org/10.1016/j.palaeo.2009.10.010

Brose, P., Schuler, T., Lear, D. Van, & Berst, J. (2001). Bringing fire back: the changing regimes of the Appalachian mixed-oak forests. *Journal of Forestry*, *99*(November), 30–35. Retrieved from https://scholar.google.com/citations?view_op=view_citation&continue=/scholar?hl=en&start=100&as_sdt=0,15&scilib=1&citilm=1&citation_for_view=j-MbVRkAAAAJ:1wZ_wKGpLuwC&hl=en&oi=p

Burton, C. A., Hoefen, T. M., Plumlee, G. S., Baumberger, K. L., Backlin, A. R., Gallegos, E., & Fisher, R. N. (2016). Trace Elements in Stormflow, Ash, and

Burned Soil following the 2009 Station Fire in Southern California. *PloS One*, *11*(5), e0153372. https://doi.org/10.1371/journal.pone.0153372

Callanan, J., Espinal, K., Grune, D., Lach, M., Pope, G., Hazen, M., & DaSilva, M. (2017a). Assessment of Water Chemistry of Bushkill Creek Following the 16 Mile Fire, Cresco PA, USA. In *American Association of Geographers Annual Meeting*. Boston: American Association of Geographers.

Callanan, J., Espinal, K., Grune, D., Lach, M., Pope, G., Hazen, M., & DaSilva, M. (2017b). Impacts to Surface Soil as a Result of the 16 Mile Fire, Cresco PA, USA. In *American Association of Geographers Annual Meeting*. Boston: American Association of Geographers.

Callanan, J., Frazier, W., Snyder, K., Reinertsen, C., Callanan, J., Frazier, W., … Reinertsen, C. (2013). Field and Laboratory Investigation of Fire-Induced Chlorite Weathering in an Inceptisol, *58*(April 2009), 9–13.

Campos, I., Abrantes, N., Keizer, J. J., Vale, C., & Pereira, P. (2016). Major and trace elements in soils and ashes of eucalypt and pine forest plantations in Portugal following a wildfire. *Science of the Total Environment*, *572*, 1363–1376. https://doi.org/10.1016/j.scitotenv.2016.01.190

Certini, G. (2005). Effects of fire on properties of forest soils: A review. *Oecologia*, *143*(1), 1–10. https://doi.org/10.1007/s00442-004-1788-8

Costa, M. R., Calvão, A. R., & Aranha, J. (2014). Linking wildfire effects on soil and water chemistry of the Mar??o River watershed, Portugal, and biomass changes detected from Landsat imagery. *Applied Geochemistry*, *44*, 93–102. https://doi.org/10.1016/j.apgeochem.2013.09.009

Davis, A. P., Shokouhian, M., & Ni, S. (2001). Loading estimates of lead, copper, cadmium, and zinc in urban runoff from specific sources. *Chemosphere*, *44*(5), 997–1009. https://doi.org/https://doi.org/10.1016/S0045-6535(00)00561-0

Debano, L. F. (2000a). The role of fire and soil heating on water repellency in wildland environments: A review. *Journal of Hydrology*, *231–232*, 195–206. https://doi.org/10.1016/S0022-1694(00)00194-3

Debano, L. F. (2000b). Water repellency in soils: A historical overview. *Journal of Hydrology*, *231–232*, 4–32. https://doi.org/10.1016/S0022-1694(00)00180-3

Demeyer, A., Voundi Nkana, J. C., & Verloo, M. G. (2001). Characteristics of wood ash and influence on soil properties and nutrient uptake: An overview. *Bioresource Technology*, *77*(3), 287–295. https://doi.org/10.1016/S0960-8524(00)00043-2

Etiégni, L., & Campbell, A. G. (1991). Physical and chemical characteristics of wood ash. *Bioresource Technology*, *37*(2), 173–178. https://doi.org/10.1016/0960-

8524(91)90207-Z

Ettensohn, F. R. (1985). Controls on development of Catskill Delta complex basin-facies. *Geological Society of America Special Papers*, *201*, 65–78.

Flannigan, M. ., Stocks, B. ., & Wotton, B. . (2000). Climate change and forest fires. *Science of The Total Environment*, *262*(3), 221–229. https://doi.org/10.1016/S0048-9697(00)00524-6

Fu, G., Chen, S., & McCool, D. K. (2006). Modeling the impacts of no-till practice on soil erosion and sediment yield with RUSLE, SEDD, and ArcView GIS. *Soil and Tillage Research*, *85*(1–2), 38–49. https://doi.org/10.1016/j.still.2004.11.009

Gallaher, B. M., Koch, R. J., & Mullen, K. (2002). Quality of Storm Water Runoff at Los Alamos National Laboratory in 2000 with Emphasis on the Impacts of the Cerro Grande Fire, 166.

Haan, C. T., Barfield, B. J., & Hayes, J. C. (1994). *Design Hydrology and Sedimentology for Small Catchments*. Academic Press. Retrieved from https://books.google.com/books?id=4rfw0FIO7BoC

Hansen, M. A., & Passchier, S. (2016). Oceanic circulation changes during early Pliocene marine ice-sheet instability in Wilkes Land, East Antarctica. *Geo-Marine Letters*, 1–7. https://doi.org/10.1007/s00367-016-0489-8

Harper, J. A. (1999). Chapert 7: Devonian. In C. H. Shultz (Ed.), *The Geology of Pennsylvania* (4th ed., pp. 108–127). Pennsylavania Geological Survey.

Hazen, M. (2016). 16MF Progression Map. PA Department of Conservation and Natural Resources.

Hernández, T., García, C., & Reinhardt, I. (1997). Short-term effect of wildfire on the chemical, biochemical and microbiological properties of Mediterranean pine forest soils. *Biology and Fertility of Soils*, *25*(2), 109–116. https://doi.org/10.1007/s003740050289

Hough, R. (2010). Copper and Lead. In P. Hooda (Ed.), *Trace elements in soil* (Vol. 1, p. 618). West Sussex, United Kingdom: Wiley. https://doi.org/10.1017/CBO9781107415324.004

Iglesias, T., Cala, V., & Gonzalez, J. (1997). Mineralogical and chemical modifications in soils affected by a forest fire in the Mediterranean area. *Science of the Total Environment*, *204*(1), 89–96. https://doi.org/10.1016/S0048-9697(97)00173-3

Johansen, M. P., Hakonson, T. E., Whicker, F. W., & Breshears, D. D. (2003). Pulsed redistribution of a contaminant following forest fire: cesium-137 in runoff. *Journal*

of Environmental Quality, *32*(6), 2150–7. https://doi.org/10.2134/jeq2003.2150

Joshi, U. M., & Balasubramanian, R. (2010). Characteristics and environmental mobility of trace elements in urban runoff. *Chemosphere*, *80*(3), 310–318. https://doi.org/https://doi.org/10.1016/j.chemosphere.2010.03.059

Marion, G. M., Moreno, J. M., & Oechel, W. C. (1991). Fire Severity, Ash Deposition, and Clipping Effects on Soil Nutrients in Chaparral. *Soil Science Society of America Journal*, *55*(1), 235. https://doi.org/10.2136/sssaj1991.03615995005500010040x

Miller, M. E., MacDonald, L. H., Robichaud, P. R., & Elliot, W. J. (2011). Predicting post-fire hillslope erosion in forest lands of the western United States. *International Journal of Wildland Fire*, *20*(8), 982–999. https://doi.org/10.1071/WF09142

Murray, R. W., Miller, D. J., & Kryc, K. A. (2000). Analysis of Major and Trace Elements in Rocks, Sediments, and Interstitial Waters by Inductively Coupled Plasma-Atomic Emission Spectrometry. *ODP Techical Note*, *29*.

Naidu, C. V, & Srivasuki, K. P. (1994). Effect of forest fire on soil characteristics in different areas of Seshachalam hills. *Annals of Forestry*, *2*, 166–173.

Neary, D. G. ., Ryan, K. C. ., & DeBano, L. F. (2005). Wildland Fire in Ecosystems. *Rocky Mountain Research Sation General Technical Rport*, *4*(RMRS-GTR-42), 250. https://doi.org/http://dx.doi.org/10.1111/j.1467-7717.2009.01106.x

Onda, Y., Dietrich, W. E., & Booker, F. (2008). Evolution of overland flow after a severe forest fire, Point Reyes, California. *CATENA*, *72*(1), 13–20. https://doi.org/http://dx.doi.org/10.1016/j.catena.2007.02.003

PA Department of Conservation and Natural Resources. (2000). Glacial deposits of pennsylvania, 80–80.

PA Department of Conservation and Natural Resources. (2016). Pocono fire contained, wildfire season still a concern in Pa. - April 27, 2016 resource - Pa. DCNR. Retrieved from http://www.apps.dcnr.state.pa.us/news/resource/res2016/16-0427-fire.aspx

Panagos, P., Borrelli, P., Meusburger, K., Alewell, C., Lugato, E., & Montanarella, L. (2015). Estimating the soil erosion cover-management factor at the European scale. *Land Use Policy*, *48*, 38–50. https://doi.org/10.1016/j.landusepol.2015.05.021

Philadelphia/Mount Holly Weather Forecast Office. (2017). National Weather Service Climate. Retrieved May 31, 2017, from http://w2.weather.gov/climate/index.php?wfo=phi

Pinedo-Gonzalez, P., Hellige, B., West, A. J., & Sañudo-Wilhelmy, S. A. (2016).

Changes in the size partitioning of metals in storm runoff following wildfires: Implications for the transport of bioactive trace metals. *Applied Geochemistry*. https://doi.org/10.1016/j.apgeochem.2016.07.016

Pope, G., Callanan, J., & Gorring, M. (2012). A reassessment of soil chemistry and pedogenesis following intense forest fires. In *2012 Annual Meeting, Middle States Division of the Association of American Geographers*. Shippensburg, Pennsylvania.

Renard, K., Foster, G., Weesies, G., McCool, D., & Yoder, D. (1997). Predicting soil erosion by water: a guide to conservation planning with the Revised Universal Soil Loss Equation (RUSLE). *Agricultural Handbook No. 703*. https://doi.org/DC0-16-048938-5 65–100.

Reynard-Callanan, J. R., Pope, G. a., Gorring, M. L., & Feng, H. (2010). Effects of High-Intensity Forest Fires on Soil Clay Mineralogy. *Physical Geography*, *31*, 407–422. https://doi.org/10.2747/0272-3646.31.5.407

Santín, C., & Doerr, S. H. (2016). Fire effects on soils: the human dimension. *Philosophical Transactions of the Royal Society B: Biological Sciences*, *371*(1696), 20150171. https://doi.org/10.1098/rstb.2015.0171

Schwertmann, U., & Fechter, H. (1984). The influence of alumimum on iron oxides: XI. aluminum-subsituted magnemite in soils and its formation. *Soil Science Society of America Journal*, *48*, 1462–1463.

Smith, H. G., Sheridan, G. J., Lane, P. N. J., Nyman, P., & Haydon, S. (2011). Wildfire effects on water quality in forest catchments: A review with implications for water supply. *Journal of Hydrology*, *396*(1–2), 170–192. https://doi.org/10.1016/j.jhydrol.2010.10.043

Taylor, S. R., & McLennan, S. M. (1995). The geochemical evolution of the continental crust. *Reviews of Geophysics*, *33*(2), 241. https://doi.org/10.1029/95RG00262

Tecle, A., & Neary, D. (2015). Water quality impacts of forest fires. *Journal of Pollution Effects & Control*, *3*(2), 140. https://doi.org/10.4172/2375-4397.1000140

U.S. Geological Survey. (1979). Geographic Names Phase I data compilation (1976-1981). 31-Dec-1981. Primarily from U.S. Geological Survey 1:24,000-scale topographic maps (or 1:25K, Puerto Rico 1:20K). Retrieved from https://geonames.usgs.gov/apex/f?p=gnispq:3:0::NO::P3_FID:1198145

Ulery, A. L., & Graham, R. C. (1993). Forest fire effects on soil color and texture. *Soil Science Society of America Journal*, *57*(1), 135–140.

United States Department of Agriculture Natural Resources Conservation Service. (2009). *NEW YORK Rapid Watershed Assessment Profile Middle Delaware-*

Mongaup-Brodhead Watershed. Syracuse.

USDA-NRCS. (n.d.). Official Soil Series Descriptions. Retrieved November 5, 2016, from https://soilseries.sc.egov.usda.gov/

Warner, F. (2016). After 8,000 acres destroyed, Poconos fire 40 percent contained, state forester says - The Morning Call. *The Morning Call*. Retrieved from http://www.mcall.com/news/breaking/mc-poconos-wildfire-may-be-90-percent-contained-20160426-story.html

Westerling, A. L., Hidalgo, H. G., Cayan, D. R., & Swetnam, T. W. (2006). Warming and earlier spring increase western US forest wildfire activity. *Science*, *313*(5789), 940–943. https://doi.org/10.1126/science.1128834

Woods, S. W., & Balfour, V. N. (2010). The effects of soil texture and ash thickness on the post-fire hydrological response from ash-covered soils. *Journal of Hydrology*, *393*(3–4), 274–286. https://doi.org/http://dx.doi.org/10.1016/j.jhydrol.2010.08.025

Yoon, J., Cao, X., Zhou, Q., & Ma, L. Q. (2006). Accumulation of Pb, Cu, and Zn in native plants growing on a contaminated Florida site. *Science of The Total Environment*, *368*(2–3), 456–464. https://doi.org/https://doi.org/10.1016/j.scitotenv.2006.01.016